UNCERTAINTY QUANTIFICATION FOR SAFETY VERIFICATION APPLICATIONS IN NUCLEAR POWER PLANTS

by

Emmanuel Boafo

A Thesis Submitted in Partial Fulfillment
of the Requirements for the Degree of

Doctor of Philosophy

in

Electrical and Computer Engineering

Faculty of Engineering and Applied Sciences

University of Ontario Institute of Technology

November 2016

ABSTRACT

There is an increasing interest in computational reactor safety analysis to systematically replace the conservative calculations by best estimate calculations augmented by quantitative uncertainty analysis methods. This has been necessitated by recent regulatory requirements that have permitted the use of such methods in reactor safety analysis. Stochastic uncertainty quantification methods have shown great promise, as they are better suited to capture the complexities in real engineering problems. This study proposes a framework for performing uncertainty quantification based on the stochastic approach, which can be applied to enhance safety analysis.

Additionally, risk level has increased with the degradation of Nuclear Power Plant (NPP) equipment and instrumentation. In order to achieve NPP safety, it is important to continuously evaluate risk for all potential hazards and fault propagation scenarios and map protection layers to fault / failure / hazard propagation scenarios to be able to evaluate and verify safety level during NPP operation. In this study, the Fault Semantic Network (FSN) methodology is proposed. This involved the development of static and dynamic fault semantic network (FSN) to model possible fault propagation scenarios and the interrelationships among associated process variables. The proposed method was demonstrated by its application to two selected case studies. The use of FSN is essential for fault detection, understanding fault propagation scenarios and to aid in the prevention of catastrophic events.

Two transient scenarios were simulated with a best estimate thermal hydraulic code, CATHENA. Stochastic uncertainty quantification and sensitivity analyses were performed

using the OPENCOSSAN software which is based on the Monte Carlo method. The effect of uncertainty in input parameters were investigated by analyzing the probability distribution of output parameters. The first four moments (mean, variance, skewness and kurtosis) of the output parameters were computed and analyzed. The uncertainty in output pressure was 0.61% and 0.57% was found for the mass flow rate in the Edward's blowdown transient. An uncertainty of 0.087% was obtained for output pressure and 0.048% for fuel pin temperature in the RD-14 test case. These results are expected to be useful for providing insight into safety margins related to safety analysis and verification.

Keywords: Uncertainty Quantification, CATHENA, Sensitivity Analysis, FSN, LOCA

Declaration

This thesis has not been submitted elsewhere for any degree or qualification.

Apart from content from other sources which have been duly referenced in the text, the content of this thesis is my own work.

Acknowledgements

My sincere thanks and appreciation go to my thesis supervisor Dr. Hossam A. Gabbar for helping to formulate this study and for guiding me throughout my doctoral studies. His valuable insight and suggestions helped in successfully completing this thesis. I am grateful for all his support, encouragement and motivation during my PhD studies.

I would like to extend my gratitude to the staff of the Thermalhydraulics branch of the Canadian Nuclear Laboratories (CNL) for their role in training me in the use of CATHENA. I also acknowledge the valuable contributions received from Dr. Eduardo Patelli and Dr. Erwin Alhassan on understanding uncertainty quantification concepts. Thanks to all my colleagues at the Energy Safety and Control Lab (ESCL) of the University of Ontario Institute of Technology for their support in various ways.

Finally, I extend my gratitude to my wife and daughter for their unfailing love, encouragement and support during the course of this study.

TABLE OF CONTENTS

TABLE OF FIGURES

LIST OF TABLES

List of Acronyms and Abbreviations

AC – Alternating Current

ACE – Alternating Conditional Expectation

AEAW – Atomic Energy Authority Winfrith

AECL – Atomic Energy of Canada Limited

AI - Artificial Intelligence

ANN – Artificial Neural Network

ANS – American Nuclear Society

ASDV - Atmospheric Steam Discharge Valve

ASDV – Atmospheric Steam Discharge Valve

BBN – Bayesian Belief Network

CANDU – Canadian Uranium Deuterium

CATHENA – Canadian Algorithm for Thermal Hydraulic Network Analysis

CIAU - Code with the Capability of Internal Assessment of Uncertainty

CNL – Canadian Nuclear Laboratories

CNSC – Canadian Nuclear Safety Commission

COSSAN – Computational Optimization Simulation and Stochastic Analysis

CSAU – Code Scaling and Uncertainty

CSDV – Condenser Steam Discharge Valve

DAG – Directed Acyclic Graph

DC – Direct Current

DID – Defense In Depth

ECC – Emergency Core Cooling

ECI – Emergency Coolant Injection

EDF – Electricité de France

ENUSA – Empresa Nacimal del Uranio, SA

ESV – Emergency Stop Valve

FDI – Fault Detection and Isolation

FES – Fuzzy Expert System

FF – Feed Flow

FM – Failure Mode

FSN – Fault Semantic Network

FTA – Fault Tree Analysis

FW – Feed Water

GA – Genetic Algorithm

GENHTP – Generalized Heat Transfer Package

GLRT – Generalized Likelihood Ratio Testing

GPM – Gaussian Process Model

GUI – Graphical User Interface

GV – Governor Valve

H – Fuzzy linguistic variable for High SG level

IAEA – International Atomic Energy Agency

IEC – International Electrotechnical Commission

IPL – Independent Protection Layer

IPSN – Institute de protection et de sûreté nucleaire

L – Fuzzy linguistic variable for Low SG level

List of Acronyms and Abbreviations

LOCA – Loss of Coolant Accident

MAE – Mean Absolute Error

MC – Monte Carlo

MCNP – Monte Carlo N-particle

MSSV – Main Steam Safety Valve

MSV – Main Steam Valve

N – Fuzzy linguistic variable for Normal SG level

NN – Neural Network

NP – Neutron Power

NPP – Nuclear Power Plant

NRC – Nuclear Regulatory Commission

OPG – Ontario Power Generation

PDF – Probability Density Function

PFDavg – Average Probability of Failure on Demand

POOM – Process Object Oriented Methodology

PSA – Probability Safety Assessment

PV – Process Variable

PWR - Pressurized Water Reactor

REGDOC – Regulatory Document

RIH – Reactor Inlet Header

ROH – Reactor Outlet Header

RRS – Reactor Regulating System

List of Acronyms and Abbreviations

SAR – Safety Analysis Report

SDG – Sign Directed Graph

SDS – Shutdown System

SDV – Steam Discharge Valve

SG – Steam Generator

SGTR – Steam Generator Tube Rupture

SIL – Safety Integrity Level

SIS – Safety Instrumented System

SUSA – Software for Uncertainty and Sensitivity Analysis

TS1 – Heated Section 1

UMAE – Uncertainty Methodology based on Accuracy Extrapolation

UQ – Uncertainty Quantification

UT – Unscented Transform

VH – Fuzzy linguistic variable for Very High SG level

VL – Fuzzy linguistic variable for Very Low SG level

VVL – Fuzzy linguistic variable for Very Very Low SG level

WIMS – Winfried Improved Multigroup System

NOMENCLATURE

$y(s)$	System output vector.
$G_{u,f}(s)$	System transfer function.
$u(s)$	System input vector.
$f(s)$	Fault vector.
λ_T	Total failure.
λ_D	Dangerous failure mode.
λ_S	Safe failure mode.
ξ_S	Diagnostic coverage for safe failures.
ξ_D	Diagnostic coverage for dangerous failures.
λ_{DD}	Dangerous detected failure rate.
λ_{UD}	Dangerous undetected failure rate.
λ_{SD}	Safe detected failure rate.
λ_{SU}	Safe undetected failure rate.
S	Sample space.
E	Restricted subspace.
p	Probability measure.

b_i	Regression coefficients.
k	Number of simulated samples.
ε	Error between predicted and calculated output values.
α_i	Input parameters.
$S_i^{(l)}$	Sensitivity measure
∂Y	Change in output parameter, Y.
∂X_i	Change in input parameter, X.
CaFr1	Frequency of cause 1
FPr1	Probability of failure 1 occurring as a result of any cause.
CoPr1	Probability of consequence 1 occurring.
Colm1	Total impact of consequence 1.
ρ_{xy}	Correlation coefficient
S_x	Standard deviation of input parameter, x.
$\bar{x}$	Mean of input parameter, x.
S_y	Standard deviation of output parameter, y.
$\bar{y}$	Mean of output parameter, y.
N	Total number of random input samples simulated.
EF	Error Function.

R_i	Risk associated with a particular fault propagation path.

CHAPTER 1: INTRODUCTION

1.1 Review

In this chapter, a brief background of the study is given and the problem statement is outlined and explained. The research objectives are also stated in this chapter. A fault is defined in the background and a description of the safety verification process is given. The chapter also identifies certain safety systems and their functions.

1.2 Background

In Nuclear Power Plants (NPPs), safety systems are represented in the form of independent layers of protections or barriers. These layers are expected to prevent or reduce the effects of all possible hazard scenarios. Typical safety systems are represented within process control systems such as alarms, process limits or control rules, which are translated into control actions [4]. An effective safety control design can improve plant operation economics, by optimizing safety margins to reduce unnecessary shutdown cases [19]. This also takes into account human factors involved in plant operation in order to ensure that safety margins are matched with required operator actions [17, 15].

Faults are abnormal conditions where deterioration occurs to plant equipment/process that can be caused by various factors including human errors, environmental stresses or material deficiencies [7]. Fault diagnosis and safety verification are important for the operation of nuclear power plants for their safe and cost effective operation. Both model based and data driven techniques have been used extensively for fault detection and diagnosis of NPPs.

These methods include Artificial Neural Networks (ANN), Neuro fuzzy, signed directed graph and fault-tree analysis. Mostly, fault diagnostic approaches are based on the sensors that measure important process variables.

1.3 Problem Statement

The conservative approach for performing safety analysis may be unrealistic due to limited knowledge of uncertainties associated with estimations of parameters important to safety by codes. Safety limits based on this approach may be overly conservative. Furthermore, it has been identified that there exist discrepancies between the results of codes that have been designed to simulate faults and transients in NPPs, such as CATHENA on the one hand, and then real time data available from the plants' operation as well as the results obtained from plant simulators. An example of steam generator level in CANDU is shown in table 1.1 to demonstrate that the difference between two states is within the error between real time and simulation results thereby implying that the transition between two plant states might not be captured by a particular method correctly.

Table 1.1. Steam Generator (SG) levels of CANDU.

	Level (meters)	Difference
Full Power	14.31	0.16
Level High Alarm	14.47	
CATHENA	2.16938	
Real Time	1.98738	0.18

These discrepancies may lead to differences in time taken to reach limits and that poses a problem for a suitable response action. Subsequently, this affects the accuracy of fault

propagation prediction and the relationship between process variables is also affected. Fault propagation is affected in terms of speed and the strength between process variables.

Currently, faults are detected in a nuclear power plant such as CANDU by the use of alarm and annunciation windows on the plant control console and the reading of parameter changes from the console by operators. However, these do not give adequate information on causes and consequences of faults.

In seeking more accurate simulation models usually from well-established codes to match real time data, some challenges arise that makes this approach an impossible task. These challenges include the uncertainties inherent in physical systems which makes modeling such systems inaccurate. Furthermore, models are based on some assumptions which make them unable to represent the physical systems exactly and finally, the complexity of multi-physics modeling of physical systems does not make their implementation in real time applications feasible.

1.4 Research Objectives

In order to achieve the stated goal of uncertainty quantification for safety verification applications in NPP, this study was carried out with the following objectives:

1. Develop FSN (static, steady state, dynamic) for given fault scenarios.
2. Develop stochastic methods to quantify uncertainty associated with code for simulations of faults/transients, and map to FSN.
3. Develop methods to model interactions between Process Variables (PV) for given faulty scenarios, and automatic update of FSN.

4. Develop a method for safety verification to link independent protection layers (IPLs) with defense-in-depth (DiD) and fault scenarios, and map to FSN.

Independent protection layers are independent layers of protection implemented to prevent fault propagation in a plant. Defense-in-depth is a concept of establishing multiple barriers in a process in order to prevent and mitigate faults and their consequences.

1.5 Thesis Organization

The following outlines the organization of this thesis:

Chapter 1

In chapter 1, a brief background of the study is given; the problem statement is outlined and explained. The research objectives are also stated in this chapter. A fault is defined in the background and a description of the safety verification process is given. The chapter also identifies some safety systems and their functions.

Chapter 2

In chapter 2, a review of existing literature related to this study is presented. Basic concepts of fault diagnosis are briefly explained in addition to a review of some fault diagnosis methods currently being used. This chapter contains a description of safety instrumented systems and safety integrity levels in relation to safety verification. Finally, the chapter concludes with an overview of the uncertainty quantification concept and methods.

Chapter 3

In chapter 3, the proposed methodology of this study is given and explained. The proposed framework for performing uncertainty quantification for safety verification applications is presented and discussed. A detailed description of the stochastic uncertainty quantification method used in this study is also given.

Chapter 4

In chapter 4, selected case studies considered for application of the proposed FSN methodology are described. The rationale for selecting these cases is explained and fault propagation scenarios related to these case studies are defined and described.

Chapter 5

In chapter 5, the proposed simulation models used in the study are presented and explained. The best estimate thermalhydraulic code, CATHENA is introduced and a sample problem described. FSN methodology is also described in this chapter.

Chapter 6

In chapter 6, results of uncertainty and sensitivity analysis performed for the RD-14 test facility are presented and discussed. Uncertainty quantification results obtained in this study compared with similar results in literature using other methods is also presented in this chapter.

Chapter 7

Results of uncertainty quantification performed for the Edward's pipe blowdown problem are presented and discussed in this chapter. This chapter also contains results of the FSN

method applied to the case studies described in chapter 4 as well as a linking of uncertainty quantification results with the FSN methodology through rule updating.

Chapter 8

Conclusions drawn from this study and recommendations to various stakeholders are presented in this chapter. The chapter also contains an outline of the innovative contributions of the study and an outlook on the future direction of this research.

CHAPTER 2: LITERATURE REVIEW

2.1 Review

In this chapter, a review of existing literature related to this study is presented. Basic concepts of fault diagnosis are briefly explained in addition to a review of some fault diagnosis methods currently being used. This chapter contains a description of safety instrumented systems and safety integrity levels in relation to safety verification. Finally, the chapter concludes with an overview of the uncertainty quantification concept and methods.

2.2 Fault Diagnosis

Fault detection and diagnosis is essential in maintaining a high level of performance, increasing system availability and taking appropriate corrective actions. This can be applied in processes such as, spacecraft, aircraft, chemical plants and nuclear power plants [30, 32, 33, and 34]. Fault diagnosis usually comprises fault detection and isolation. Fault detection involves distinguishing between normal and faulty conditions. Fault isolation deals with determining the source of the fault, i.e. which sensor, actuator or component is the source of the fault. Hence the abbreviation FDI (fault detection and isolation) is normally used in literature.

Several methods have been extensively utilized and reported for fault diagnosis and safety verification of complex systems such as nuclear power plants, aircrafts, chemical processing plants and space vehicles. These methods include the following: fault tree analysis (FTA) [11]. FTA can be used to detect causes of faults and their subsequent

propagation, however FTA is limited because it is implemented manually and not suitable for real-time fault diagnosis [18]. Zhao and Upadhyaya [29] and Gross et al. [10] also used model based methods for fault diagnosis. The sign directed graph (SDG) is a logic based method [14] that can be used to perform fault diagnosis. Although SDG is a useful method for fault diagnosis and propagation, its usage is undesirable since it requires robust mechanisms to construct fault models [7]. Data-driven solutions based on computational intelligent methodology have gained popularity in fault diagnosis of nuclear power plants. They include, Artificial Neural Networks (ANN), Genetic Algorithms (GA), fuzzy logic and Neuro fuzzy techniques. These computationally intelligent methods have been widely used in recent times due to their learning abilities for fault diagnosis and their inherent parallel structures. They have therefore been applied in different types of industries including geophysical [23], oil and gas [9] and in nuclear steam supply system of a nuclear power plant [12]. The following sections present some basic concepts of model-based FDI methods as well as a review of some methods that have been used for fault diagnosis reported in literature.

2.2.1 Basic Concepts of Model-based FDI Methods

Model-based methods for fault diagnosis have been a major research subject in the past few decades [31]. These methods are mainly based on analytical redundancy which entails comparison between signals generated by mathematical models of a system and actual process measurements. The difference between model values and actual measurements is known as residual quantities [35, 30, 36, and 37]. A major advantage of analytical redundancy is that a process computer alone can be used to implement a FDI algorithm

without the need for additional hardware resources [38]. Model-based FDI require only input-output data and consists of two stages; residual generation and residual evaluation (decision making) as shown in figure 2.1.

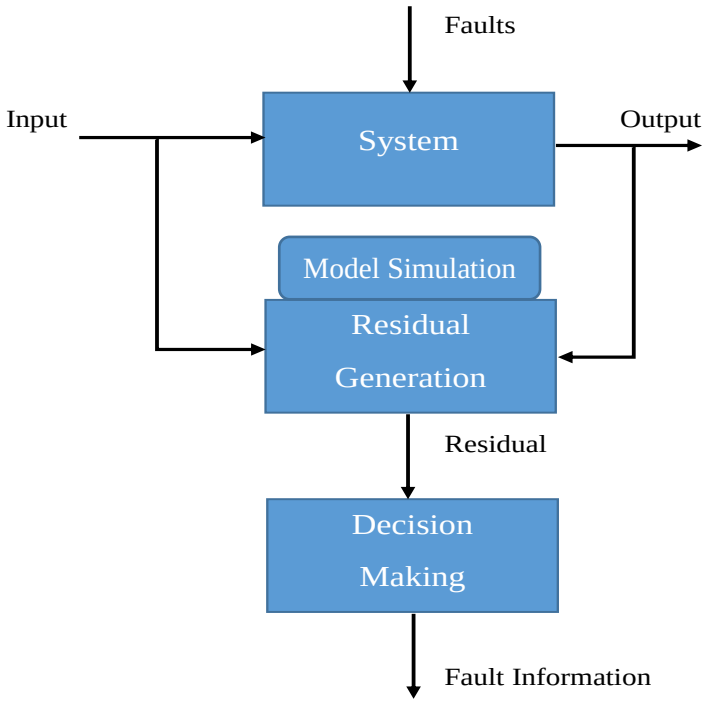

Figure 2. 1 General structure of model-based FDI [33]

2.2.2 Residual Generation for Fault Diagnosis

A system with possible faults is given by [38],

$$y(s) = G_u(s)u(s) + G_f(s)f(s) \tag{2.1}$$

Where $G_u(s)$ and $G_f(s)$ are input and fault transfer matrices respectively, u, y are system input and output vectors respectively. $f = [f_1, f_2, \dots, f_q]^T$ is a fault vector, with each element representing a particular fault. The fault vector is usually considered as an unknown time function. Residuals generated for FDI must satisfy the following condition;

$$r(t) \neq 0 \; iff \; f(t) \neq 0 \tag{2.2}$$

The general structure for residual generation is expressed mathematically as [33],

$$r(s) = H_u(s)u(s) + H_y(s)y(s) \tag{2.3}$$

Where $H_u(s)$ and $H_y(s)$ are transfer matrices that can be obtained using stable linear systems. In a system without a fault, $H_u(s)$ and $H_y(s)$ must satisfy the condition,

$$H_u(s) + H_y(s)G_u(s)=0 \tag{2.4}$$

The parameterizations of $H_u(s)$ and $H_y(s)$ is dependent on the choice of the residual generation method. A suitable selection of $H_u(s)$ and $H_y(s)$ can result in the desired performance of the residual.

2.2.3 Review of Model-based Residual Generation Methods

2.2.3.1 Observer-based Methods

These methods involve the estimation of the system output based on inputs and outputs of the monitored system by an observer. The (weighted) difference between the estimated and the actual outputs is the residual [39, 30, 40, 33 and 37]. The Main advantages of this approach include: 1) fast reaction to incipient faults, 2) suitable for fault detection and isolation in sensors and actuators, 3) the design procedure is systematic and simple and 4) it is easy to implement and execute the algorithm. Some disadvantages include: 1) difficulties may arise when applying linear observers to highly nonlinear systems [39, 30, and 40], 2) nonlinear observers are direct and accurate but are only applicable for some

classes of nonlinearities, 3) requires a fairly accurate system model for a priori modelling. This approach is also not fully verified [40, 41].

2.2.3.2 Parity Relation Methods

This method entails checking inconsistencies between inputs and outputs of the monitored system. The mismatched term is used as the residual signal [42, 43, 44 and 45]. The method has been shown to be similar to the use of a dead-beat observer [33]. Observer-based methods are similar to parity relation methods with a few differences such as; 1) use of directional residual which may be difficult, 2) the method can be applied to only linearized models, and 3) advanced techniques such as optimally robust parity relations may be used to ensure robustness of the fault diagnosis system. Both observer-based and parity relation methods can be designed in the frequency as well as time domains. In the frequency domain, advantages such as the use of frequency distribution of faults, noise and modelling uncertainty can be used to achieve a robust fault diagnosis system [38].

2.2.3.3 Parameter Estimation Methods

The method involves the online estimation of model parameters and the residual is based on a comparison between estimated and actual parameter values. The error between the actual and predicted output can be considered as the residual signal [46, 47, 48 and 40]. Some advantages of the parameter estimation methods are: 1) detection and isolation of faults in sensors and actuators is quite straight forward, 2) noise is easily handled in this method, and 3) can have a good self-learning capability if the estimation method is adaptive. Some disadvantages include: 1) fault isolation is difficult because the physical

parameters do not correspond to model parameters and make the design of the directional residual impossible [46, 47, 48 and 40], 2) the detection and isolation of faults in sensors and actuators is complicated. And 3) the method requires a large amount of computations during implementation.

2.2.3.4 Neural Network Methods

This method is similar to observer-based methods with the observer replaced by a neural network. The neural network estimates the system output and the residual is the difference between the estimated and the actual outputs [49]. The following are some advantages of this method: 1) convenient for detecting faults in sensors and actuators, 2) has good ability to detect and isolate parameter faults, 3) detection of multiple faults is possible, 4) excellent in fault detection in nonlinear systems. Some disadvantages include: 1) requires a large amount of computation during implementation, 2) Neural networks need to be trained extensively during the design stage. This method forms part of the FDI framework proposed in this study because of its capabilities in performing accurate fault diagnosis by learning the system as has been demonstrated in subsequent chapters of this thesis.

2.2.4 Residual Evaluation (Decision Making)

It is important for a FDI system to be robust, which is avoiding errors in fault diagnosis resulting in false alarms due to parameter uncertainty, disturbances and noise. Robustness can be enhanced at the residual evaluation stage of FDI [50, 51]. Residual evaluation can be carried out by threshold logic, fuzzy logic or neural networks. These methods are briefly described in the following sections.

2.2.4.1 Threshold Logic

This method involves the comparison between a residual evaluation function, $DF(r(t))$ and a defined threshold, $T(t)$ in a test shown below [52, 53, and 54].

$$DF(r(t)) \begin{cases} \leq T(t) & no\ fault \\ > T(t) & likely\ fault \end{cases}$$

A positive test result is indication of a likely fault while $DF(r(t)) \leq T(t)$ indicates a no fault system. The determination of a residual evaluation function and the threshold are the main tasks to be performed.

2.2.4.2 Residual Evaluation Function

The norm of the instantaneous residual value can be used as an evaluation function if the residual is robust and the noise is small. In stochastic systems, statistical testing theory is used to determine residual functions and thresholds [54]. Chi-squared testing, generalized likelihood ratio testing (GLRT) are some methods that have been utilized in residual evaluation [55, 37].

2.2.4.3 Threshold Determination

Thresholds are positive fixed values determined either by experience or by experiments. Fixed thresholds, optimal thresholds from Markov theory or adaptive thresholds [56, 57 and 58] are some of the methods used for threshold determination. The adaptive thresholds that involve the variation of the thresholds according to the control activity of the process was found to be the most suitable threshold determination method.

2.2.5 Fuzzy Logic

Fuzzy logic is used in residual evaluation to make decisions which produce weighted alarms instead of Boolean decisions. The fuzzy inference system aids the plant operator in taking the final decision [59, 60]. Fuzzy logic translates analytical information and expert knowledge into a rule-based knowledgebase with the capability to make intelligent decisions even when information is uncertain. The introduction of fuzzy logic into residual evaluation provides a reliable decision making tool which can be applied in real industrial systems.

2.2.6 Neural Networks for Residual Evaluation

Neural networks learn and store information from residual history. They can distinguish noise, thereby providing a stable, automated and highly sensitive diagnostic tool. In pattern recognition, an input feature vector is mapped unto various decision classes. The decision classes correspond to various faults that might exist in a particular system. A neural network can be used as a pattern recognizer to partition residual patterns and activate alarm signals [61, 62]. Fault patterns can be stored in neural networks during training and can be used to detect and isolate specific faults. Neural networks are therefore suitable for feature extraction and recognition of complex features in residuals to aid in FDI.

The structured identification of faults, causes and consequences is still a major problem in fault diagnosis [7] as it requires a multi discipline approach as well as factors such as plant degradation.

2.2.7 Optimum Sensor Placement

Sensor placement plays an important role in an FDI system. Process variables are affected by the onset and propagation of a fault. The main objective of the FDI system is to identify these faults and also to determine the root cause of the fault identified. The efficiency of the FDI system is thus dependent on the ability of the sensor network to detect failure modes and abnormal conditions. With several process variables in a NPP that need to be measured, the selection of optimum sensor locations presents a unique problem. The solution to the sensor placement problem can be summarized as:

1) Generating a set of process variables that are affected by the onset of a fault by means of fault modeling.

2) Use of the generated set to identify sensor locations based on the design criteria of the plant. The cause-effect information is represented in a fault-sensor maximum connectivity matrix.

2.2.8 Fault Observability and Resolution

This refers to the condition that every fault defined for the process has to be observed by at least one sensor. For a given process, the observability problem becomes finding the minimum number of sensors that would cover all faults (root nodes). This is commonly known as minimum set covering problem [25]. Resolution refers to the ability to identify the exact fault that has occurred. The fault observability and resolution could be solved by linking the root nodes and sensor locations, but this becomes difficult due to increasing number of faults and sensor locations. Heuristics often give a quick and reasonably accurate solution. A greedy search heuristic was developed for solving the single and

multiple fault observability and resolution problem as reported in [21, 2]. Not all faults are distinguishable by using the sensor placement sets obtained from the above method. However, these methods provide essential information to the PCA-based FDI system.

2.3 Safety Analysis and Verification

2.3.1 Safety Instrumented System (SIS)

SIS include sensors, logic solvers and final elements that ensure that a plant operates under safe conditions within defined limits and free from hazards. In a NPP such as the CANDU, the shutdown system number one (SDS#1) which consists of 32 control rods made of cadmium and stainless steel is an example of a SIS. The system does not take part in the plant normal operation but is poised and on standby to be deployed when necessary to restore the plant to a safe operating mode.

2.3.2 Safety Integrity Level (SIL)

It is defined as the likelihood of a SIS to satisfactorily perform the required safety functions under all stated conditions, within a stated period of time (IEC 61508). SIL is a discrete level (from 1 to 4) for specifying the safety integrity requirements of safety functions. The design of an SIS determines the overall SIL. It is a target probability of the system average probability of failure on demand (PFD_{avg}). Table 2.1 shows the safety integrity levels and PFD_{avg} for a low demand operation.

Table 2.1. SIL for a low demand operation [93].

SIL	**PFD_{avg}**
1	10^{-1}- 10^{-2}
2	10^{-2}- 10^{-3}
3	10^{-3}- 10^{-4}
4	10^{-4}- 10^{-5}

2.3.2 Fault Tolerance

This is the ability of a system to prevent a fault from progressing into system failures and is achieved by incorporating some redundancy (using multiple instruments to serve the same purpose) into the system design.

2.3.3 Failure Modes

SIS failure modes are described as either safe or dangerous. Failures that do not pose any threats to the safety of the system are described as safe while those that have a potential to compromise system safety are described as dangerous failures. Both safe and dangerous failures may either be detected or undetected by the fault diagnosis system. It is generally more acceptable to detect safe failure modes including false alarms than not to detect dangerous failure modes. Equations 2.5-2.7 illustrate this concept based on the standard in [93].

$$\lambda_T = \lambda_D + \lambda_S \tag{2.5}$$

Where,

λ_T is the total failure.

λ_D is the dangerous failure mode.

λ_S is the safe failure mode.

$$\lambda_T = \xi_D\lambda_D + (1-\xi_D)\lambda_D + \xi_S\lambda_S + (1-\xi_S)\lambda_S \quad (2.6)$$

Where,

ξ_S is the diagnostic coverage for safe failures.

ξ_D is the diagnostic coverage for dangerous failures.

$$\lambda_T = \lambda_{DD} + \lambda_{DU} + \lambda_{SD} + \lambda_{SU} \quad (2.7)$$

Where,

$\lambda_{DD}, \lambda_{DU}$ is the dangerous detected and dangerous undetected failure rates, respectively.

$\lambda_{SD}, \lambda_{SU}$ is the safe detected and safe undetected failure rates, respectively.

2.3.4 Common Cause Failure

This is the failure of more than one item as a result of the same stress or cause. Certain complexities are encountered in dealing with this category of failures due to the difficulty in identifying all possible consequences that may result from a common cause.

2.3.5 Protection Layers and Defense-in-depth

In NPPs, safety is achieved by the implementation of various barriers that are meant to ensure that processes are carried out in a safe and reliable manner and also to prevent and control any abnormal/accident conditions that may occur as well as to mitigate any consequences of accidents if they occur. This is the defense-in-depth concept. Safety protection layers are mapped to defense-in-depth levels in which each defense-in-depth level should be covered by more than one protection layer. Independent protection layers (IPLs) include: IPL1: safety design; IPL2: basic process control/alarm; IPL3: critical alarm; IPL4: safety instrumented system (SIS); IPL5: relief devices; IPL6: physical protection; IPL7: site emergency procedures; and IPL8: community protection. Table 3.1 shows the defense-in-depth levels.

Table 3.1. Defense-in-depth levels

Level	Description
Level 1	Prevention of abnormal operation and malfunctions
Level 2	Control of abnormal operation and detection of malfunctions
Level 3	Control of accidents included in the design basis.
Level 4	Control of severe accident conditions of the plant, including the prevention of accident progression and mitigation of consequences.
Level 5	Mitigation of environmental/radiological consequences of significant releases of harmful products.

2.3.6 CANDU Shutdown Systems

CANDU has two shutdown systems called shutdown system number one (SDS#1) and shutdown system number two (SDS#2). SDS#1 is made up of solid neutron absorbing rods that are dropped into the reactor core while a liquid poison (Gadolinium nitrate) is introduced into the moderator for SDS#2. They are functionally and physically independent of each other and are able to shut down the reactor separately. The two shutdown systems respond automatically to neutronic and process signals and their independence is achieved by using diversity in areas such as types of instruments used, source of electric and pneumatic power and the software languages used. The shutdown systems are activated by trip parameters that include; high neutron power, high rate of neutron power, low coolant flow, high coolant pressure, low pressurizer level, low steam generator level and high reactor building pressure [73]. Figure 2.2 shows SDS#1 and SDS#2.

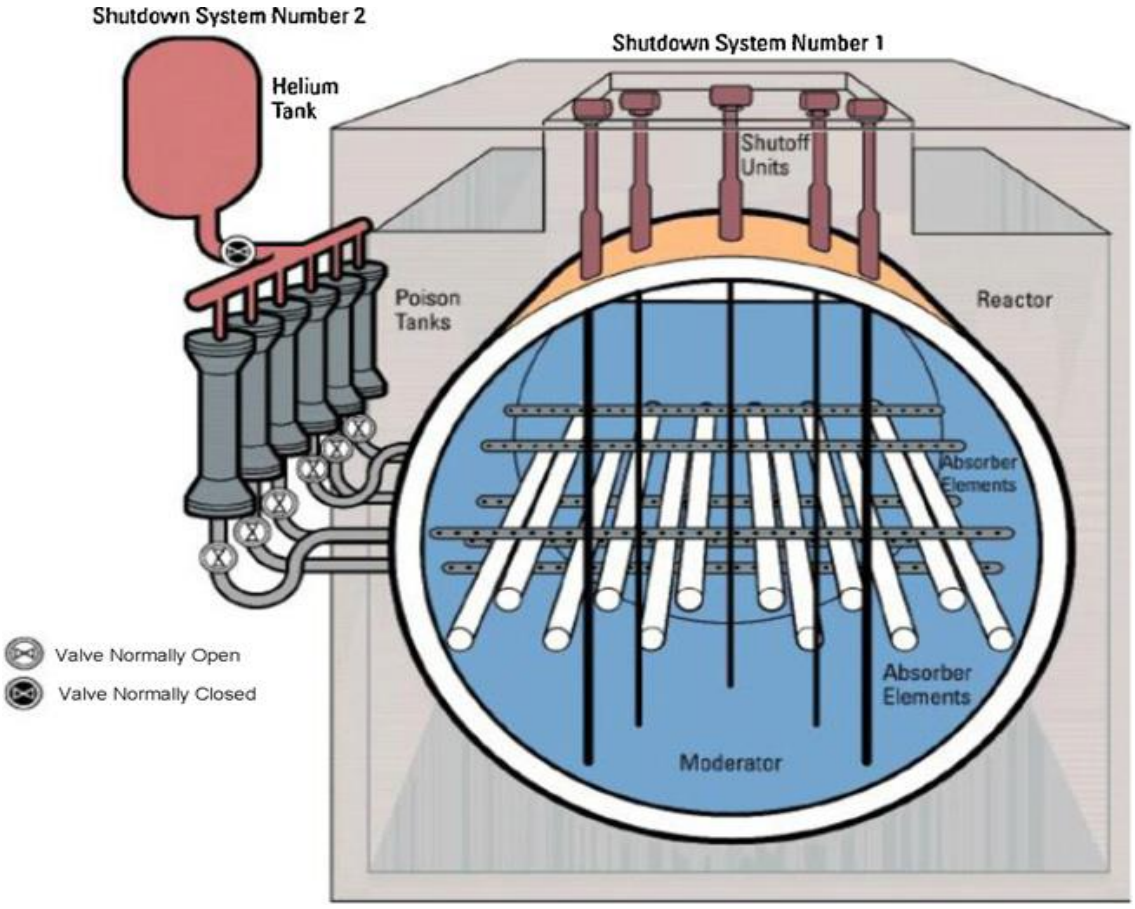

Figure 2.2 Shutdown systems SDS1 and SDS2 [73]

2.3.7 Safety Verification

Verification is the evaluation of an implementation to determine that applicable safety-critical requirements for any plant and its operations as specified are satisfied. The verification process ensures that the design solution meets all validated safety requirements. [22]. A verified system shows measurable evidence that it complies with the overall system safety needs by incorporating an integrated framework.

2.3.8 Current Safety Assessment and Verification Practices for NPPs

Safety assessments are undertaken for NPPs to evaluate the compliance with safety requirements. According to the IAEA standard for Safety Assessment for Facilities and Activities [63], an independent verification of the safety assessment must be carried out prior to its use by the operating Organization (such as Bruce Power or OPG) or before it is submitted to the regulatory body. The following guidelines are provided by the IAEA standard [63] for carrying out independent verification of the safety assessment:

1. Verification is carried out by qualified experts. The objective of an independent verification is to determine whether safety assessment was done in an acceptable way.
2. The verification is expected to review and determine whether the safety assessment carried out was comprehensive. It should also identify any radiation risks that had not been taken into account.
3. The accuracy of models used to represent the design and operation of the plant must be determined by the verification.
4. The regulatory body (CNSC/NRC) is required to carry out an independent verification to satisfy itself that the safety assessment is acceptable.

2.3.9 Requirements for Safety Analysis and Assessment

Safety assessment according to the CNSC's REGDOC-2.4.1 [74] involve structured processes that enable the verification of applicable safety requirements during the entire life cycle phases of NPPs. Areas covered by safety assessment include design adequacy, safety analysis, equipment fitness for service and emergency preparedness.

Safety analysis forms part of safety assessment and it is mainly an analytical quantitative study that is performed to demonstrate the safety of a NPP as well as to test the adequacy of its design and performance. Safety analysis can be performed either quantitatively (deterministic) or probabilistically (PSA).

The guide [74] outlines requirements for the establishment of a process by operating organizations of NPPs to ensure that the safety analysis reflects the following; current condition of the plant, current operating limits, experience obtained from operating the plant as well as experimental research findings, new modeling and computational capabilities to determine likely impacts on the conclusions of safety analysis. It also requires the use of human performance estimation in the safety analysis.

As a result of the above requirement, this study is conducted to explore various computational methods that will enhance fault propagation analysis and to perform safety verification.

2.4 Multiphysics Simulations for Safety Analysis in NPPs

In NPPs, various computational tools are used to perform safety analysis and safety verification. These tools are designed to simulate transients and in some cases, accident

scenarios for various systems in a NPP. For example, for thermal hydraulics; RELAP5, STAR CCM+ and CATHENA are used. For neutronics; MCNP, DRAGON and WIMS are used. The codes mentioned above are used by regulators, operating organizations and researchers to perform safety assessment and verification of NPPs.

2.5 Uncertainty and Safety Analysis

Uncertainty is a range attached to a measurement or computed parameter within which the true value is believed to lie. It is the most widely accepted way of expressing the accuracy of results and it covers both systematic and random errors including noise. In safety analysis, uncertainty quantification plays a crucial role mainly because knowledge of uncertainties associated with estimations of parameters important to safety will ensure that safety limits are not violated under any circumstance. Additionally, uncertainty quantification helps industry regulators to accept more realistic safety margins rather than relying on single value conservative estimates.

A number of studies on uncertainty quantification applied to safety analysis have been reported in literature. The Software for Uncertainty and Sensitivity Analysis (SUSA) developed in Germany was used to perform uncertainty quantification for a large break loss of coolant accident on a German pressurized water reference reactor. The results showed instances during the transient where the upper limit of the maximum clad temperature was not bounded by the conservative calculation of same [65]. In a similar study, uncertainty and sensitivity analysis was performed on the TALL-3D facility by coupling ANSYS CFX (CFD) and ATHLET codes. The results provided uncertainty estimates on output parameters given uncertain input parameters which can be compared

with experimental data in order to assess agreement between simulations and experimental data [90]. In other studies, uncertainty in selected input parameters was estimated using RELAP5-3D and VIPRE -01 codes for a small modular reactor. The uncertainty quantification results obtained showed that the output parameter range estimates were within regulatory accepted limits [91].

2.6 Uncertainty Quantification in NPP Simulations

Uncertainty quantification (UQ) is an important exercise that needs to be conducted as part of NPP simulations. This is due to the fact that uncertainties arise from various sources during the modeling and simulation process, these sources include; uncertainties in the input parameters used, model uncertainties arising from assumptions made in modeling a physical system as well as the type of numerical methods used in solving the problem. UQ basically asks the question, what range of outputs will be observed given the range of uncertain input parameter values? The UQ process therefore involves the determination of the range and probability of the outputs or the output probability density function (PDF). UQ methods can be broadly classified into the following: a) sampling based methods, b) Code Surrogates and c) Ad joint methods. Both sampling based methods and code surrogates can be described as computer codes in black box mode. Examples of these category include regression analysis and Monte Carlo methods. Code surrogates are simplified mathematical models of inputs and outputs, examples include; Unscented Transform (UT), Alternating Conditional Expectation (ACE) and Gaussian Process Model (GPM). In regression analysis, input/output relationships are estimated from datasets.

2.6.1 Uncertainty Propagation

The process of uncertainty propagation involves the selection of input parameters and quantifying the effects of uncertainty in these inputs on selected output parameters. Variability in input parameters affects output or response parameters. These effects are analyzed in order to estimate uncertainties on the outputs. Input parameter uncertainty propagation is executed by the identification of uncertain input parameters, followed by the characterization of these inputs using probability distributions and ranges, then performing model recalculations with variations of the input. This process can be done either deterministically or using probabilistic approaches.

Uncertainties in the input parameters are propagated through the model to produce an output. Performing a number of model recalculations enables an output distribution to be obtained. This distribution can then be analyzed to estimate the uncertainty of the output due to the input uncertainties [88; 89]. Input parameter uncertainty propagation was performed in this study with details given in subsequent chapters.

2.6.2 Deterministic Uncertainty Quantification Methods

In deterministic methods, probability distributions are not used to quantify the parameter uncertainties. Uncertainty ranges based on available experimental data are specified and uncertainty results are deterministic. Sensitivity analysis performed using these methods are based usually on local sensitivity values. These are derived from computing the change in model output divided by the change in a particular input parameter. Examples of deterministic tools developed and used are the Atomic Energy Authority Winfrith (AEAW) and the Electricité de France which is part of the Framatome methods.

2.6.3 Stochastic Uncertainty Quantification Methods

This method consists of: the identification of the NPP, the best estimate code and the transient to be analyzed, followed by the identification of uncertain input parameters (initial conditions and boundary conditions), then a screening of input parameters to be included in the analysis based on a priori knowledge if it exists. Examples of stochastic methods for UQ which have been used include, the Code Scaling and Uncertainty (CSAU) method used in Canada, the Software for Uncertainty and Sensitivity Analysis (SUSA) developed in Germany, the Institute de protection et de sûreté nucleaire developed in France and the Empresa Nacimal del Uranio, SA developed in Spain.

The use of stochastic methods to perform UQ has gained significant interest in recent times. These methods include Bayes and Laplace's subjective interpretation of probability as a state of information and their wide acceptance relative to other methods is due to the well-developed concept of probability. In the stochastic methods, uncertainties are represented mathematically by random variables and by suitable probability distributions. The stochastic analysis allows for UQ and its propagation to the outputs, which may be mathematically perceived as random variables adequately described by their probability distribution. UQ yields certain benefits including assessing the reliability and variability of outputs as well as providing useful information that would enhance the design process and increase the fidelity of the prediction. Closely related to UQ is sensitivity analysis which involves mainly uncovering the quantities responsible for the variability of the outputs. The uncertainties that may be due to the lack of knowledge would be reducible by obtaining more information on the quantities causing the variability in the output. Irreducible uncertainties must be factored in the design such that the safety of the system is not

compromised [64]. Sensitivity measures such as the Spearman rank correlation is used and it provides the variation of the output in terms of standard deviations when the input uncertainties vary by one standard deviation [65].

2.6.4 Sources of Uncertainty

Uncertainties associated with the use of best estimate codes to perform safety analysis arise from the following sources:

1. Uncertainties arising from the model or code.
2. Uncertainties due to the numerical solution method used.
3. Uncertainties resulting from modelling the nuclear power plant.
4. Input parameter uncertainties (initial and boundary conditions).

In this study, the focus has been on uncertainties due to input parameters. A more detailed list of sources of uncertainties can be derived from the already mentioned ones and summarized below:

I. The conservation of mass, energy and momentum equations solved are approximate. Geometric discontinuities are not considered and not all interactions between steam and liquid are accounted for.

II. Velocity profiles are not considered within a particular geometry. The use of cross section averaging at the geometry level is a source of uncertainty.

III. The use of empirical correlations to close the balance equations is another source of uncertainty. Validity ranges for these correlations may not be fully specified.

IV. Steady state conditions under which correlations are derived do not exist in NPP during transients.

V. The use of approximate material properties.

VI. The code user effect is another source of uncertainty. This can arise from the process of nodalization, interpreting transient results or interpreting information supplied in code user manuals. Differences in these areas with different users may give rise to uncertainties.

Although there are several sources of uncertainty as noted above, the focus of this study is input parameter uncertainty propagation through the code. The models implemented in the code are assumed to be good enough and the effect of uncertainty in selected input parameters is quantified by observing their effect on output parameters.

The above sources of uncertainties present a formidable challenge to the scientific community and active research is ongoing to address these issues in order to enhance code prediction accuracy [89]. This study is also expected to contribute to such efforts.

2.6.5 Modeling Uncertainties

Probability can be used to effectively model uncertainties. In this way, scalar values of inputs and outputs can be represented by random variables. The uncertainty modeling approach used in the software OpenCOSSAN is described in this section. Details of the software implementation are given in chapter 3, methodology.

Various distributions are used to specify a random variable, they include normal, log-normal and uniform. If experimental data is available, these maybe used to construct the set of random variables. A maximum likelihood method is then used to determine parameters that result in an optimal fit of the experimental data by a particular distribution. The maximum likelihood method is an efficient tool that obtains estimators of the distribution parameter having optimal statistical properties [66].

An uncorrelated multivariate distribution is obtained by transformation of the multiple correlated distribution. This is achieved in the standard normal space which is a multi-dimensional random variable space with zero mean, a unit standard deviation and Gaussian marginal probability density functions. This step is necessitated by the fact that pseudo-random number generators usually generate independent samples.

Stochastic processes such as Monte Carlo (MC) and random fields can be applied to model parameters which vary randomly and are functionally dependent in a multi-dimensional continuous space [67, 68]. If the stochastic process is Gaussian, then it is adequately defined by the mean function and the covariance function. The covariance function may be considered the mutual influence of the process at two different spatial-coordinates or time-instants [64]. The MC method is applied in the OpenCOSSAN software and used in this study to model uncertainties of input parameters used to simulate a transient by CATHENA.

2.6.6 Sensitivity Analysis

Sensitivity analysis is performed in order to estimate the effect of uncertain input parameters on an output parameter. The results from such analyses are useful in providing

information on areas where designs can be changed in order to improve performance. It identifies variables that affect model results the most [16, 24] and can be used for model calibration and validation.

Local sensitivity analysis, screening methods and global sensitivity analysis are the major types of sensitivity analysis used. The computationally intensive nature of global sensitivity analysis makes the local sensitivity analysis the most utilized method in practical applications [31]. In local sensitivity analysis, the response of a model is obtained by varying the inputs one-at-a time while holding the other inputs fixed. Global sensitivity analysis considers the entire range of variation of input parameters with the aim of accounting for the entire output uncertainty according to the different sources of uncertainties in the model inputs [16].

The first order derivative of an output with respect to an uncertain input parameter gives the most common sensitivity measure, $S_i^{(l)}$

$$S_i^{(l)}=\frac{\partial Y}{\partial X_i} \tag{2.8}$$

Where Y is the output and X_i is the uncertain input parameter. A more informative form of equation 2.8 is obtained by normalizing the derivatives by standard deviations of inputs and outputs as follows,

$$S_i^{(\sigma)}=\frac{\sigma_{X_i}\partial Y}{\sigma_Y \partial X_i}=\frac{\sigma_{X_i}}{\sigma_Y}S_i^{(l)} \tag{2.9}$$

A MC method is known to give accurate estimates of the gradient of a function [34]. The gradient in this method is obtained by random sampling in the neighborhood of an arbitrary reference point. Since the MC method requires a large sample size (usually N>1000) to

obtain accurate estimates of sensitivity indices, the computational time involved for complex models is huge. This makes it necessary for model reduction methods to be implemented prior to performing the stochastic analysis [64].

CHAPTER 3: METHODOLOGY

3.1 Review

In chapter 3, the thesis framework is presented and the stochastic uncertainty quantification methodology used in the study is introduced and explained.

3.2 Methodology Framework

In this study, a methodology is proposed for uncertainty quantification and sensitivity analysis for safety verification in NPPs and other applications. The proposed method seeks to achieve more accurate transient/fault propagation analysis by estimating the uncertainties associated with process variable prediction. To this end, normal and transient simulations by a best estimate thermalhydraulic code, CATHENA were utilized. The various steps that would achieve the objectives of the study are represented in figure 3.1 and the various components are described in the subsequent sections. The proposed framework can be extended to other systems and for any number of input and output parameters.

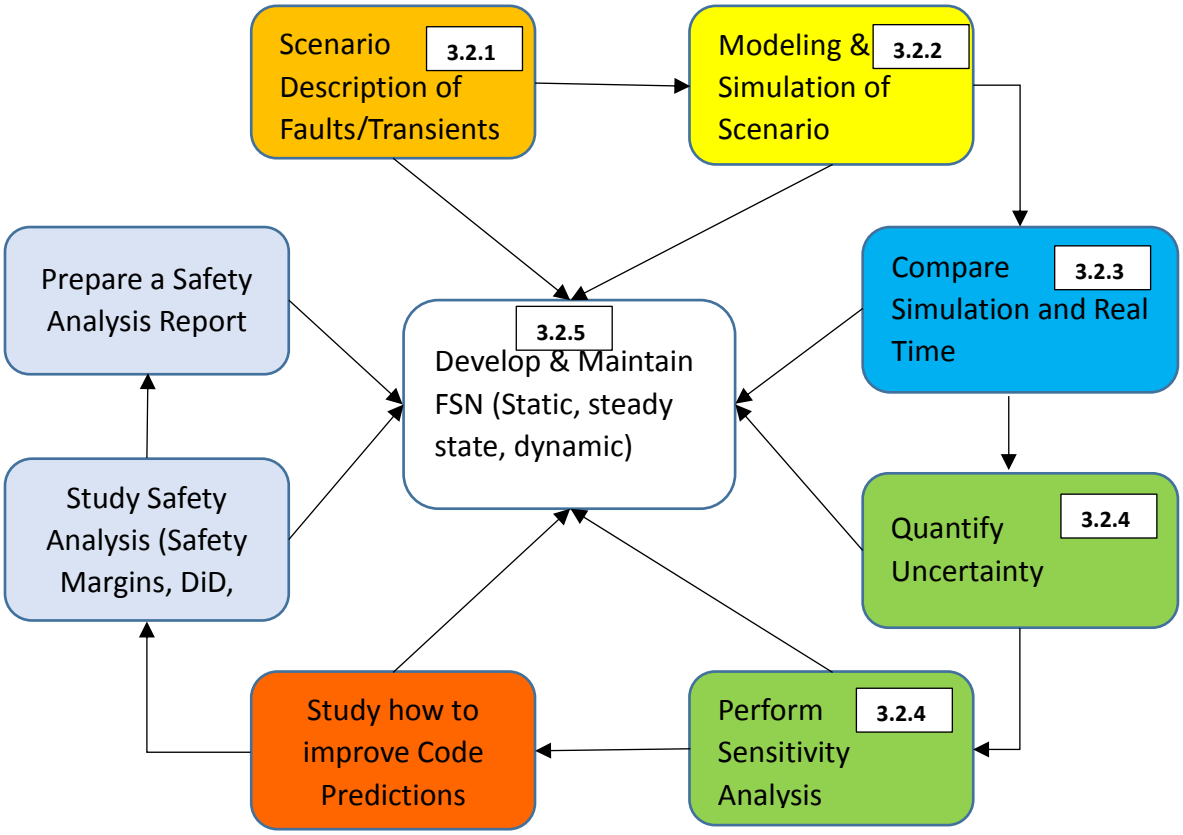

Figure 3.1 Proposed Methodology Framework for performing Uncertainty Quantification for safety verification applications

In figure 3.1, the framework begins with scenario description of faults. This entails a detailed definition and description of a fault or transient. Two standard transient scenarios which are related to the loss of coolant in the primary heat transport system of a CANDU reactor were used in this study. The research then proceeded with the modelling and simulation of the fault scenarios from the previous step. Both transients were modelled by the Canadian Nuclear Laboratory and the best estimate thermal hydraulic code, CATHENA was utilized to simulate these transients. A comparison between the simulated results and experimental data was then made in order to quantify the uncertainty associated with selected input parameters. In the next step, a sensitivity analysis was performed to

determine the contribution of various input parameters to the global uncertainty observed in the output parameters. All the preceding steps mentioned were linked with the development and maintenance of the fault semantic network (FSN). This was achieved by using the uncertainty quantification results to update the fuzzy rule base of the FSN for safety verification applications. Other blocks included in the proposed framework but were not studied as part of this thesis are; improving code predictions and preparing a safety analysis report. These would be considered for future studies. More information on the blocks mentioned above have been provided in the following sections.

3.2.1 Scenario Description of Faults

Various fault scenarios or transients may occur during the lifetime of NPPs. These scenarios are usually simulated by dedicated codes in order to estimate plant response should they occur. One important fault associated with the primary heat transport system is the loss of coolant accident (LOCA). The thermal hydraulic code, CATHENA was developed mainly to simulate LOCA scenarios in CANDU. In this study, two fault scenarios were simulated using CATHENA. Transients related to the steam generator and the turbine systems were also used to demonstrate the fault semantic network methodology. The scenarios considered in this study were selected based on their likelihood of occurrence and their importance to performing safety analysis of any NPP.

3.2.2 Modelling and Simulation of Scenario

Two transient scenarios were simulated in this study: a small break LOCA in the RD-14 test facility and the Edward's pipe blowdown problem. Both scenarios were modelled by

the CNL and the input files were modified and adapted to suit the objectives of this study. Additionally, two case studies were used to demonstrate the proposed FSN methodology: faults associated with the steam generator in a nuclear power plant and a turbine trip scenario. These faults were created and simulated using the IAEA CANDU 9 simulator. Details of the above simulation models and results are presented in subsequent chapters of the thesis.

3.2.3 Compare Simulation and Real time

Results obtained from executing experiments for certain fault scenarios exist. These results can be considered the real time data that is compared with simulation results from codes. Uncertainty associated with code simulations is possible without the experimental data. In this study, experimental results of the RD-14 test obtained from the CNL were utilized in performing uncertainty quantification.

3.2.4 Stochastic Uncertainty and Sensitivity Analysis Framework

The uncertainty and sensitivity analysis methodology used in this study is based on the framework presented in figure 3.2.

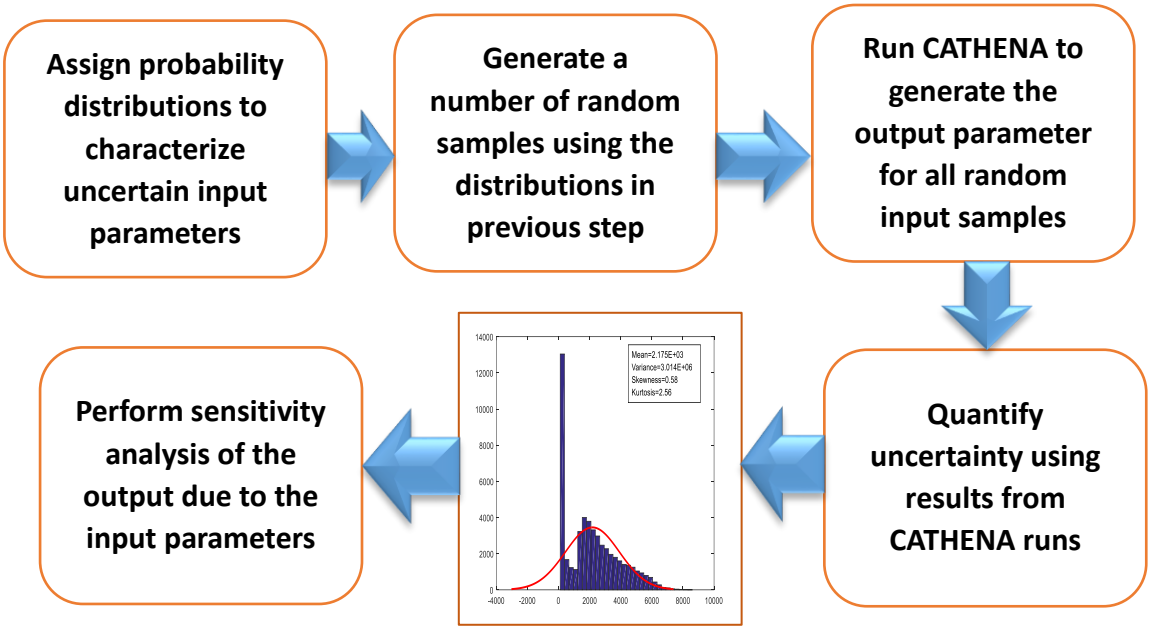

Figure 3.2 Uncertainty and Sensitivity Analysis Framework

The stochastic uncertainty quantification methodology utilized in this study is shown in figure 3.2. Generally, uncertainties may either be model-related or input parameter related. In this study, the models implemented in the best estimate code were assumed good enough and the code was treated as a black box. The effect of propagating uncertainties in input parameters through the code was the main goal in the above framework.

Assign probability distributions to characterize uncertain input parameters: this step is one of the most important steps in the framework. Studies had been conducted in this area due to its fundamental importance. Examples of such studies reported in literature include, Hora and Iman [85]; Bonano and Apostolakis [86]. Practical experience over the years has shown that specifying quantile (minimum, maximum) values would yield better outcomes compared to specifying particular distributions to characterize uncertain input parameters. The distributions are assigned usually based on expert review and knowledge.

Experts may find it easier to justify specific quantile values than to justify specific distributions. Normal, uniform or lognormal are the types of distributions that are used. These distributions are available for use in the OpenCOSSAN software. A probability space is defined after assigning distributions to input parameters of interest. This space comprises three components; a sample space, a restricted subspace and a probability measure. The probability space can be represented as (S, E, p). Where S is the sample space, E is the restricted subspace of S and p is the probability measure.

Generate a number of random samples using the distributions in previous step: This step consists of sampling in the probability space. Random sampling involves selecting observations within the sample size according to the probability distribution defined by (S, E, p). Each sample point is independently selected and there is no certainty of selecting sample points from any sub region of the sample space. Importance sampling procedure was developed to avoid inefficient sampling due to inadequate coverage of the sample space. This procedure ensures that parameters with low probability of occurrence but with significant effect on the response parameter are captured in the analysis. The Latin Hypercube sampling procedure further extends the concept of covering the parameter range [92]. The procedure essentially involves randomly pairing parameter values generated from each parameter space to form a Latin Hypercube sample. This process is however suited for only uncorrelated parameters. Inaccurate results will be obtained if it is applied to correlated parameters. Random sampling is a preferred statistical technique due to its easy implementation and the fact that it yields unbiased estimates of the means, variances and distribution functions. Large sample sizes are however required for implementing this method. The computational time needed to generate large samples for complex systems

and processes makes the stratified random sampling a desirable option. A priori knowledge is however necessary before this type of sampling can be implemented. Fault trees and event trees used in performing safety assessment in NPPs may be useful as a priori knowledge in defining stratified sampling procedures. On the whole, Latin Hypercube sampling yields a compromise importance sampling in the absence of a priori knowledge of relationships between input and output parameters [92].

The Monte Carlo method, a random sampling technique which is used in OpenCOSSAN was utilized for this study.

Run CATHENA to generate the output parameter for all random input samples: This step involves model recalculations for all generated input samples in order to obtain the response parameter. This step constitutes the most computationally expensive part of the process. The best estimate thermal hydraulic code, CATHENA was used to perform model recalculations. A convergence test was performed to ascertain the adequacy of the number of random input samples simulated for the uncertainty and sensitivity analysis.

Quantify uncertainty using results from CATHENA runs: the means and variances calculated from the simulation results are displayed as part of uncertainty quantification. The mean and variance may be less useful in deducing information on the response parameter of interest. This is due to the fact that useful information is lost during the process of calculating the mean and variance [92]. Distribution functions such as density functions provide more complete information on the sample being analyzed. In this study, the first four moments (mean, variance, skewness and kurtosis) of the response parameter were computed and the probability distributions of the response parameters were estimated.

Perform sensitivity analysis of the output due to the input parameters: This step comprises performing sensitivity analysis to assess the effects of uncertainty in the input parameters on the output parameter. Methods used include, scatter plots, regression analysis, rank transformation and correlation analysis. Regression analysis is performed on a linear model between the predicted output parameter ($Output_{predicted}$) and the input parameters (α_i) as a formal method for performing sensitivity analysis. This can be written as, $Output_{predicted} = b_0 + \sum_{i=1}^{I} b_i \alpha_i$ (3.1)

The actual input parameters α_{ki} can be used to express the calculated output values in the following; $Output_{calculated} = b_0 + \sum_{i=1}^{I} b_i \alpha_{ki} + \varepsilon_{calculated} \quad (k = 1, \dots, M)$ (3.2)

Where $\varepsilon = Output_{calculated} - Output_{predicted}$ is the error between the calculated and predicted value of the output parameter and M is the number of samples simulated. The predicted output values can be obtained from experiments. The unknown regression coefficients can be determined by minimization of the sums of squared errors,

$$\sum_{calculated} (Output_{calculated} - Output_{predicted})^2 \equiv \sum_{calculated} \varepsilon^2$$

The regression coefficients and other indicators computed can be used to estimate the effect of individual input parameters on the global uncertainty observed in the output parameter [80]. In this study, the Pearson correlation coefficient was used as a sensitivity measure to determine the linear relationship between the input parameters and the output parameters [92]. Details of this procedure are presented in chapter 7.

3.2.4.1 Uncertainty Quantification using OpenCOSSAN

OpenCOSSAN is a general purpose software developed by the Institute for Risk and Uncertainty at the University of Liverpool which can be applied to solve various engineering problems including uncertainty quantification, sensitivity analysis, reliability analysis and optimization. The software implements state of the art algorithms and methods in user friendly environments to produce reliable analytical results.

The main features of OpenCOSSAN are user interfaces, software core components and interaction with 3rd party software. User interfaces comprise a graphical user interface (GUI) and a high-level programming language which is Matlab based. These Matlab scripts provide a flexible programming environment allowing users to modify solution sequences, exploration of data, and definition of algorithms and creating custom tools in order to solve specialized problems. Deterministic solvers such as CATHENA can be connected to OpenCOSSAN for stochastic analysis. Both intrusive and non-intrusive methods are used to enable such connections with deterministic solvers. Non-intrusive methods treat the deterministic solvers as black boxes where no modification is made to the solver [52]. In this method, interaction between third party solvers and OpenCOSSAN is achieved using input/output files usually in ASCII format for generating input configurations for the numerical analysis. This is the method that has been adopted in this study to link CATHENA to OpenCOSSAN in order to perform uncertainty quantification of selected input parameters and their estimated effect on output parameters in simulating a transient. Post-processor tools are used to extract output parameters from the deterministic solver. The interaction with the 3rd party solver involving input file manipulation and extraction of outputs of interest is completely automated in the OpenCOSSAN environment.

An additional feature of the OpenCOSSAN software is the possibility to utilize high performance computing in problem solving. Since the stochastic analysis requires several computations of the deterministic models and these models are usually complicated, the use of distributed computer resources is desired. Running various components of the software on different platforms such as clusters comprising both Windows and Linux operating systems would significantly reduce computational times associated with solution sequences. The OpenCOSSAN software structure is summarized in figure 3.3 as adapted from [64].

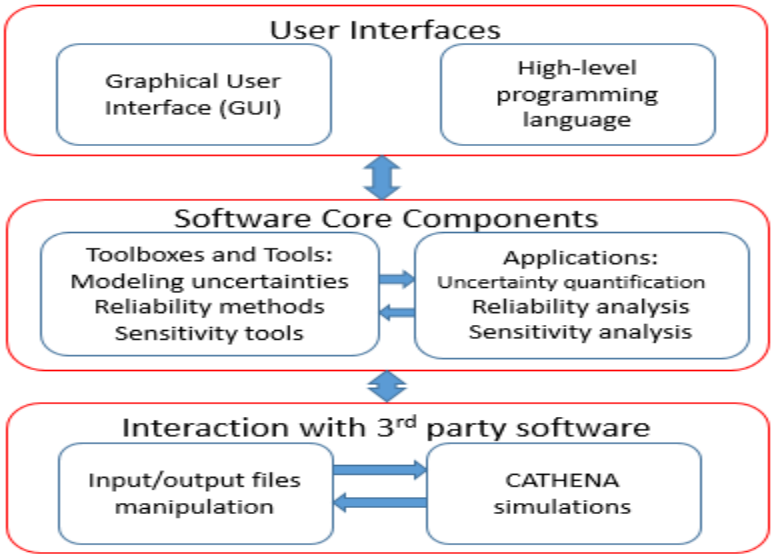

Figure 3.3 OpenCOSSAN software structure

As part of this study, a MATLAB script was written to link OpenCOSSAN with CATHENA. The script constituted the connector section of OpenCOSSAN which enabled the generation of random CATHENA input files based on the Monte Carlo method. The generated input files were simulated and the results were used to quantify input parameter uncertainty as well as to perform sensitivity analysis.

3.2.5 Develop and Maintain FSN

The dynamic tuning of the Fault Semantic Network (FSN) enables the representation of the dynamic nature of fault propagation in a plant. This process can be applied with the inclusion of protection layers and failure probabilities of these layers for risk estimation and safety verification. The development of FSN commences with the static, then the steady state and the dynamic. The static FSN comprises equipment details, process variables, possible faults and different plant states. The steady state involves the normal operation of the plant while the dynamic FSN deals with the dynamic nature of fault propagation usually simulated by CATHENA in this study. A more detailed description of the dynamic FSN is given in section 3.2.4. In this study, results obtained from CATHENA simulations were used to tune the dynamic FSN for the selected case.

CHAPTER 4: CASE STUDIES

4.1 Review

In this chapter, selected case studies considered for application of the proposed FSN methodology are described. Fault propagation scenarios related to these case studies are defined and described. The steam generator is the primary heat sink of the reactor which removes the heat generated in the core. Faults associated with the steam generator are therefore important to be studied as they may pose significant threats to reactor safety. A study of a turbine trip scenario is also essential as its occurrence is credible and may have significant safety and economic impacts on operating plants. These scenarios were created as part of the simulator design. The various faults were therefore inserted into the simulation and results were analyzed for the purpose of the study.

4.2 Case Study 1: Steam Generator

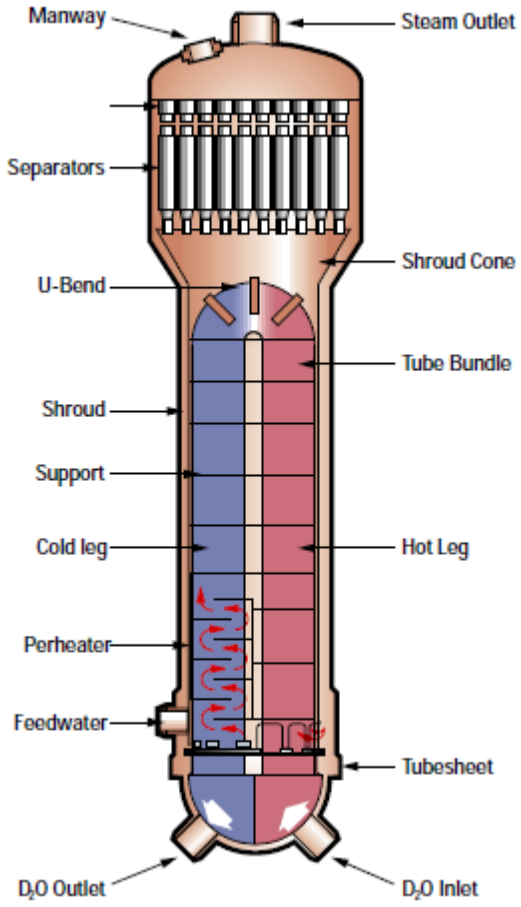

Figure 4.1 A CANDU steam generator [13]

The Steam Generator (SG) is an equipment system in which heat from the primary heat transport system heavy water is transferred to the secondary side light water. CANDU is made up of four steam generators and most of the steam from the SG flows to the Turbine during normal operation. The Turbine converts the latent heat of the steam to rotational energy which is converted by the generator into electricity. Steam pressure in the SGs is controlled by regulating the flow through the Governor valves (GVs) and Atmospheric and Condenser discharge valves are opened if the pressure rides above the set point. Emergency

stop valves (ESV) and GVs are fully opened under normal operating conditions, however the ESV can be closed to prevent steam flow to the Turbine to avoid damage to the Turbine during certain malfunctions. Since the SG is the major heat sink for the reactor primary heat transport system, the process variables associated with the SG have effects on other process variables such as reactor power, reactivity and the neutron flux which are neutronic parameters.

The SG level is controlled within required limits to ensure adequate volume of water in the SG for the effective heat removal from the heat transport system. Steam flow, feed water flow and SG level measurements comprise the control algorithm that is used to control the SG level. Steam flow is compared with feed water flow and the difference gives the flow error. A positive error signal will increase the feed water control valve opening while a negative error signal will decrease the feed water control valve opening thereby either increasing or decreasing the SG level.

4.2.1 Fault propagation Analysis of Feedwater Liquid Control Valve (FW LCV101) fails closed

LCV101 is the feed water control valve that regulates flow from the condenser to SG1. After the above malfunction was inserted using the CANDU simulator, the effect on other process variables was monitored and this is described as follows to demonstrate the interconnection between process variables of various systems in the nuclear power plant.

4.2.2 Effect on Reactor Neutron Power

The reactor neutron power increased slightly at the initial stage of the malfunction. This is because the malfunction led to a decrease in the SG1 level, and this meant the heat produced in the reactor core was not being effectively removed and thus resulting in the initial power increase. The neutron power however decreased after about 250 seconds and this is due to the response of the reactor regulating system (RRS) to the initial reactor power increase. The RRS inserted negative reactivity into the system in order to achieve reactor stepback and this led to the subsequent power decrease.

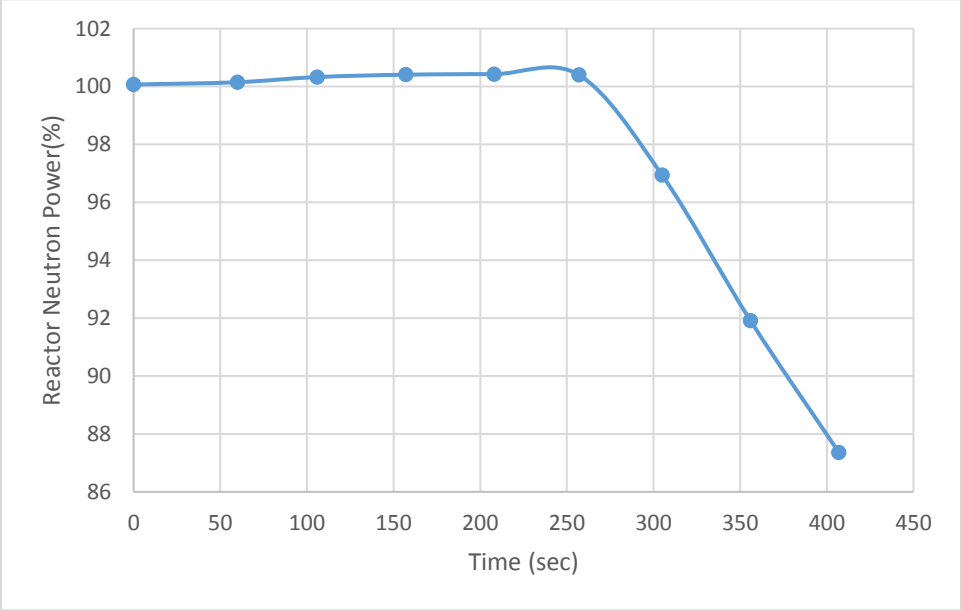

Figure 4.2 Reactor neutron Power as a function of time during "FW LCV101 fails closed" transient

4.2.3 Effect on SG1 Level

As can be seen from figure 4.3, the SG1 level decreased following the insertion of the malfunction. As expected, the SG1 level decreased because of the lack of feed water flow as a result of the closure of LCV101.

4.2.4 Effect on SG1 Pressure

The decrease in SG1 level led to a corresponding increase in SG1 pressure however, SG1 pressure decreased subsequently after the decrease of the reactor neutron power.

4.2.5 Effect on Average Zone Level

The CANDU consists of 14 liquid zone compartments that contain light water for the purpose of reactivity control. Increasing the water in the zones implies the addition of negative reactivity to the system as more neutrons are absorbed by the light water. Following the reactor power increase after the insertion of the malfunction, the average zone level increased in order to decrease the reactor power.

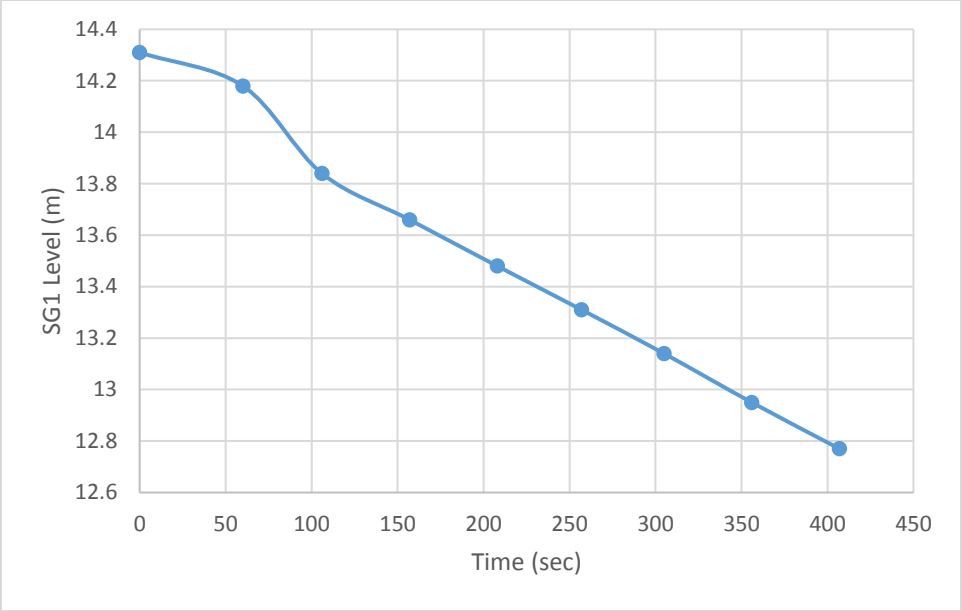

Figure 4.3 SG1 level as a function of time during “FW LCV101 fails closed” transient

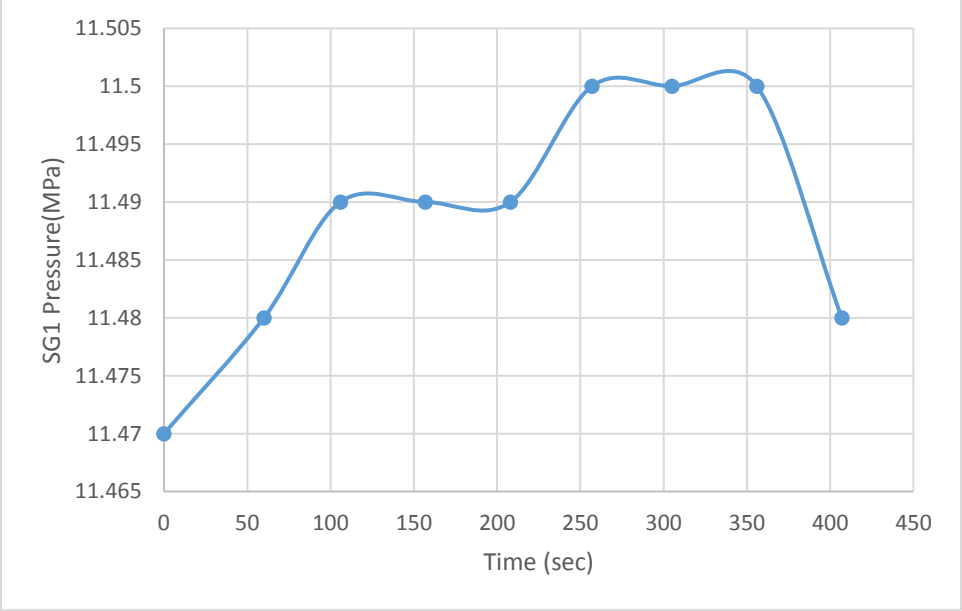

Figure 4.4 SG1 pressure as a function of time during “FW LCV101 fails closed” transient

4.2.6 Effect on Pressurizer Level

The pressurizer controls the pressure and inventory of the heavy water in the heat transport system. The pressurizer level is a function of reactor power. An increase in reactor power results in an increase in the pressurizer level in order to accommodate the swell in the coolant due to temperature changes. In similar manner, a decrease in reactor power results in a decrease in pressurizer level in order to accommodate the shrink in the coolant as a consequence of temperature drop. As can be seen in figure 4.6, the pressurizer level increases because of the initial power increase and decreases subsequently following the decrease of the reactor power.

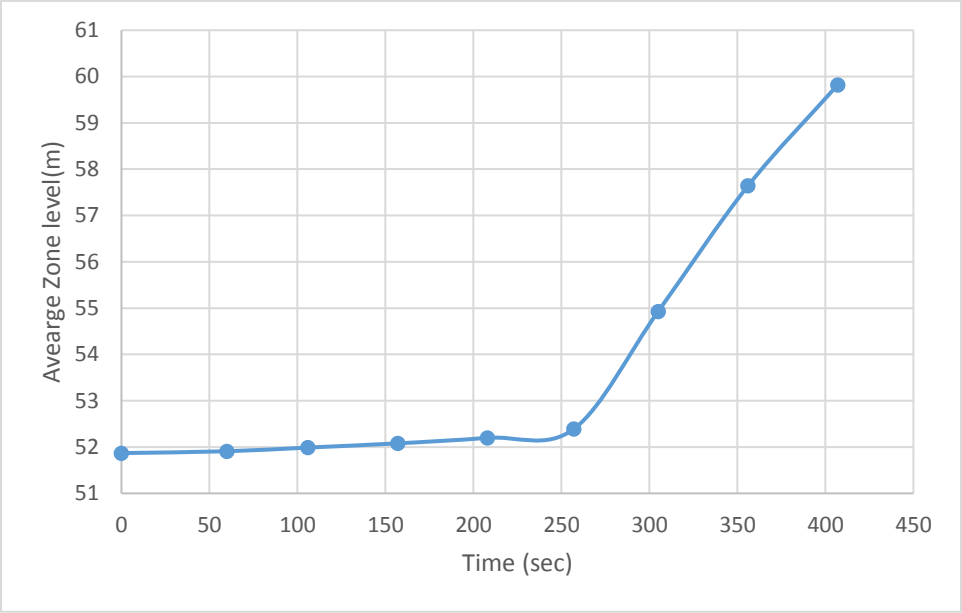

Figure 4.5 Average zone level as a function of time during “FW LCV101 fails closed” transient

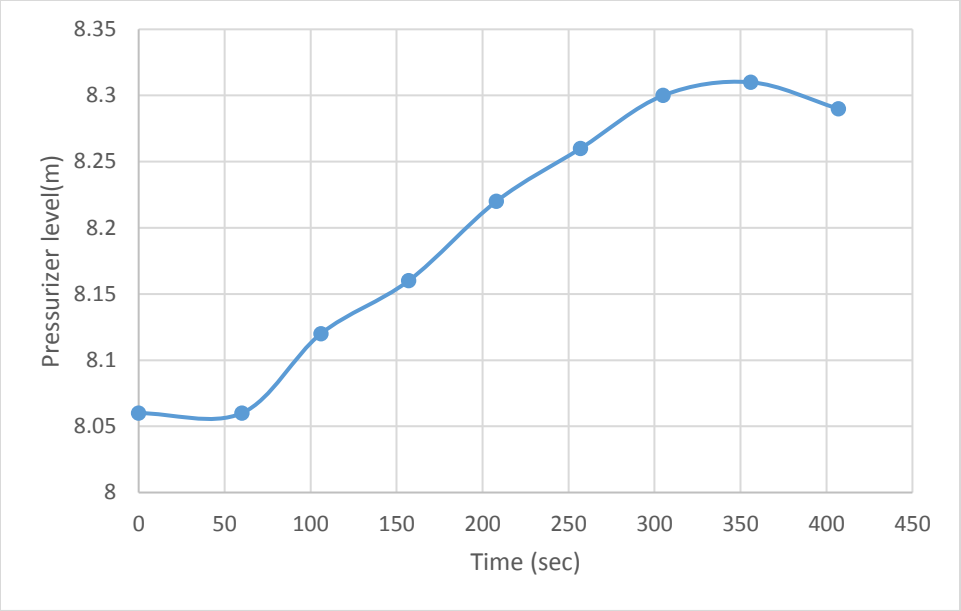

Figure 4.6 Pressurizer level as a function of time during "FW LCV101 fails closed" transient

The relationship between these process variables are explored using FSN in order to understand fault propagation and to take appropriate remedial actions following the occurrence of a fault. In table 4.4, some NPP systems and associated faults as well as process variables are listed. From figure 4.7, the FSN model of the fault propagation is seen. This illustrates the interconnection between process variables associated with various systems in the NPP where ΔT represents the time delay between states. As an example from figure 4.7, failure of the valve which is a mechanical component (FM-M1) led to an increase in reactor neutron power (FM-N1) which is a neutronic parameter. This resulted in steam generator 1 level increase (FM-T3) which is a thermal parameter. The relationships between the process variables helps in the understanding of fault propagation in terms of time delay between reaching different plant states as well as the strengths between the various connections.

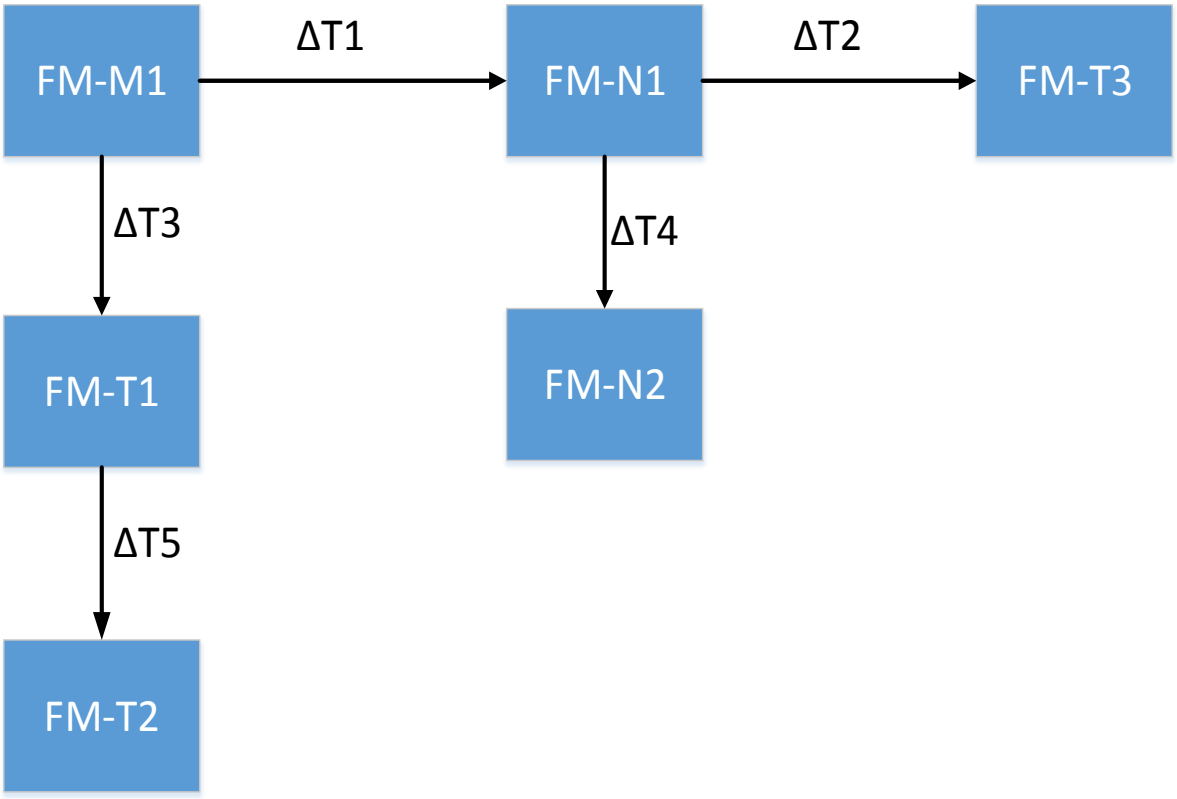

Figure 4.7 FSN model of Case study 1: Steam Generator

Table 4.1 gives the definitions and descriptions of the codes used in the FSN model of the case study. From figure 4.7, it is clear that a fault in a mechanical component affects both neutronic and thermal hydraulic components with the respective time delays shown in figure 4.7. This makes it important for establishing the interactions between process variables of various components to understand fault propagation.

Table 4.1. Definition of codes

Code	Definition	Description
FM-M	Failure mode in mechanical component	FW LCV101 fails closed
FM-M1		
FM-N	Failure mode in neutronic system	
FM-N1		Neutron power increase
FM-N2		Average zone level increase
FM-T	Failure mode in thermal hydraulic component	
FM-T1		SG1 level decrease
FM-T2		SG1 pressure increase
FM-T3		Pressurizer level increase
FM-S	Failure mode in structural component	
FM-E	Failure mode in electrical component	
FM-R	Failure mode in radiation component	
FSNN	Fault Semantic Network Node	

The construction of FSN is commenced by the development of a database comprising; hazard scenarios, equipment, failure modes and process variables. The hazard scenarios are defined and linked with the propagation of each failure mode. The consequences of failures are also defined as well as the associated risks. Table 4.2 and 4.3 show examples of the FSN knowledge base associated with the current case study.

Table 4.2. FSN knowledge base example 1

Equipment	Equipment ID	Process Variables	
		Input	Outputs
Steam Generator	1	20%-100% nominal thermal power in CANDU	- SG level - FW flow rate - Steam flow - Steam pressure - LCV101opening - LCV102opening - LCV102opening

Table 4.3. FSN knowledge base example 2

Failure Mode	Failure ID	Description	Consequences
LCV fails open	F1	Liquid control valve fails in open position.	- Low SG1 level. - Low reactor neutron power. - High pressurizer level. - Turbine trip - Reactor trip.
LCV fails closed	F2	Liquid control valve fails in the closed position.	
SG1 FW FT irrational	F3	Steam Generator 1 feedwater flow transmitter irrational	

4.3 Case Study II: Turbine Trip in a NPP

The Turbine converts the heat energy of the steam from the Steam Generator (SG) to rotational energy. In a CANDU, the Turbine is made up of a high pressure stage followed by three parallel low pressure stages. The steam, Turbine, Generator and Feedwater system is very important to CANDU operation since it serves as the normal heat sink for the energy produced by the reactor. The Generator which is connected to the Turbine converts the rotational energy of the Turbine to produce electricity. The CANDU Turbine, Generator system is shown in figure 4.8.

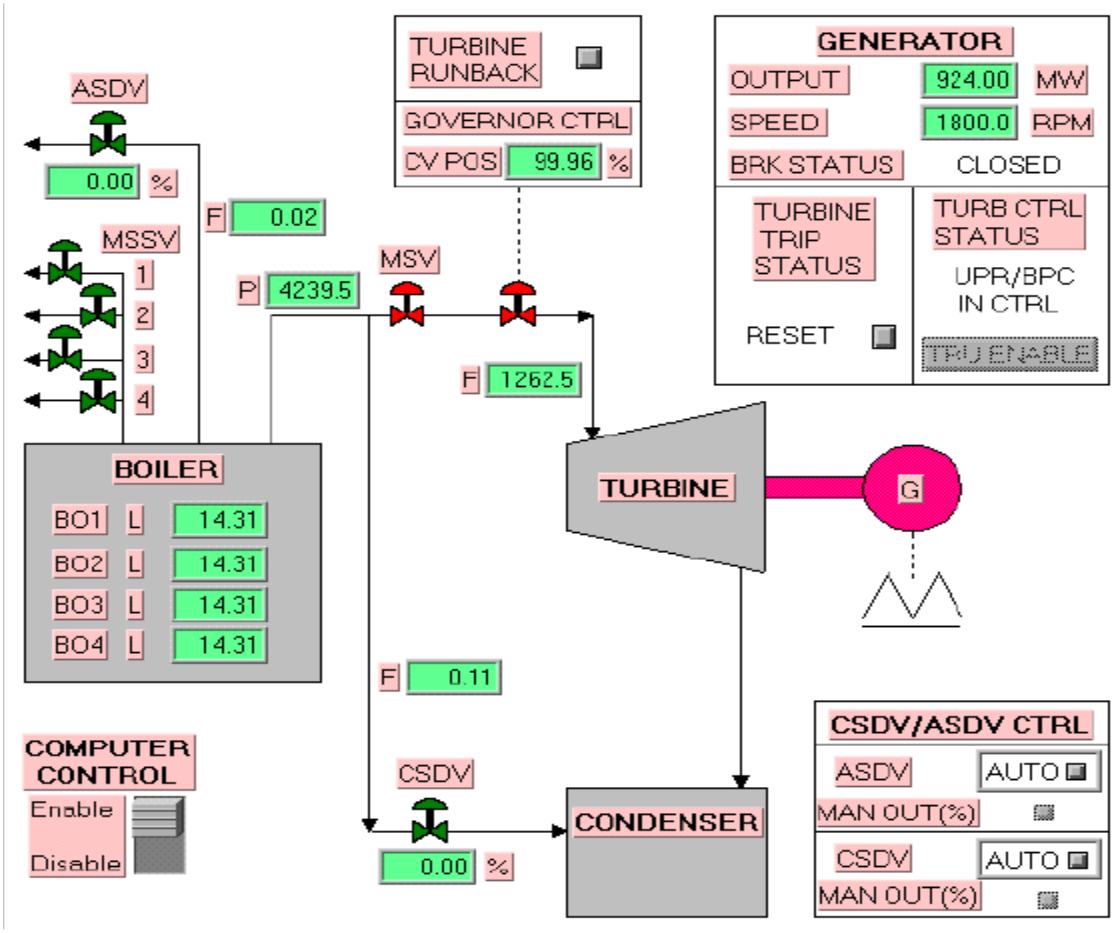

Figure 4. 8 CANDU Turbine, Generator system [84]

4.3.1 Fault Scenario Description

A turbine trip event is classified as an American Nuclear Society (ANS) condition II and may result in a reactor trip, at worst. A turbine trip can be initiated by different initiating events including, generator trip, low condenser vacuum, low bearing oil, turbine thrust bearing failure, turbine overspeed, steam generator HI-HI water level, Electro-Hydraulic (E-H) DC power failure or by a manual trip. Following a Turbine trip, steam flow to the Turbine is abruptly stopped and steam dump is initiated (Krsko SAR, 2012). The loss of steam flow leads to an increase in the steam generator temperature and pressure. In the event of a Turbine trip, steam discharge valves (Condenser Steam Discharge Valves (CSDVs) and Atmospheric Steam Discharge Valves (ASDVs)) are open to bypass steam to the Condenser and to the Atmosphere in order to prevent a 'poison-out'. The Main Steam Safety Valve (MSSV) can however be opened if a failure of CSDV and ASDV should occur. In this study, the following process variables are used; SG flow (kg/s), SG pressure (MPa), SG level (m), Reactor Thermal Power (%), Reactor Outlet Header (ROH) pressure (MPa), Reactor Inlet Header (RIH) temperature (^{0}C) and the Reactor Regulating System (RRS) reactivity insertion (mk). And the components of the CANDU involved in this case study include, SG, Steam Discharge Valves (ESVs, GVs, CSDVs, ASDVs, MSSVs), RIH, ROH and pressurizer. Table 4.4 shows the list of equipment, process variables, and faults.

Table 4.4. Equipment, Process variables and Faults

Equipment	Equipment ID	Process Variable	Process Variable ID	Fault	Fault ID
Turbine	EQ1	Core Thermal Power	PV1	Generator trip	F1
Generator	EQ2	ROH Pressure	PV2	Low Condenser vacuum	F2
Steam Generator	EQ3	SG Pressure	PV3	SG HI HI	F3
CSDV	EQ4	SG Level	PV4	Turbine Over speed	F4
ASDV	EQ5	SG flow	PV5	SG Temp. High	F5
GV	EQ6	Pressurizer Level	PV6	Reactor Power Low	F6
MSSV	EQ7			SG flow Low	F7
RIH	EQ8			Pressurizer level Low	F8
ROH	EQ9				

4.3.2 Fault Propagation Scenario

We consider the fault propagation of a Turbine trip for our analysis and this scenario is summarized in figure 4.9. A Turbine trip results in temperature and pressure increase in the SG shell as well as an initial increase in coolant temperature and pressure. The Emergency stop Valves (ESVs) and Governor Valves (GVs) are closed immediately after a Turbine trip. This is to stop steam flow to the Turbine, the CSDVs and ASDVs are then open to bypass steam to the condenser and the atmosphere respectively. It is expected that

the Steam Discharge Valves (SDVs) work properly to prevent a reactor trip or the opening of MSSVs.

A reactor trip is undesirable because it leads to loss of electrical power to the grid and could be a very huge financial loss. Also a reactor trip may lead to loss of offsite power and both of these situations are extremely undesirable.

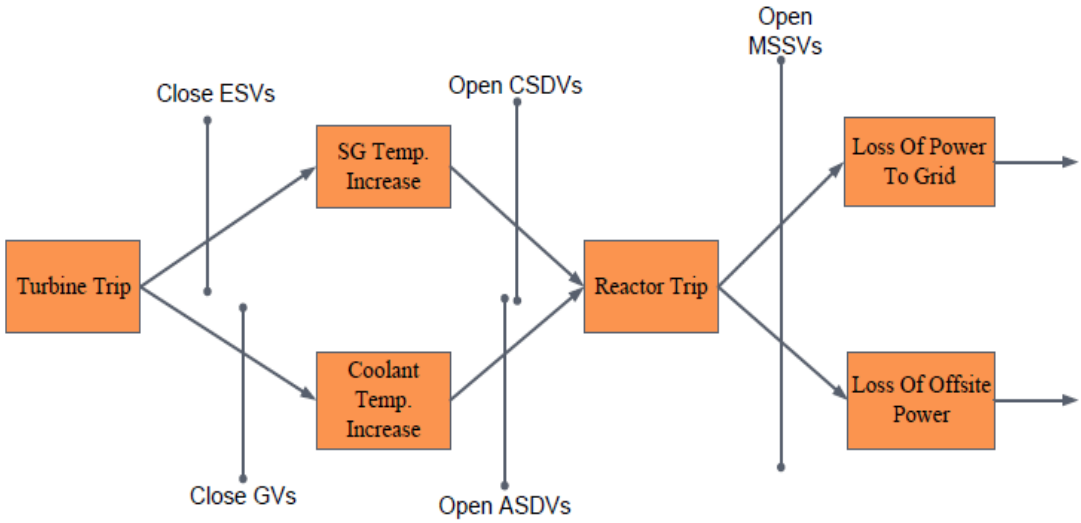

Figure 4.9 Fault propagation scenario of case study 2: Turbine trip

In figure 4.9, the vertical lines represent the independent protection layers that have been designed to prevent the propagation of the fault from one stage to the next while the boxes represent various plant states. In the event that these protection layers do not work properly as expected, the figure shows the likely propagation of the fault to the next stage.

4.3.3 Updating FSN

Fault propagation scenarios are defined based on historical data initially and later updated using real time data. Figure 4.10 shows the FSN model where each node represents equipment, component, and failure mode as well as associated process variables.

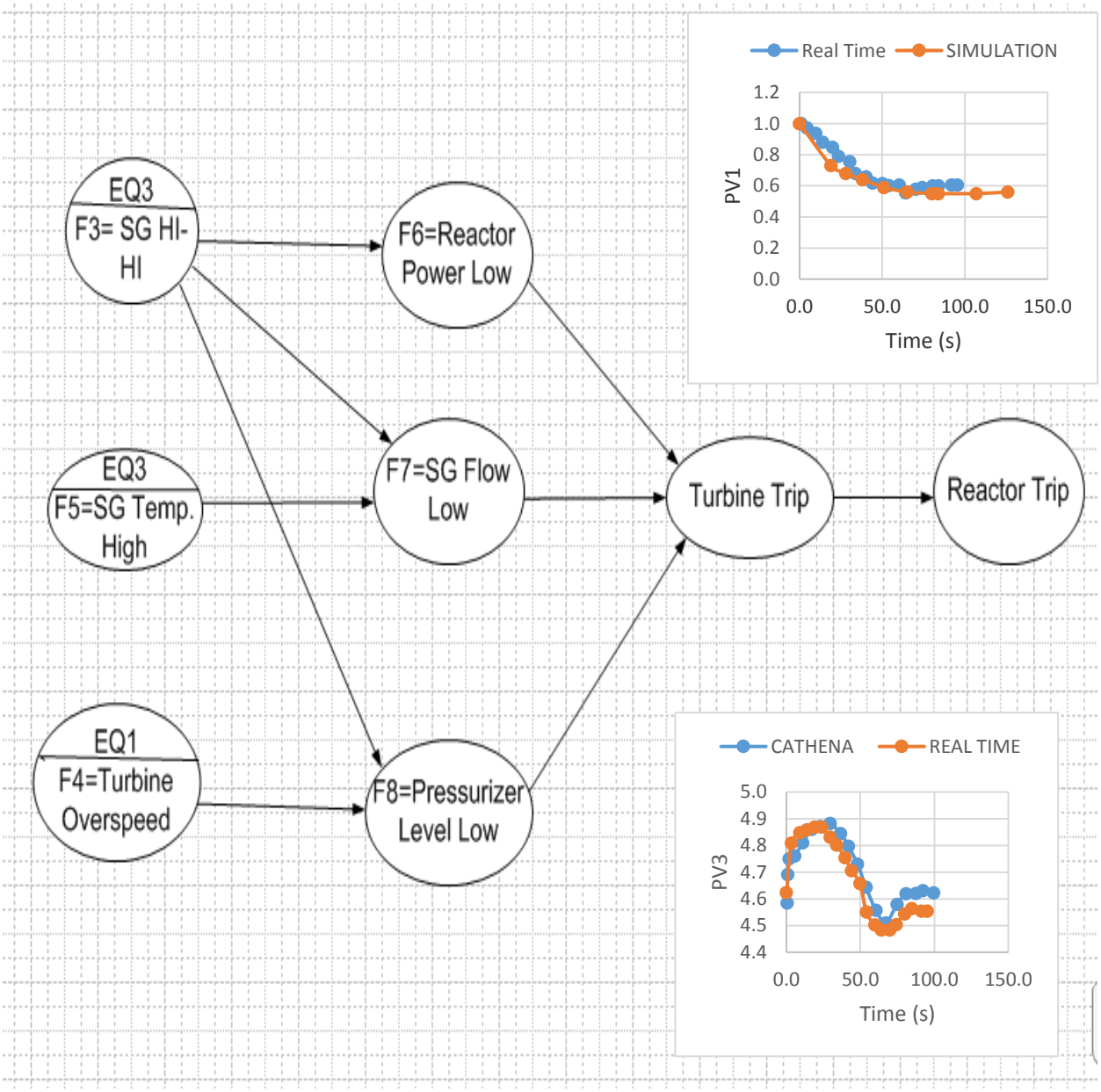

Figure 4.10 FSN model of Case Study II

CHAPTER 5: PROPOSED SIMULATION MODELS

5.1 Review

In this chapter, the proposed simulation models are presented and described. The Fault Semantic Network methodology proposed to be applied for fault propagation analysis and safety verification is explained in detail. The best estimate code, CATHENA used for simulating transients is also described with a sample problem. The chapter concludes with a presentation of the stochastic uncertainty quantification model applied to the Edward's pipe blowdown problem.

5.2 Fault Semantic Network

In view of the challenges mentioned in section 1.2, this study proposes the use of Fault Semantic Network (FSN) to perform fault propagation analysis with reduced error between simulation and real time. This approach will involve the establishment of relationships between process variables associated with different components of the NPP following the occurrence of a fault. Examples of systems and components in the NPP with some associated faults and process variables are illustrated in table 5.1. FSN can be utilized as a fault detection, prediction as well as propagation analysis tool making its use advantageous compared with other methods discussed in chapter 2.

Table 5.1. NPP systems, faults and process variables

System	Components	Associated faults	Associated process variables
Neutronic	Fuel	• Fuel defect • Fuel failure • High neutron flux • High neutron power	• Reactivity • Neutron flux • Reactor power • Average zone level
Thermal hydraulic	• Coolant • Pressurizer • Steam generator • Bleed condenser	• Loss of coolant accident (LOCA) • High pressure • High temperature • High coolant inventory • Low coolant inventory	• Pressurizer pressure • Pressurizer level • SG pressure • SG level • Feed water flow • Steam flow
Electrical	• Power lines • Cables • Service transformers	• High voltage • Low voltage • Loss of AC power	• Transformer load • Voltage • Current
Mechanical	• Pumps • Valves • Pipes • Vessels	• Leakage • Corrosion • Valve failure	• Valve opening • Flow rate
Structural	• Calandria • Pressure tubes • Containment	• Pressure tube sag • Pellet-cladding interaction	• Containment building pressure
Radiation	• Detectors • Shielding materials • Dosimeters	• High dose • Low dose • Radioactive components	• Dose • Activity

	in secondary side

Semantic Networks are structures used to depict the relationship between various concepts. These networks consist primarily of nodes and arcs. The nodes represent concepts while the arcs represent the relationship between the nodes. An example of a semantic network is shown in figure 5.1.

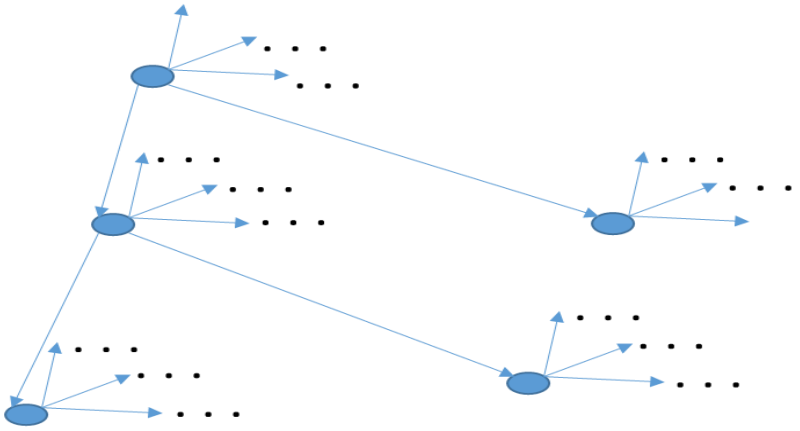

Figure 5. 1 Semantic Network Structure

Semantic networks are applied in different fields to model systems by linking various concepts based on the relationship that exist between them. Connections between nodes is achieved by means of a reasoning mechanism. FSN is an application of Semantic Networks to represent various faults, their causes as well as consequences in a system. The nodes in FSN represent various faults/causes/process variables and the link between the nodes represent the dependencies between them. Directed arcs are used to indicate the connections between the nodes. For instance, two nodes randomly selected are linked by a directed arc which shows how a plant state may lead to another state during the occurrence

of a particular fault. The strength of connections between nodes depend on the type of interaction that exist between them.

In applying FSN to a complex system such as a NPP, certain steps need to be followed. These steps are illustrated by describing a faulty condition in a Steam Generator. A decrease in steam generator level as monitored on a plant control console maybe caused by various conditions. Some of these causes may include decrease feed water flow, irrational flow sensor or a faulty control valve. FSN is used in this study to construct fault propagation scenarios in order to enhance the performance of the Fault diagnostic systems and to achieve real time safety verification of NPPs. FSN is constructed based on ontology structure of fault models based on process object oriented methodology (POOM) in which failure mode (FM) is described using symptoms, anablers, variables, causes and consequences. Rules are associated with each transition of the causation model in FSN. For example, failures related to loss of feedwater might be associated with rules such as

Table 5.2. Rules associated with feedwater flow

IF	(Structure= steam Generators) And (PV= SG Level) And (Dev= Low feedwater flow)
THEN	(FM= Loss of feedwater)

5.2.1 Process Variable Representation by Nodes

Nodes in FSN represent various process variables and plant states. It is important to identify which variable each node represents and what initial values must be assigned to each node as well as the state of each node. In a dynamic system, the values of nodes change however, at any time nodes must be assigned one value. Nodes are either classified as Boolean, ordered values or integral values. Boolean nodes take binary values such as true (T) or false

(F). Ordered values are qualitative description of the node such as high, low or medium. Integral values are quantitative values assigned to nodes.

5.2.2 FSN Structure

The FSN represent both qualitative and quantitative relationship between process variables. This structure is based on POOM. POOM enables the construction of a process model in either static, dynamic or functional states. In the static FSN, faults are related with structures such as steam generator, feed valve, bleed valve or control valve. In the dynamic FSN, faults are related with the dynamic behaviour of a system such as less flow, more flow and power surge. In the functional FSN, faults are related with the operation of a system such as start-up, normal operation and shutdown.

5.2.3 Node Connections

The relationship between nodes in FSN which is a representation of the interactions between process variables and various plant states can be done using different methods such as probabilistic, fuzzy logic and mathematical models.

For the probabilistic method, a probability value is assigned to each possible combination of a node to other neighbouring nodes as either parent or child. The probability values assigned indicate the likelihood of progressing from one node to the other. This is useful in fault propagation analysis in which various stages of a fault can be predicted based on these probabilities that may be obtained from historic data and expert knowledge.

For the Fuzzy method, IF-THEN rules are used to describe the transition from one node to the other. Since each node in FSN represents various faults, causes or consequences, the

fuzzy rules give estimations of likely plant states during a fault or transient. For instance, fuzzy rules applied to the steam generator in NPP may include; IF feedwater flow=Low THEN Failure Mode=Low Steam Generator Level.

For the Mathematical modeling approach, mathematical equations comprising various functions are used to specify the relationship between nodes. These equations express the relation between dependent and independent process variables. Genetic Programming is a method that can be used to establish these types of relations between nodes/variables.

5.2.4 Dynamic FSN

Changes in plant conditions and states can be modeled by the FSN. In the dynamic FSN, new data obtained from sensors or by running simulations is used to update process variables by implementing a reasoning process. The reasoning process enables the mapping between process variables both qualitatively and quantitatively. Bayesian Belief Network (BBN) was implemented as a tool to achieve reasoning in FSN and applied to fault propagation analysis in this study. The reasoning maybe diagnostic, predictive, inter-causal or combined.

In diagnostic reasoning, symptoms of a fault are first identified and the likely causes are obtained as output of the reasoning. A low steam generator level maybe considered a symptom and a low feedwater flow or irrational flow sensor maybe likely causes.

In predictive reasoning, faults are predicted without the knowledge of symptoms. For example, decreasing the feedwater control valve will result in low steam generator level. In inter-causal reasoning, multiple causes result in a single consequence.

In combined reasoning, a combination of any or all the other types of reasoning is used to achieve the desired outcome.

5.2.5 Implementing FSN

Formal language is proposed to represent process domain knowledge and safety control rules as explained in [7]. These rules are initially defined in generic form based on domain knowledge, i.e regardless of plant specific knowledge and then further explained for plant specific knowledge based on observations. A risk element is identified for each hazard or fault propagation scenario from the root causes to the final consequences. Three possible risk elements associated with consequence-1 are shown in figure 5.2, they include

- Cause-1 → failure-1 → consequence-1
- Cause-2 → failure-1 → consequence-1
- Cause-3 → failure-1 → consequence-1

Where

CaFr1= frequency of cause-1

FPr1= Probability of failure 1 occuring as a result of any cause.

CoPr1= Probability of consequence-1 occuring.

Colm1= Total impact of consequence-1.

For independent events, the total risk associated with consequences 1, 2 and 3 are represented in equations 5.1 to 5.3.

Risk (Consequence-1)= [(CaFr1+CaFr2+CaFr3)×FPr1×CoPr1]×Colm1 (5.1)

Risk (Consequence-2)= [(CaFr1+CaFr2+CaFr3)×FPr2×CoPr2]×Colm2 (5.2)

Risk (Consequence-3)= [(CaFr1+CaFr2+CaFr3)×FPr3×CoPr3]×Colm3 (5.3)

For dependent events, Bayesian theorem can be used to determine the total risk based on dependencies for cause-1, 2 and 3.

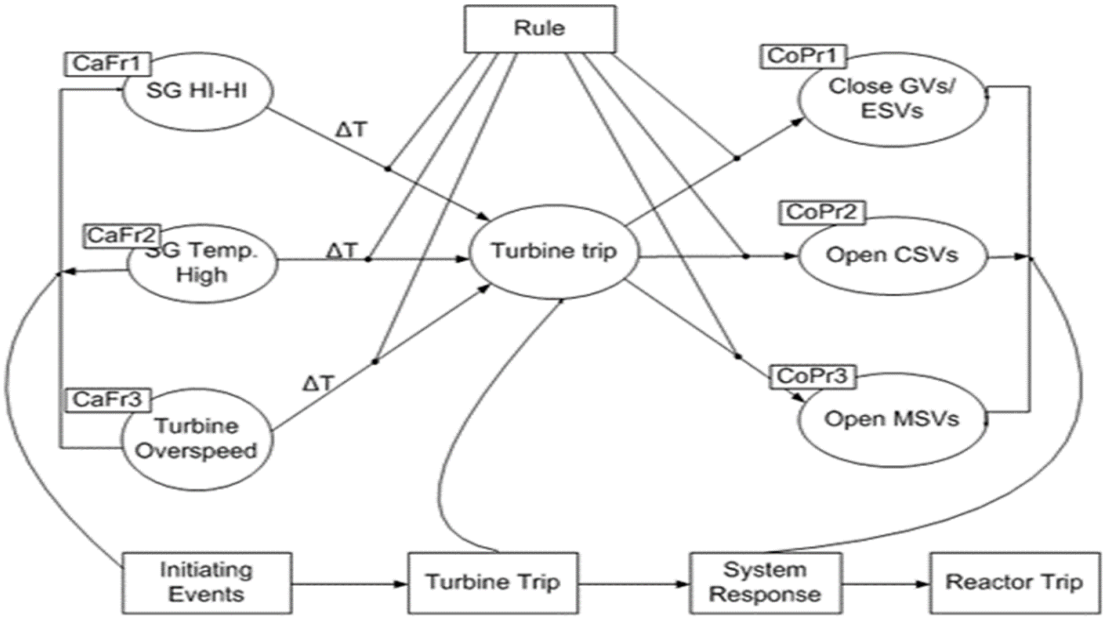

Figure 5. 2 FSN model for NPP

The FSN consists of two parts of static off-line and dynamic online models. Static FSN comprises faults, failures, hazards and accidents that are linked in the form of causation models associated with process equipment while dynamic FSN involves the use of dynamic simulated or real time data that can be obtained from sources such as, operation, maintenance, safety and control. In this study, static FSN is constructed for different fault

propagation scenarios after which operational scenarios for different fault propagation scenarios from real time data or simulation are identified.

5.2.6 FSN Implementation in Existing NPPs

The FSN methodology as described in the preceding sections can be implemented in existing NPPs for fault diagnosis and safety verification. This process is represented in figure 5.3.

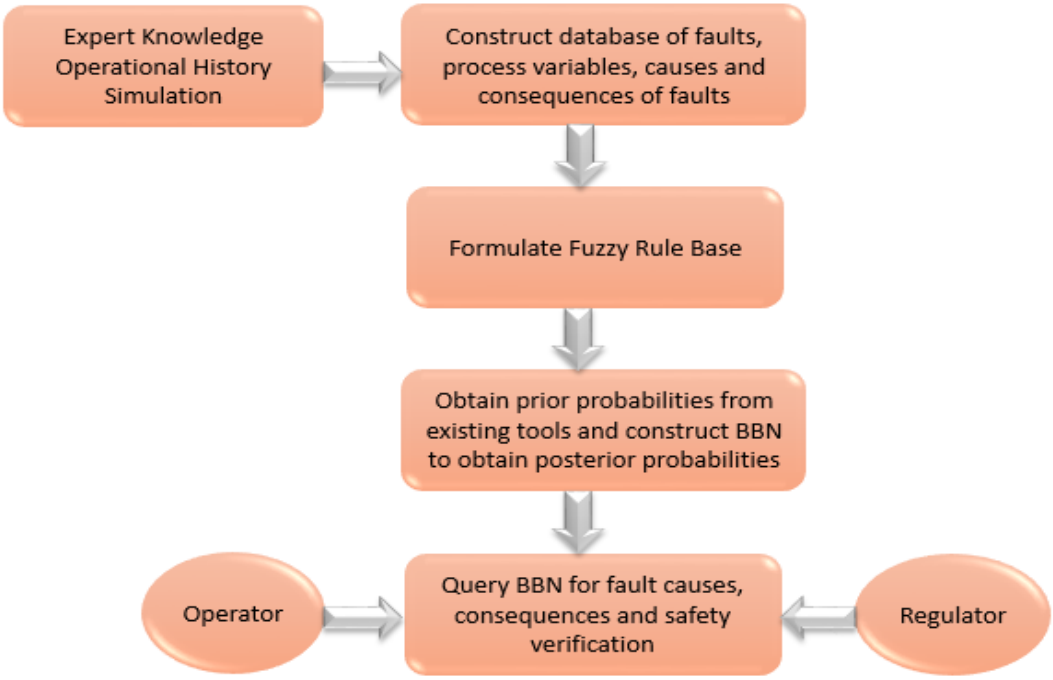

Figure 5.3 FSN application in existing NPPs

In figure 5.3, a database is constructed consisting of various faults, process variables and consequences of faults. This database is based on expert knowledge of the NPP, operational history as well as from simulation. A fuzzy rule base is then formulated from the database for various systems and associated faults in an NPP. After the rule base is completed, the BBN is constructed. The BBN utilizes prior probability estimates from tools currently

available at the operating stations. Posterior probabilities can then be obtained after simulating the BBN. Both plant operators and regulators can query the BBN for various purposes including:

1. Estimating fault propagation scenarios based on evidence entered in the BBN using the inference mechanism.

2. Diagnosing likely causes of faults based on process variable observation.

3. For safety verification which is useful for safety protection system design.

In the proposed method above, the FSN is the structure of the solution approach while BBN and fuzzy logic are both computational engines utilized in the FSN structure.

5.3 CATHENA

Canadian Algorithm for Thermalhydraulic Network Analysis (CATHENA) is a one dimensional, two-fluid non-equilibrium system thermalhydraulics code developed by AECL/CNL mainly for the analysis of postulated Loss of Coolant (LOCA) events in CANDU reactors. The use of CATHENA to perform reactor simulations for transient and postulated accident scenarios is relevant to this study since the safety analysis of a reactor based on fault propagation scenarios is the main objective of this study. The conservation equations for mass, momentum and energy are solved for the two phases (liquid and vapour) in CATHENA. Flow-regime-dependent constitutive relations for wall shear account for momentum transfer between the fluid and the pipe surfaces.

The numerical solution method used is a staggered mesh (i.e. a node consists of scalars such as void fraction, phase enthalpies, phase pressures and inflow and outflow velocities

of liquid and vapour between nodes), semi-implicit, finite-difference method that is not transit-time-limited [69]. Conservation of mass is obtained using a truncation error correction technique. Mass conservation is important in predicting 2-phase flow because of its known sensitivity to small changes in mass inventory. Additionally, the length of the transients makes them vulnerable to the accumulation of small errors which can adversely affect the solution. Sparse matrices are therefore solved in the code due to the stiffness of the problem.

Heat transfer from metal surfaces is handled by a complex wall heat transfer package known as the Generalized Heat Transfer Package (GENHTP). A set of flow regime-dependent constitutive relations describe energy transfer between the fluid and the pipe wall or fuel element surfaces. Heat transfer by conduction within the piping and fuel is modelled in the radial and circumferential directions. Radiative heat transfer and the zirconium-steam reaction can also be included during modeling. Component models which describe the behavior of pumps, valves, steam separators, and discharge through breaks are available to complete the modelling of reactor systems. A more detailed description of the CATHENA code can be found in [70, 71].

5.3.1 Edward's Blowdown Problem

In order to demonstrate the use of CATHENA for transient simulations, a simple pipe blowdown problem is selected [72]. A 4.0 m. long pipe filled with water at 240 deg C pressurized to 7 Mpa (70 atmospheres). The pipe has a rupture disc at one end which is opened starting at t=0 over a period of 0.003 seconds, and the pipe allowed to depressurize. The setup is shown in figure 5.4. It is observed that the water at the open end of the pipe

immediately flashes into steam and begins to rapidly exit the pipe into the environment. Depressurization moves along the pipe towards the closed end, resulting in vapor generation and continued flow out of the opening.

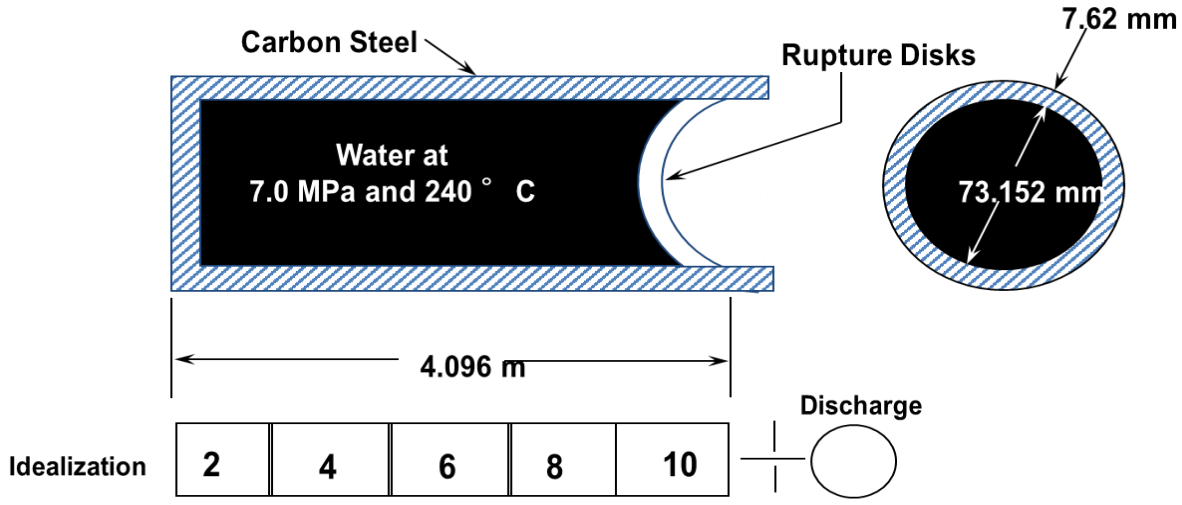

Figure 5. 4 Edward's Pipe Blowdown Problem [72]

5.3.1.1 Input Description

The CATHENA [69] Idealization/modelling contains various sections that describe the problem and defines control parameters for the simulation. They include:

1. " PROBLEM TITLE"- this describes the problem.
2. "CONTROL PARAMETERS"– this contains data that specify start/end times, output frequency and time step control.
3. "COMPONENTS"- describes the geometry of the various systems in the model. Pipe (length, volume, pressure losses), volume, tank, reservoir, etc.

4. “COMPONENT CONNECTIONS” – shows how the components are connected to form a hydraulic network.

5. “BOUNDARY CONDITIONS”- identifies the conditions at the boundaries of the problem. These are classified as reservoir, flow or heat boundary conditions.

6. “SYSTEM MODELS”- enables the modelling of physical systems such as pumps, valves, discharge and junction resistance.

7. “SYSTEM CONTROL MODELS”- contains the output models. Writes selected data to user-specified disk files.

8. “INITIAL CONDITIONS”- describes the physical conditions (pressure, enthalpies and void) that apply to each component in the network at the start of the simulation.

The results of the above example are presented and discussed in chapter 7.

5.3.2 Uncertainty Quantification for Edward’s Pipe Blowdown Problem

The stochastic method for uncertainty quantification was applied in the form of the Monte Carlo method to the Edward’s pipe blowdown problem. The OpenCOSSAN software was used with modifications to simulate this scenario. Three input parameters were selected namely, the initial pressure, the initial temperature and reservoir pressure which was a boundary condition. The details of the stochastic model for this problem are as follows: the reservoir pressure was considered to be a constant value of 1.013E+05 for all input samples, a random variable set was generated for the initial pressure which was assumed to be normally distributed with mean 7.0E+06 and covariance 0.1 (10 %) and a random

variable set was generated for the initial temperature which was assumed to follow a uniform distribution with a lower bound of 200 and an upper bound of 300.

Random variable sets were generated for the input parameters described above. A cossan readable input file was created which is a modification of the main CATHENA input file. This file contains information that is scanned and used to generate sample input files subsequently. The connection between OpenCOSSAN and CATHENA is established using the connector script. A total number of 420 random variable input parameter sets were generated from the Monte Carlo model thereby creating 420 different CATHENA input files after simulation. All the CATHENA input files created were subsequently executed and the outputs were analyzed for uncertainty quantification. Results and analysis are presented in chapter 7.

Table 5.3. Stochastic input model description

Random Variable	Distribution		Covariance
Initial Pressure	Normal	(mean=7MPa)	0.1
Initial Temperature	Uniform	(Lower bound=200,) (Upper bound=300)	

CHAPTER 6: UNCERTAINTY QUANTIFICATION FOR RD-14 TEST FACILITY

6.1 Review

In this chapter, uncertainty quantification performed using the methods developed in chapter 3 is presented. A small break LOCA transient simulated by the RD-14 test facility is described in detail and the uncertainty quantification results for this facility are presented. Uncertainty in selected input parameters was quantified by estimating their effect on the output parameters. The transient scenario was created by CNL based on postulation. The scenario was simulated and results were used for subsequent analyses.

6.2 RD-14 Facility Description

The RD-14 is a thermal–hydraulic test facility which has most of the important characteristics of a CANDU primary heat transport system. Figure 6.1 shows a simplified schematic of the RD-14 facility [72] and figure 6.2 shows the nodalization of the facility used for CATHENA simulation. The facility is a pressurized-water loop (10 MPa nominal) with a geometry similar to a typical CANDU reactor. It has two horizontal channels of length 6 meters and total power of 11 MW. These are connected to end-fitting simulators representing 2 passes through a reactor core. Each test section consists of 37 electrically heated fuel-element simulators of almost the same heat capacity as reactor fuel. Heat removal from the primary circuit is achieved through 2 recirculating U-tube type steam generators. Primary fluid circulation is provided by 2 high-head centrifugal pumps, which generate channel flowrates similar to a single reactor channel. Full length feeders connect test sections. The elevation of the above-header piping is also similar to a CANDU. The

above-header piping includes the piping connected to two full-height, U-tube steam generators, and two bottom-suction centrifugal pumps. Steam generated in the secondary side of the steam generators is condensed in a jet condenser and returned as feedwater to the steam generators. A pressurizer (a surge tank) controls the primary-side pressure. The test facility is also equipped with ECC systems.

The test sections, steam generators, pumps, and headers are arranged in order to obtain a scale similar to a typical CANDU reactor. The steam generators are also scaled such that their dimensions and characteristics are similar to those in a CANDU. The facility was designed to produce the same conditions in its primary system as those in a typical reactor under both forced and natural circulation [71; 81].

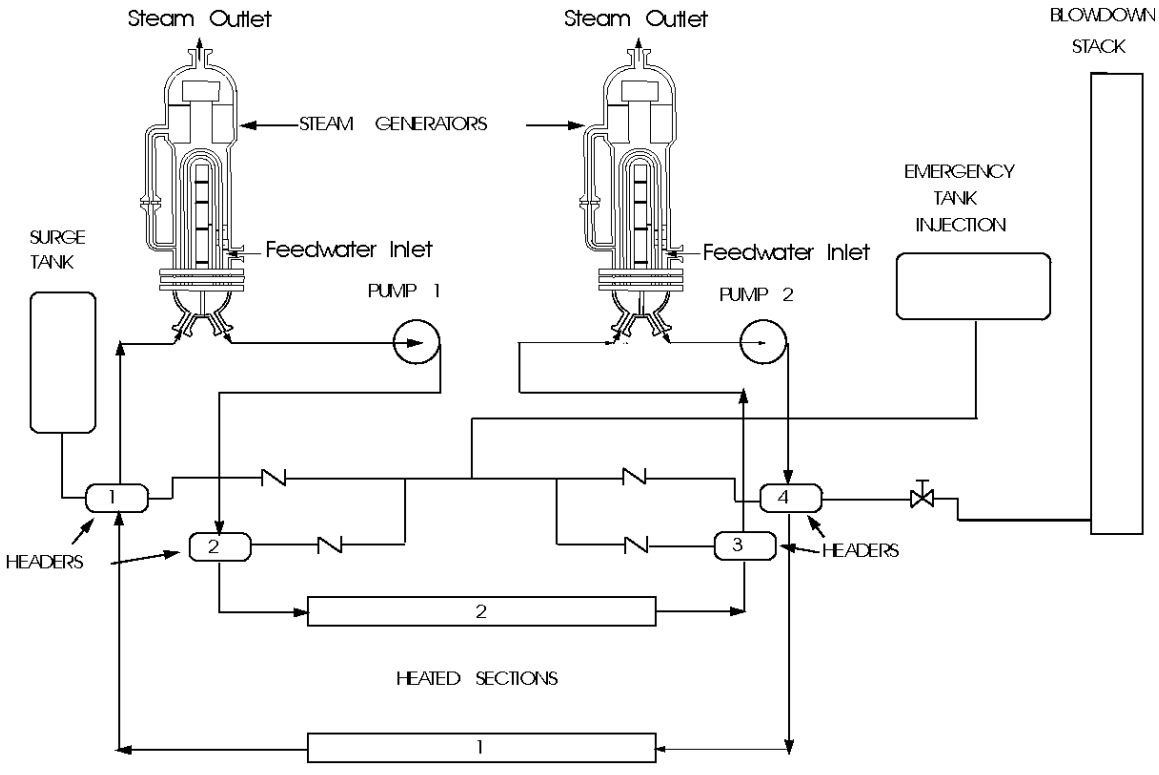

Figure 6.1 Schematic diagram of the RD-14 facility [72]

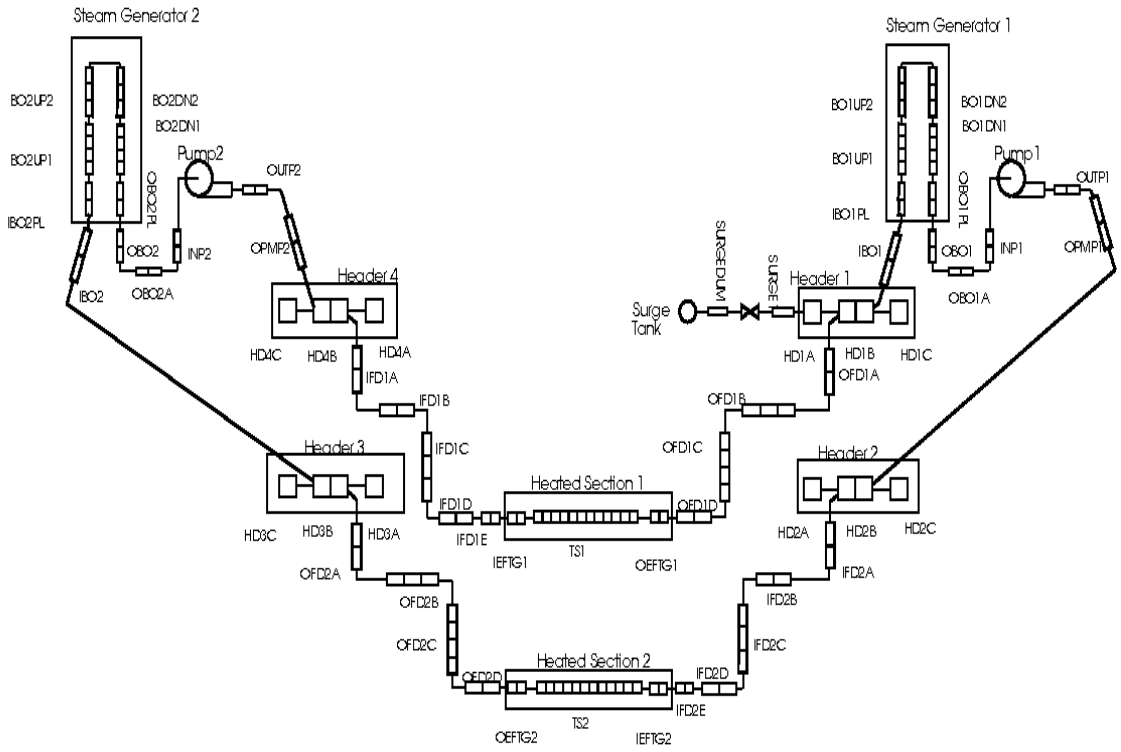

Figure 6.2 RD-14 Nodalization [72]

6.2.1 Test B8603

For the purpose of this study, the CATHENA model for test B8603 was simulated and the results were used to perform uncertainty quantification. Test B8603 is a small break LOCA in the inlet header conducted in the RD-14 facility and was reported in [82]. The break diameter was 7 mm, which is proportional to the cross sectional area of two feeders for a CANDU reactor LOCA. The break was located at the inlet header 4 [83]. The break was represented in the simulation by a fast-opening valve connected to an inlet header, and an orifice plate, scaled by the ratio of break area to loop volume to represent a feeder-sized break. Once the break valve was opened, single-phase liquid was discharged through the orifice, changing to two-phase flow when the inlet header pressure reached saturation.

This scenario was simulated for 200 seconds to capture most of the events of interest such as: the blowdown, exponential pump ramp, secondary pressure ramp (crash cool), high-pressure ECC and ECC refill. The secondary side pressure was set to 4.5 MPa and the emergency coolant injection (ECI) system was set to 5.5 MPa for the high pressure ECI and 1.3 MPa for the low pressure ECI. In this test, the surge tank was isolated 4 s before break initiation, and the power was tripped 20 seconds after break initiation to establish decay heat conditions [83].

6.3 Stochastic Uncertainty Quantification Model

The uncertainty in output parameters due to input parameter uncertainty was estimated using the stochastic method as implemented in the OpenCossan software discussed in chapter 3. The RD-14 CATHENA model [72] was simulated and the results were used to quantify uncertainty. Two random variables were selected: the initial pressure in heated section 1 (TS1) and pressure in the surge tank which was treated as a boundary condition. A constant value of 10 MPa was chosen for the boundary condition pressure random variable while a uniform distribution with a lower bound of 10.4 MPa and an upper bound of 10.9 MPa was chosen as the initial pressure distribution. A matlab script was written in the OpenCossan environment which takes the original RD-14 model input and a cossan readable file as inputs. The cossan readable input file contains scripts that replace the selected input parameters with the random variable sets created. After, running the matlab script, a number of input files are created corresponding to the total number of samples specified in the script. All the random input files generated are simulated using CATHENA and the results analyzed to quantify uncertainty. Figure 6.3 shows the distribution of the

initial pressure in four nodes of TS1. This represents the uniform distribution that was assigned to the input parameter (initial pressure). The distribution was assigned based on similar studies in literature as well as expert judgement.

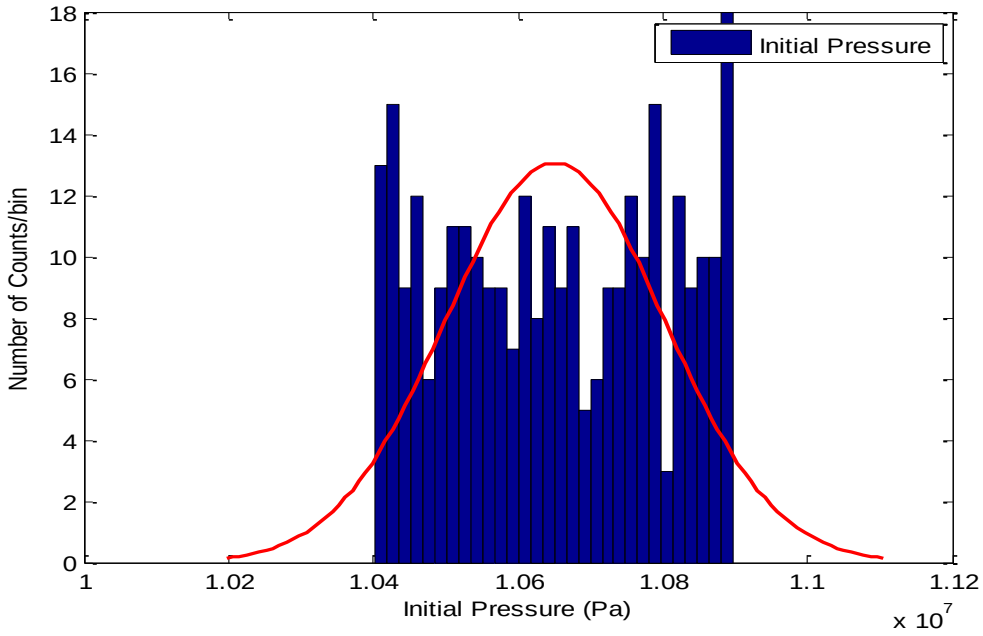

Figure 6.3 Initial Pressure in TS1 distribution

6.4 Output Pressure Results

In this section, uncertainty quantification results for the output pressure in header 4 are presented. These results represent the effect of uncertainty in the initial pressure in 4 nodes of heated section 1 (TS1). Figure 6.4 shows the output pressure plotted against time for the simulated random input files. The total number of samples simulated was 300. In figure 6.5 the output pressure distribution is presented. The distribution is fitted to a normal distribution and the first four moments (mean, variance, skewness and kurtosis) are computed and indicated on the figure. In comparison to the normal distribution, the output distribution is observed to be positively skewed implying the output pressure distribution

has an asymmetric tail extending out towards more positive pressure values. The distribution also shows a spread of about 1.8 MPa around the mean pressure as well as a positive kurtosis.

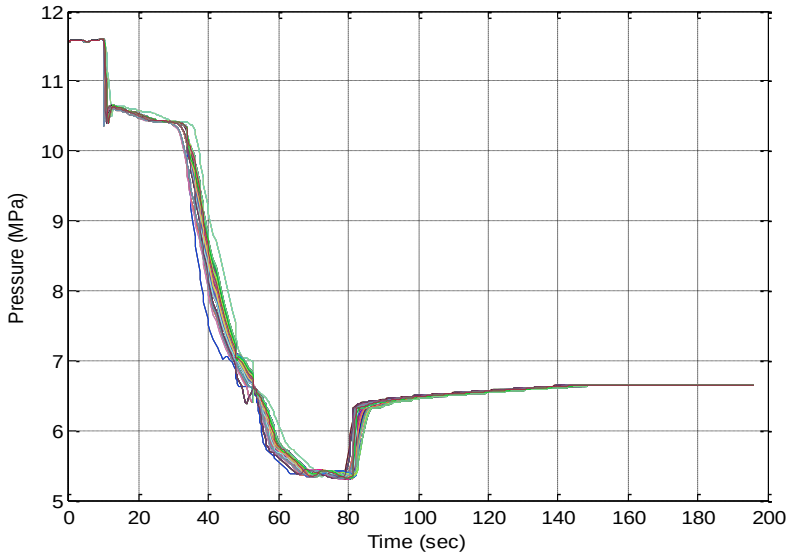

Figure 6.4 Output pressure plots for random input samples

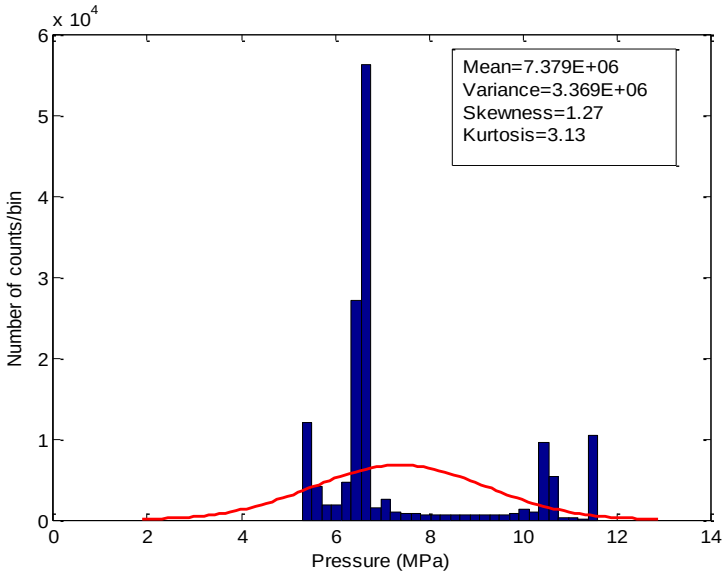

Figure 6.5 Output pressure distribution

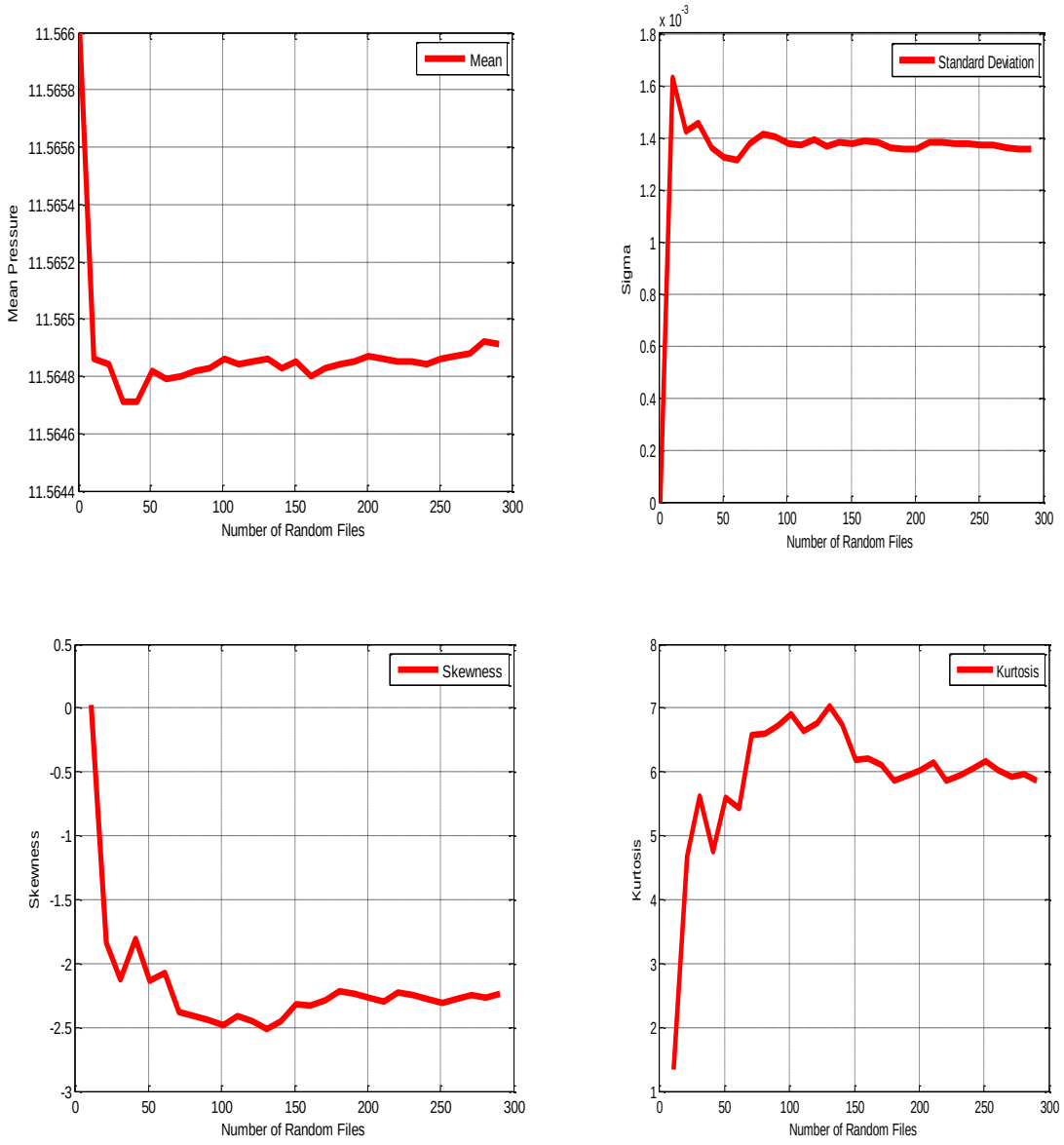

Figure 6.6 Output pressure convergence test: Top left (Mean Pressure), Top right (Standard deviation), Bottom left (Skewness), Bottom right (Kurtosis)

Figure 6.6 shows results of the convergence of output pressure after simulating 300 random input samples. This is demonstrated by the convergence of the first four moments implying the adequacy of the number of random samples simulated to estimate the output parameter distribution. The uncertainty computed was 0.087% signifying a 1.84 MPa change in

output pressure expected given uncertainty in initial pressure of values uniformly distributed between 10.4 MPa and 10.9 MPa.

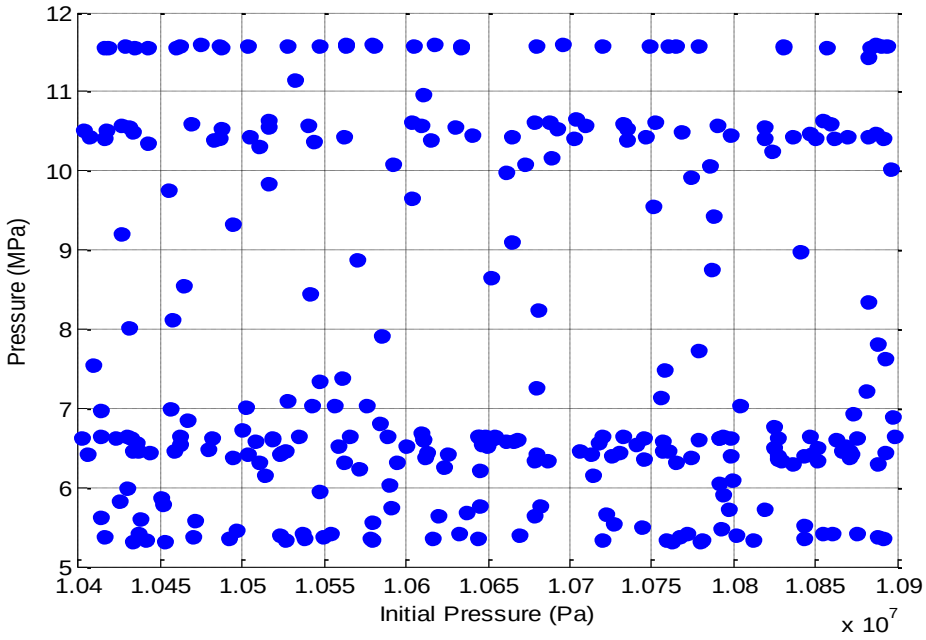

Figure 6.7 Scatter plot of output pressure

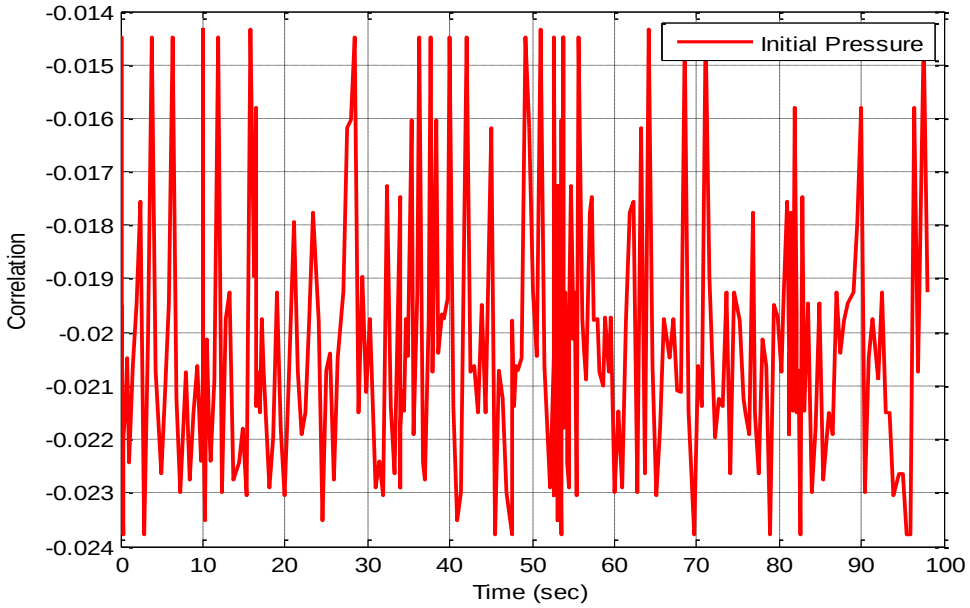

Figure 6.8 Correlation coefficient between initial pressure and output pressure

Figure 6.7 shows a scatter plot of output pressure against the input parameter (initial pressure). Figure 6.8 is a plot of the correlation coefficient between the initial pressure and the output pressure for a specified number of time steps. The figure indicates that there is a negative correlation between the initial pressure and the output pressure.

6.5 Fuel Pin Temperature Results

The effect of perturbing the initial pressure in 4 nodes of heated section 1 were investigated. Results presented in this section focus on the fuel pin temperature as output. Uncertainty associated with the input parameter is quantified by creating and simulating random CATHENA input files. A total of 300 random files were simulated and analyzed.

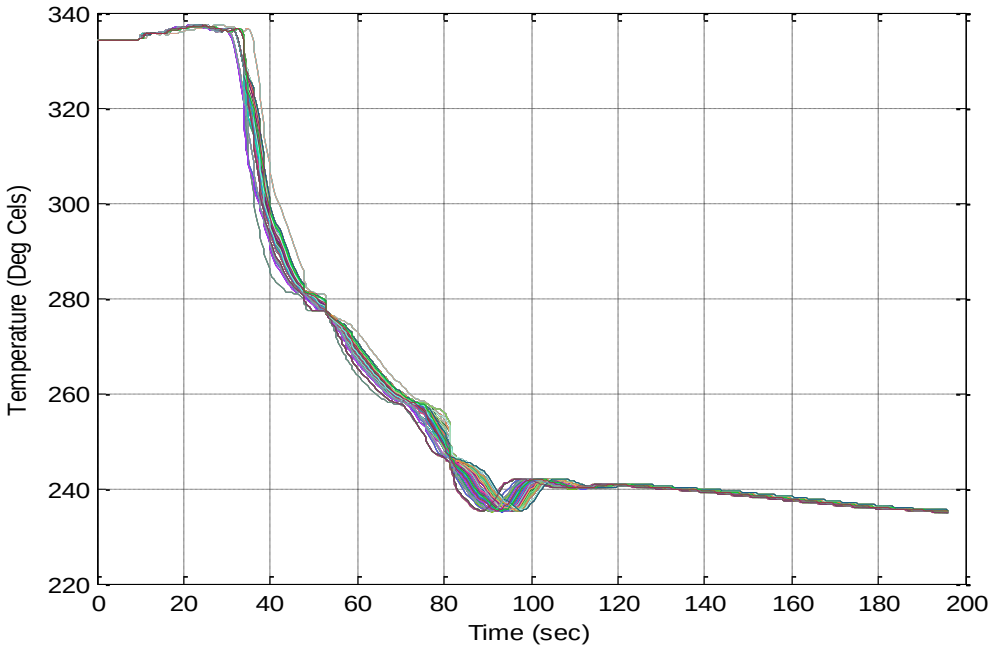

Figure 6.9 Fuel pin temperature plots for random input samples

Figure 6.9 shows a plot of the fuel pin temperature against time during the LOCA for all the random input samples. This figure indicates the range of the output parameter to be obtained given the range of input parameter variation due to uncertainty.

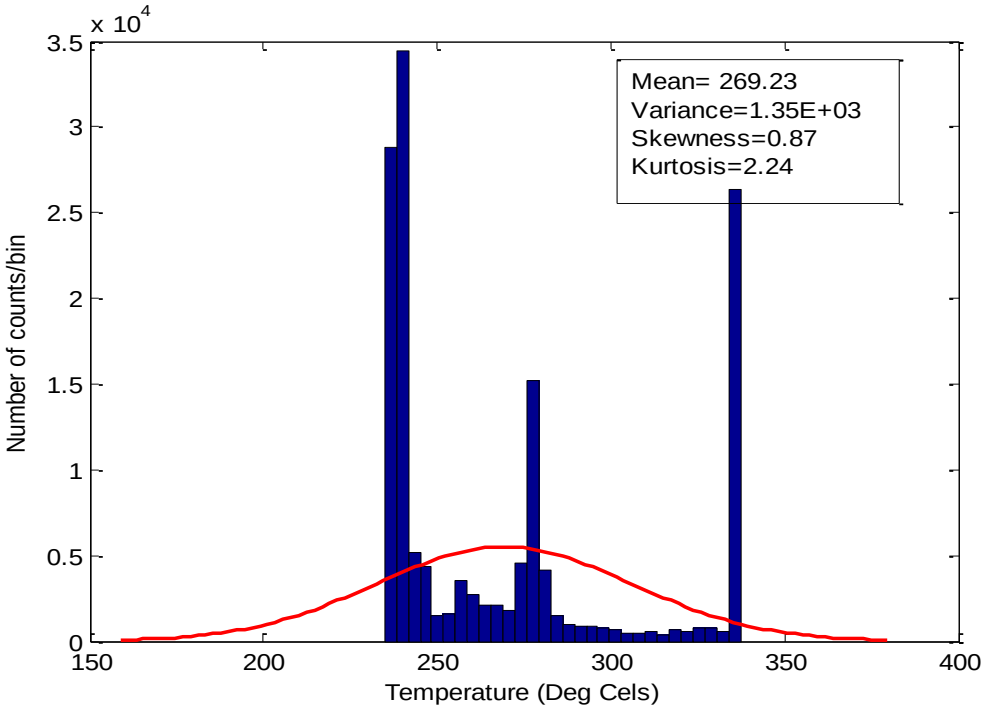

Figure 6.10 Fuel pin temperature distribution

Figure 6.10 presents the fuel pin temperature distribution obtained from simulating the 300 random input samples. Also included in this figure are the first four moments (mean, variance, skewness and kurtosis) computed from the simulation results. The important characteristics of this distribution are; a spread of about 36.8 degrees Celsius around the mean temperature, a positive skewness and a positive kurtosis. The shape of the output parameter distribution is largely influenced by the distribution assigned to the input parameter. The uncertainty in fuel pin temperature estimated was 0.048%. This was obtained after taking a ratio of the standard deviation of fuel pin temperature to the experimental results expressed as a percentage. This signifies that a 36.79 degrees' Celsius change in fuel pin temperature is expected given a change in initial pressure between 10.4 and 10.9 MPa which is uniformly distributed.

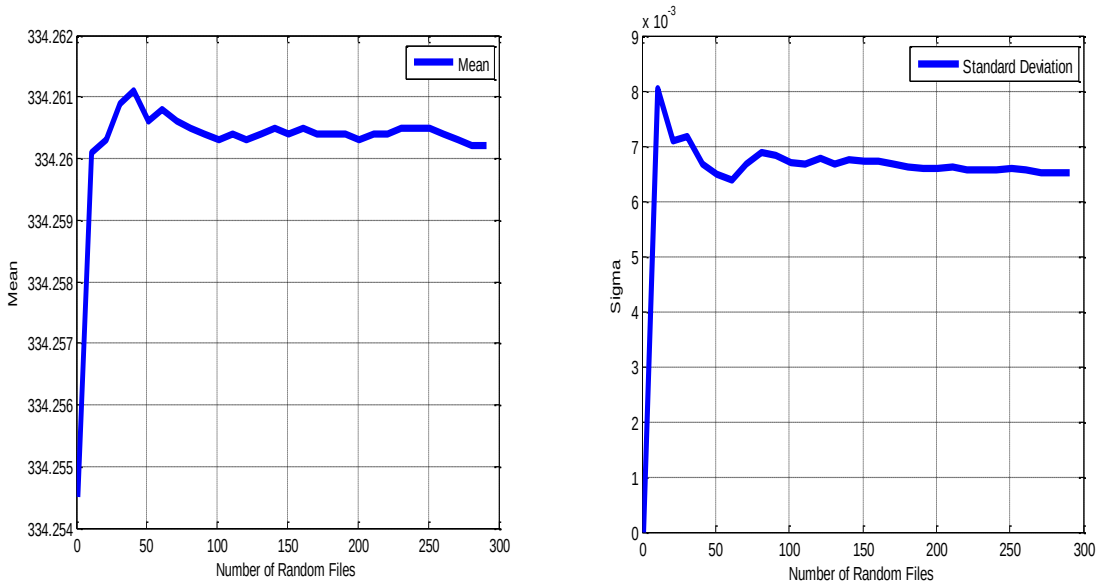

Figure 6.11 Fuel pin temperature convergence: Left (Mean), Right (Standard Deviation)

In figure 6.11, the convergence of fuel pin temperature is shown by plotting the mean (left) and standard deviation (right) for the random input samples. By the convergence theorem, it was not necessary to simulate additional samples in order to estimate the output parameter distribution accurately. The 300 input samples therefore proved to be adequate.

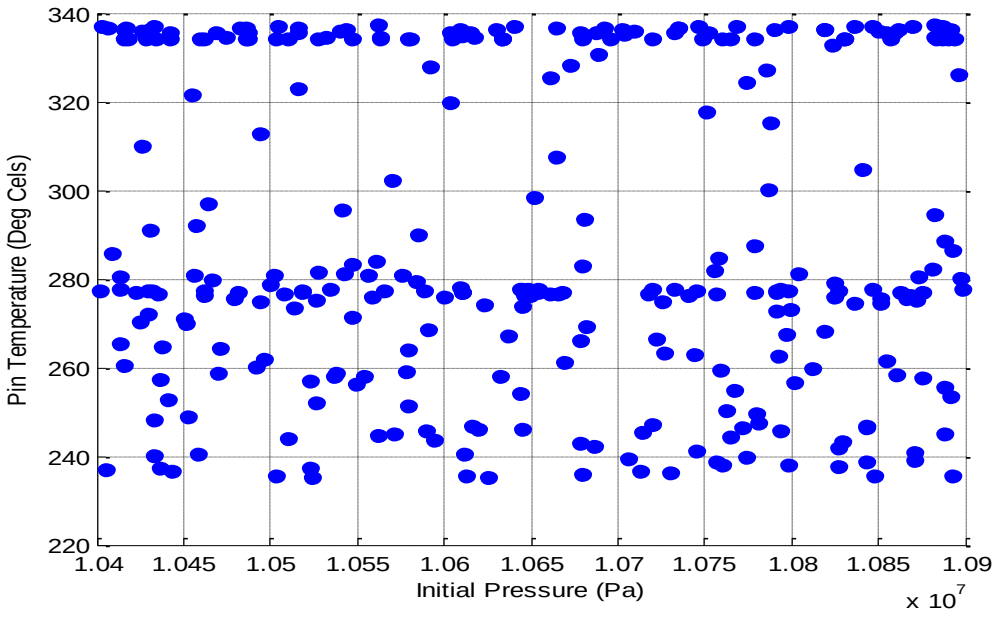

Figure 6.12 Fuel pin temperature against Initial pressure scatter plot

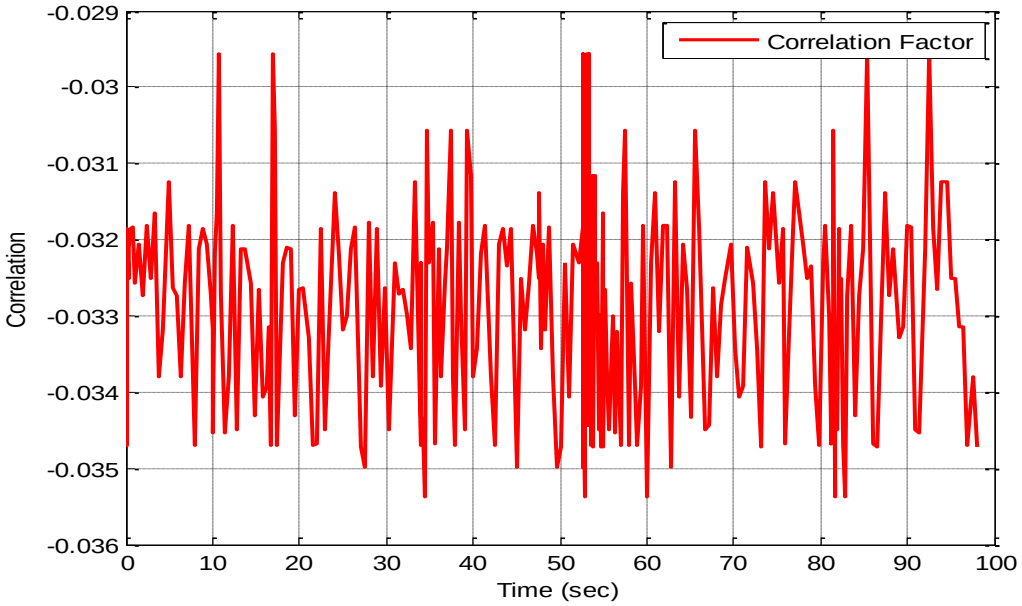

Figure 6.13 Correlation coefficient between Fuel pin temperature and Initial pressure

A scatter plot of the output parameter (fuel pin temperature) against the input parameter (initial pressure) is presented in figure 6.12. The input parameter was generated randomly

using the lower and upper ranges specified earlier. In figure 6.13, the correlation coefficient between the initial pressure and fuel pin temperature is plotted for a specified number of time steps. The correlation coefficient is used in this study as a sensitivity measure to show the linear relationship between the input parameter and the output parameter. From figure 6.13, it is seen clearly that there exists a negative correlation between the fuel pin temperature and the initial pressure.

The results presented in this chapter are expected to be useful to regulators in providing further insights on safety margin reduction. With uncertainty quantification extended to capture other input parameters and systems in NPPs, a fair idea of code accuracies can be evaluated and confirmed. Additionally, code developers and users would also find these results useful, as they would be able to further understand the effect of input parameter uncertainties on output parameter predictions.

6.6 Comparison of Uncertainty Quantification Results

Uncertainty quantification results obtained in this study were compared with results obtained using other methods reported in literature. In table 6.1, this comparison is shown with 23% and 13% lower uncertainty estimates from this study for output pressure and temperature respectively. The results from literature were based on the CIAU methodology applied for a small break LOCA in a PWR. CIAU is an uncertainty quantification methodology that is made up of the UMAE method and RELAP5/MOD 3.2 [89]. It is worth bearing in mind the differences between the RD-14 test facility (based on CANDU design) considered in this study and the PWR considered in the CIAU study. Additionally, the authors of that study attributed the high uncertainty values to a low number of data points

for the scenario simulated [89]. In view of the similarities and differences in both studies as identified above, the most significant inference from this comparison is the fact that uncertainty results from this study are far below generally accepted limits.

Table 6.1. Uncertainty quantification results

Parameter	Uncertainty (%)	
	This study	CIAU
Pressure	0.087	0.38
Temperature	0.048	0.35

CHAPTER 7: RESULTS AND DISCUSSION

7.1 Review

In this chapter, uncertainty quantification results obtained for the Edward's blowdown problem are presented. Error reduction in Case Study 2 and risk estimation for a steam generator tube rupture as well as FSN results for case study 1 are also presented and discussed. The chapter concludes with a demonstration of the link between uncertainty quantification results and FSN.

7.2 Uncertainty Quantification with OpenCOSSAN

Uncertainty quantification was performed by studying the effect on output pressure obtained from CATHENA simulations by randomly varying the initial pressure and initial temperature as input parameters in the Edward's pipe blowdown problem. Results presented here were obtained after connecting CATHENA with OpenCOSSAN for quantifying uncertainty in a stochastic manner. A total of 420 random variables were generated from the Monte Carlo simulation to represent the number of input samples that were simulated by CATHENA.

Figure 7.1 shows a plot of output pressure against time for all the 420 input samples. This demonstrates varying outputs that can be obtained when the input parameters are varied. Figures 7.2 and 7.3 show scatter plots of output pressure against the inputs (initial pressure and initial temperature respectively). These plots show various levels of correlation between the inputs and the output parameter. A sensitivity analysis is however necessary in order to ascertain the exact effect of varying input parameters on the response parameter.

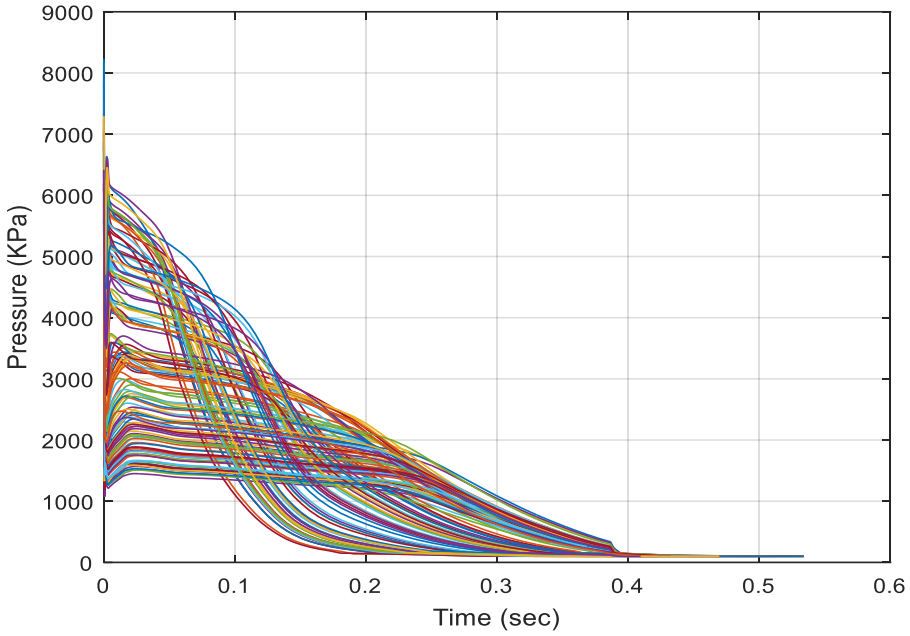

Figure 7.1 Plots of Pressure for Random Input Samples

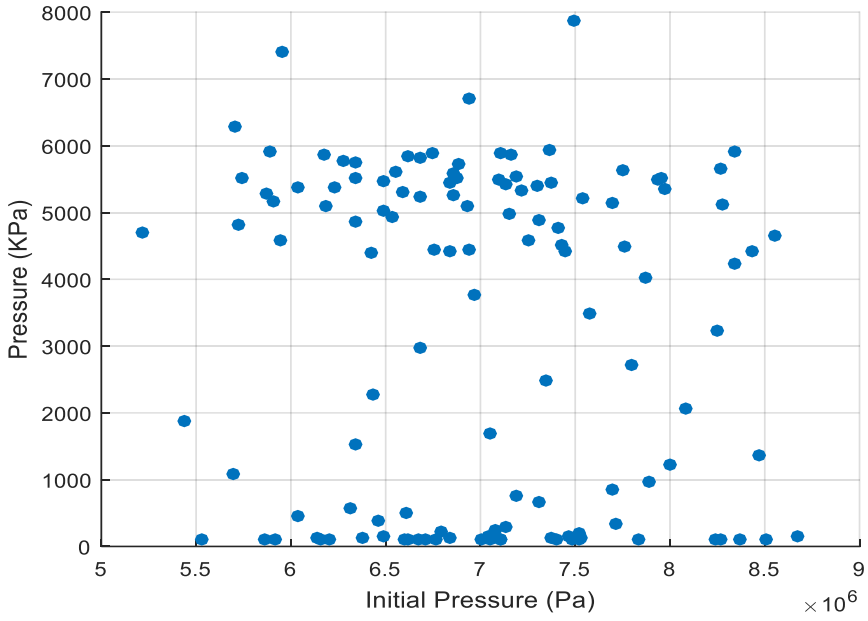

Figure 7.2 Scatter plot of Output pressure vrs. Initial pressure

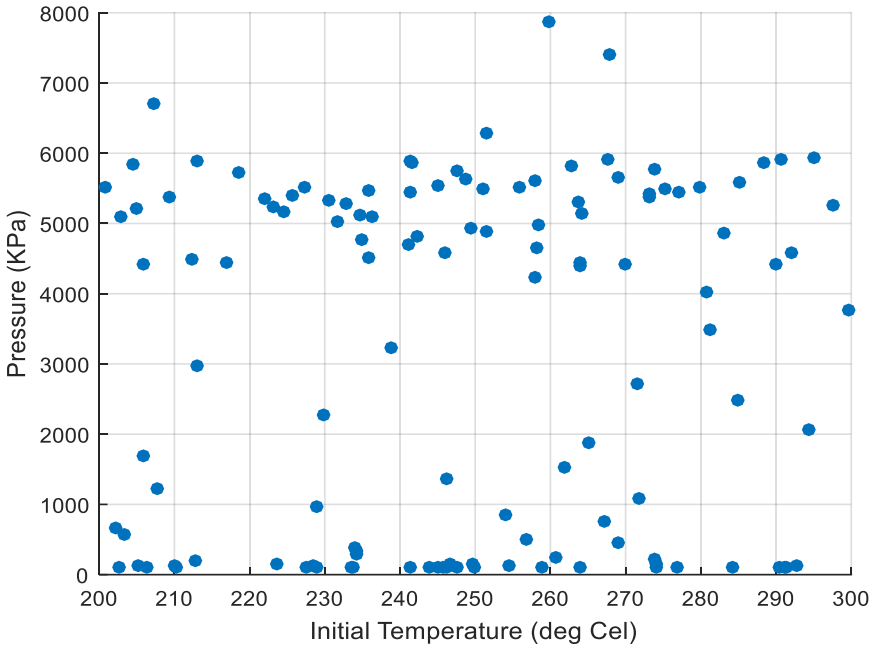

Figure 7.3 Scatter plot of Output pressure vrs. Initial Temperature

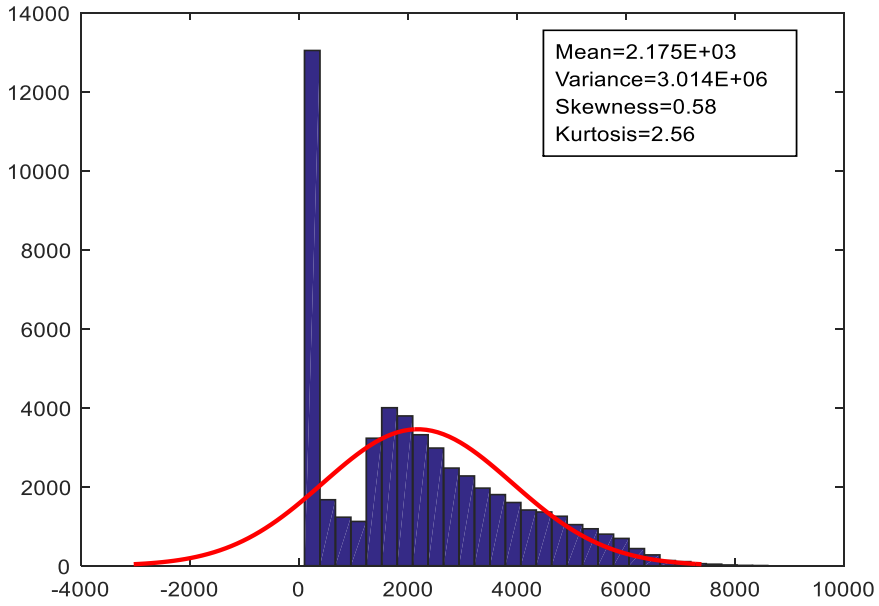

Figure 7.4 Histogram of output pressure for sampled inputs

Figure 7.4 shows a histogram fit of the output pressure obtained for all the 420 input samples simulated. The fit compares the output probability distribution to the normal distribution. The first four moments (mean, variance, skewness and kurtosis) are computed and shown on this figure. The output probability is rightly skewed.

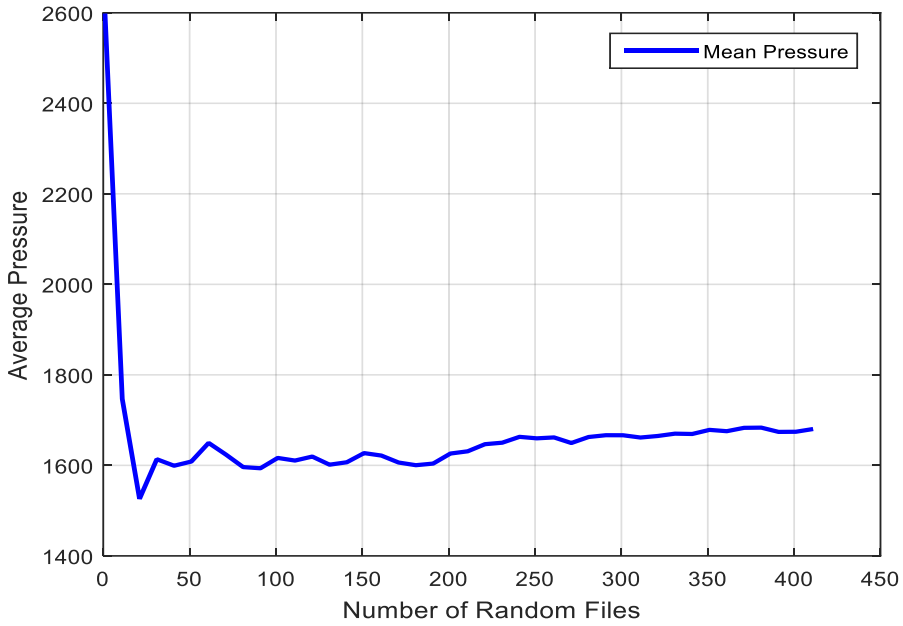

Figure 7.5 Convergence of average output pressure

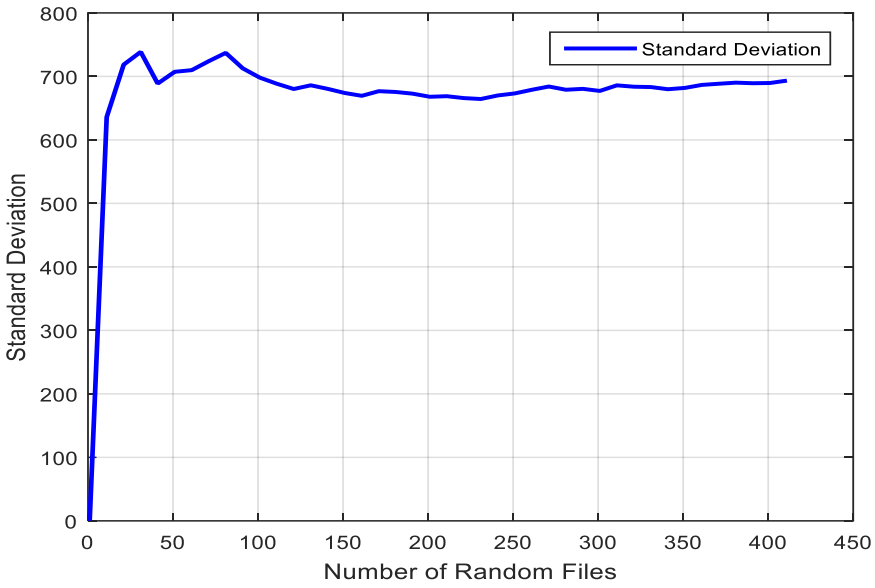

Figure 7.6 Convergence of output pressure standard deviation

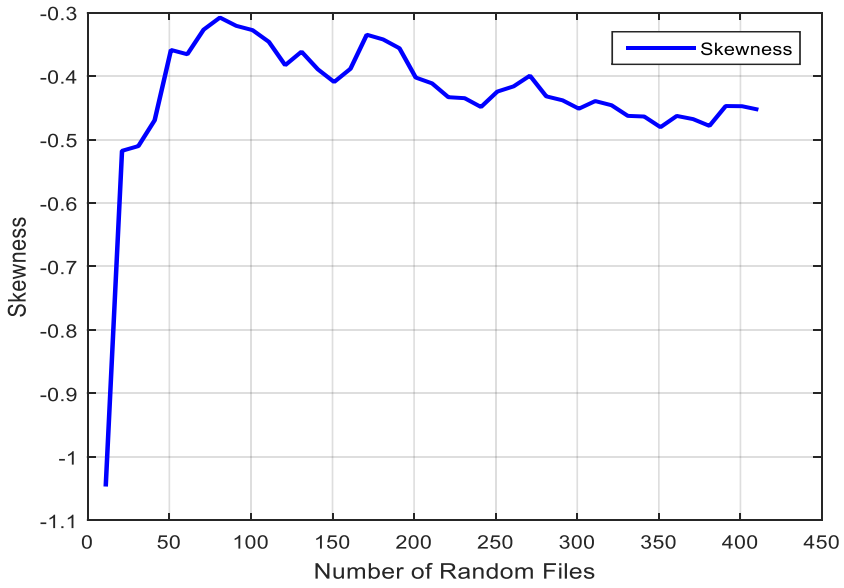

Figure 7.7 Convergence of output pressure standard deviation

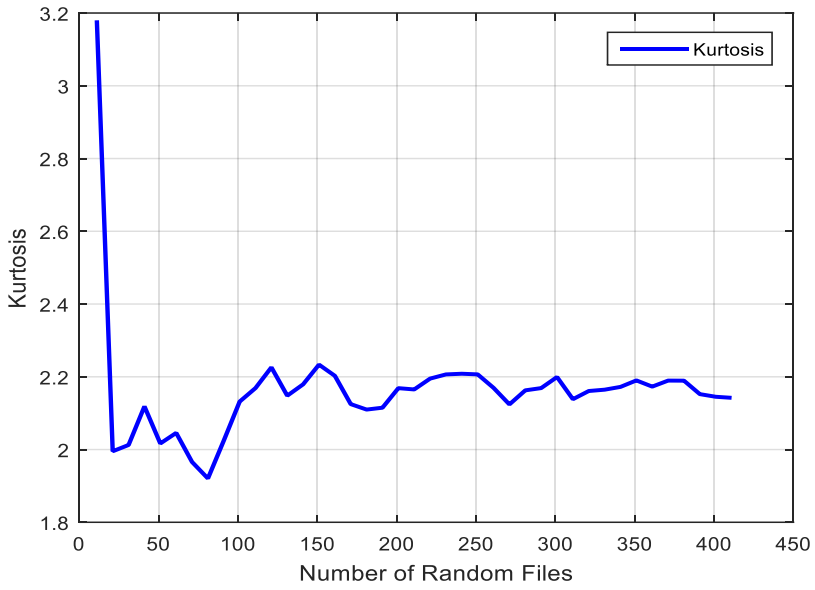

Figure 7.8 Convergence of output pressure kurtosis

Figures 7.5-7.8 show the convergence of the output pressure which is demonstrated by computing the first four moments. From these figures, small fluctuations of output pressure are observed initially prior to its convergence as seen in the mean pressure (figure 6.5), standard deviation (figure 7.6), skewness (figure 7.7) and kurtosis (figure 7.8). The convergence indicates that sufficient samples have been simulated to give information on the probability distribution of the output parameter.

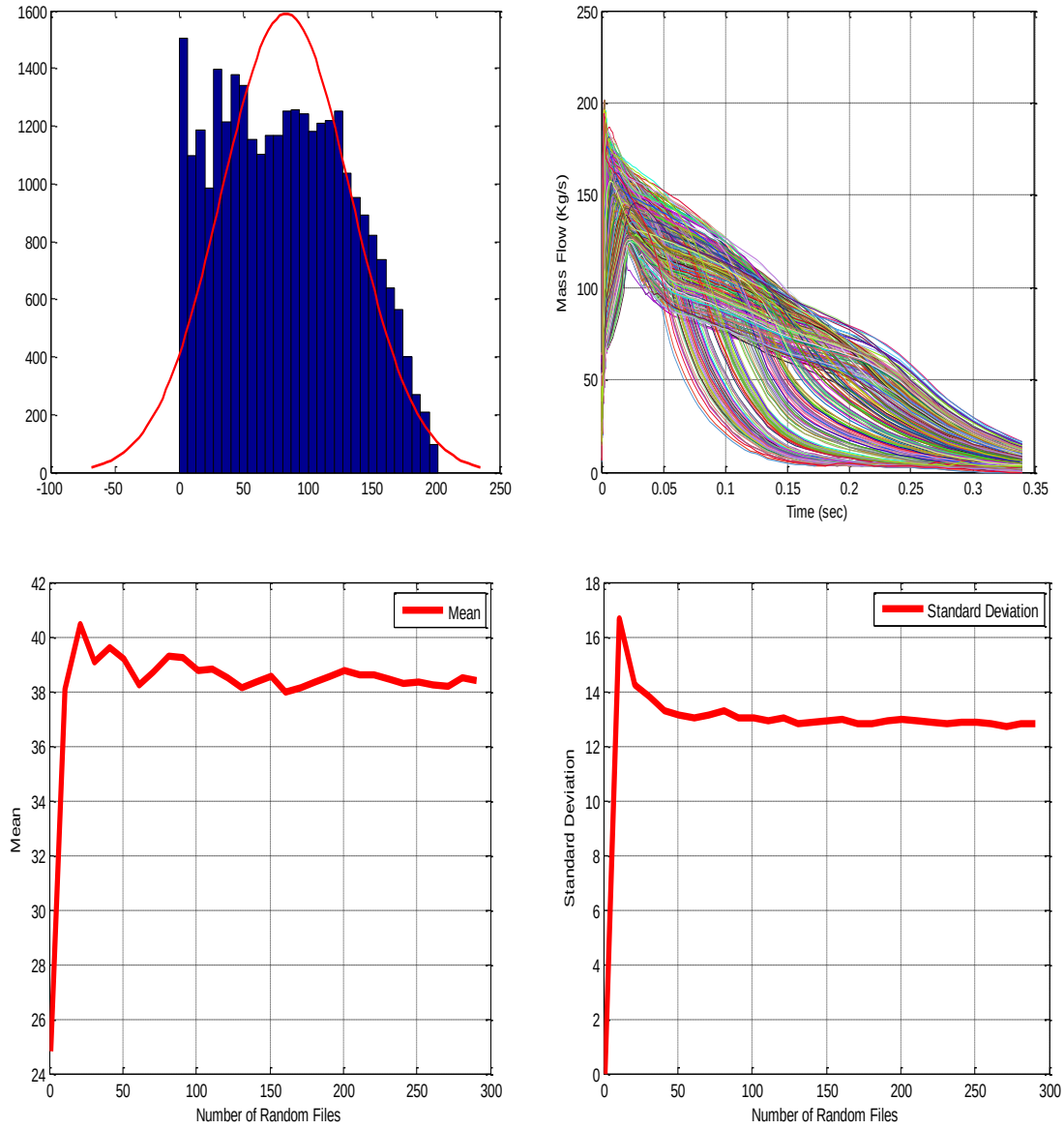

Figure 7.9 Mass flow rate results: Top left (mass flow rate distribution), Top right (mass flow rate plots for random input samples), Bottom left (mean mass flow rate convergence), Bottom right (standard deviation convergence of mass flow rate)

In figure 7.9, results of the mass flow rate are presented. The mass flow rate values were obtained at the rupture disc end of the pipe. In this figure, the mass flow rate distribution, profiles for the simulated random input files and convergence of its mean and standard deviation are shown.

7.2.1 Sensitivity Analysis for Sample Problem

In order to investigate the contribution of selected input parameters to the total output parameter uncertainty estimated in the previous section, a sensitivity analysis was performed. The sensitivity measure used is the correlation coefficient (ρ_{xy}) or factor given as;

$$\rho_{xy} = \frac{\sum_{i=1}^{N}(x_i-\bar{x})(y_i-\bar{y})}{(N-1)S_xS_y} \tag{7.1}$$

Where x_i is the random input parameter, $\bar{x}$ is the input parameter mean, y_i is the output parameter for the ith random file, $\bar{y}$ is the output parameter mean, N is the number of samples, S_x is the input standard deviation and S_y is the output standard deviation. The correlation coefficient provides a measure of the linear dependence between an input parameter and the output parameter.

For the Edward's blowdown problem simulated in this study, sensitivity analysis was performed by computing the correlation coefficient between the output pressure and two input parameters (initial temperature and initial pressure) for random input samples generated using the Monte Carlo sampling method. Figure 7.10 shows a plot of the computed correlation coefficient for different time steps.

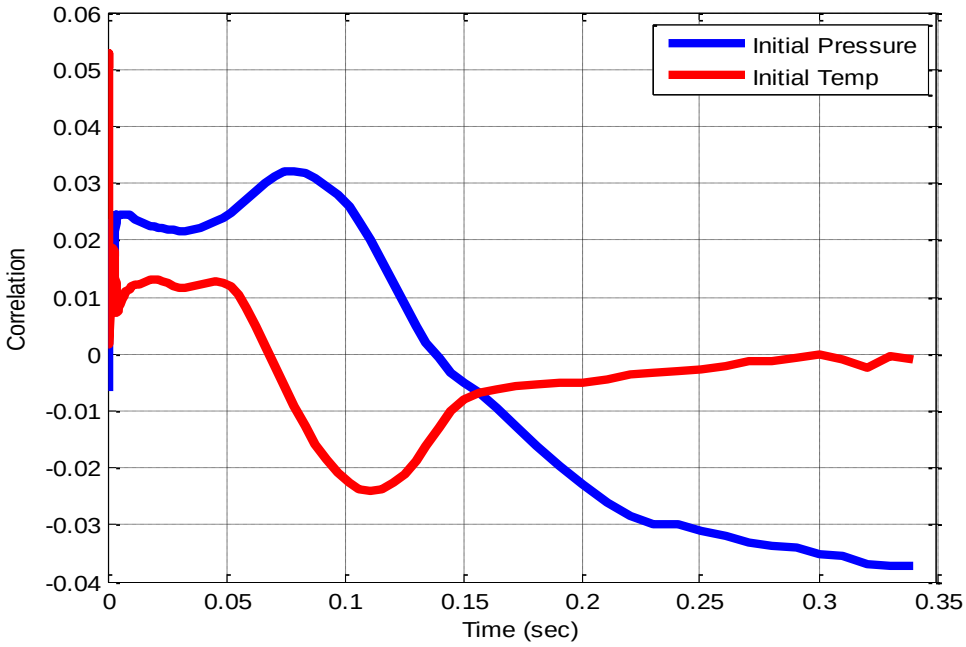

Figure 7.10 Output pressure sensitivity to initial temperature and pressure for various time steps

It can be observed from figure 7.10 that initially, the initial pressure contributed more to the uncertainty associated with the output pressure estimation. After about 0.15 seconds, although the plot shows a reversal of trends where the initial temperature seems to contribute more to output pressure uncertainty, the effect was in fact much less when comparing the effect of the two input parameters. Taking into consideration the total value of the correlation coefficient for the two input parameters for a specified number of time steps, it was determined that the contribution of the uncertainty in initial pressure to the global uncertainty observed for the output pressure was more compared to the contribution from uncertainty in the initial temperature.

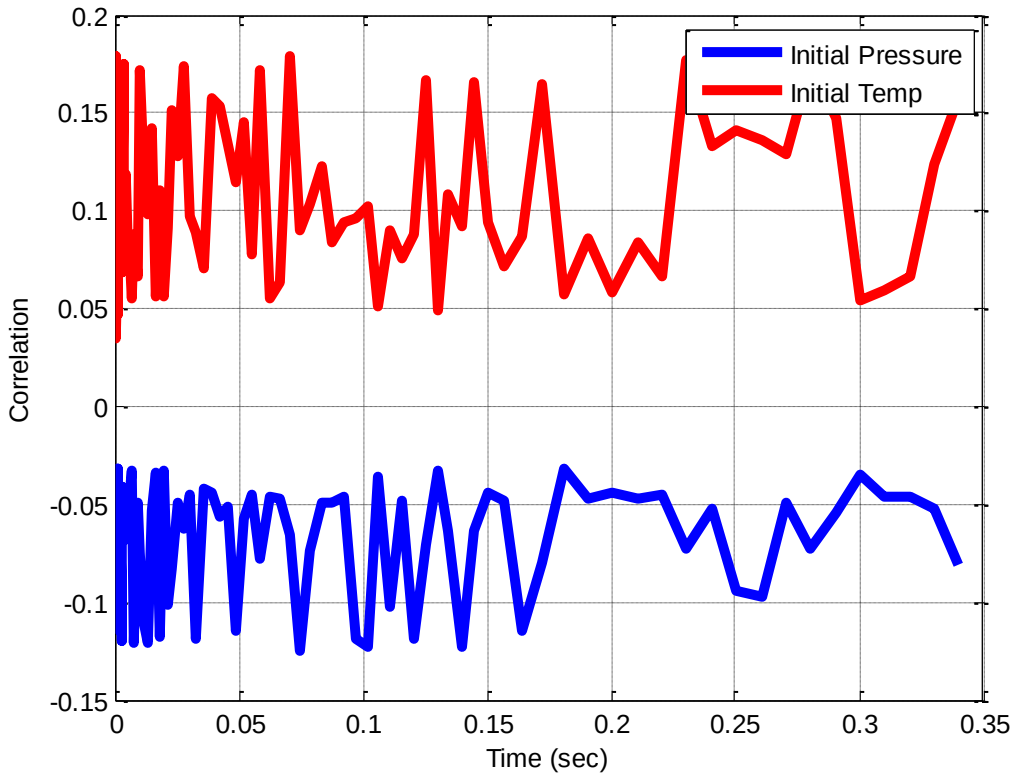

Figure 7.11 Mass flow sensitivity to Initial temperature and pressure

In figure 7.11, the correlation coefficient is plotted against time to establish the linear relationship between the input parameters (initial temperature and pressure) and the mass flow rate. From the figure it is evident that there is a positive correlation between the initial temperature and mass flow rate while a negative correlation is observed between the initial pressure and mass flow rate. The contribution of uncertainty in the initial temperature to the global uncertainty in mass flow rate is therefore expected to be more in comparison to uncertainty contribution from initial pressure.

7.3 Error Reduction for Turbine trip scenario

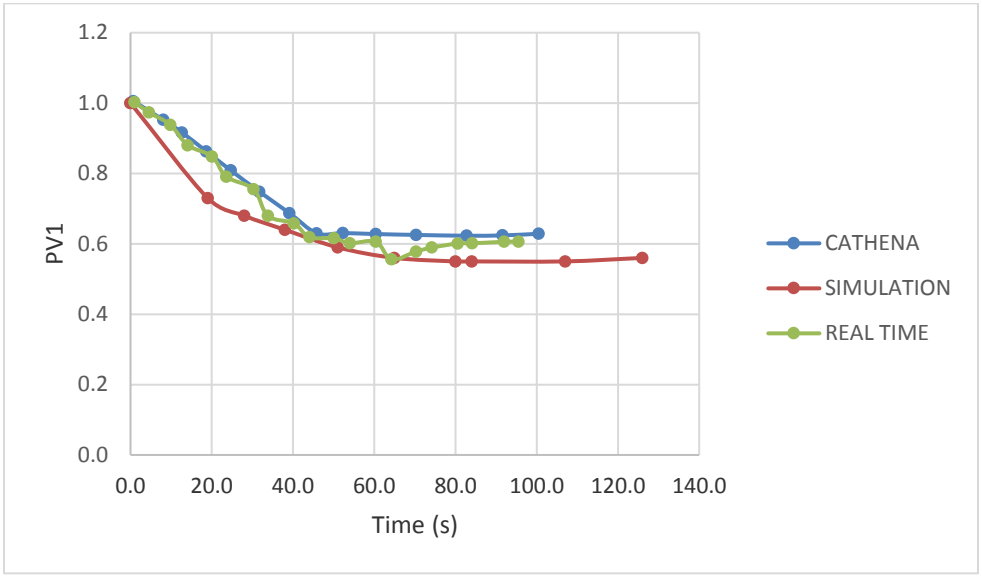

Figure 7.12 CATHENA, simulation and Real time results following a Turbine trip

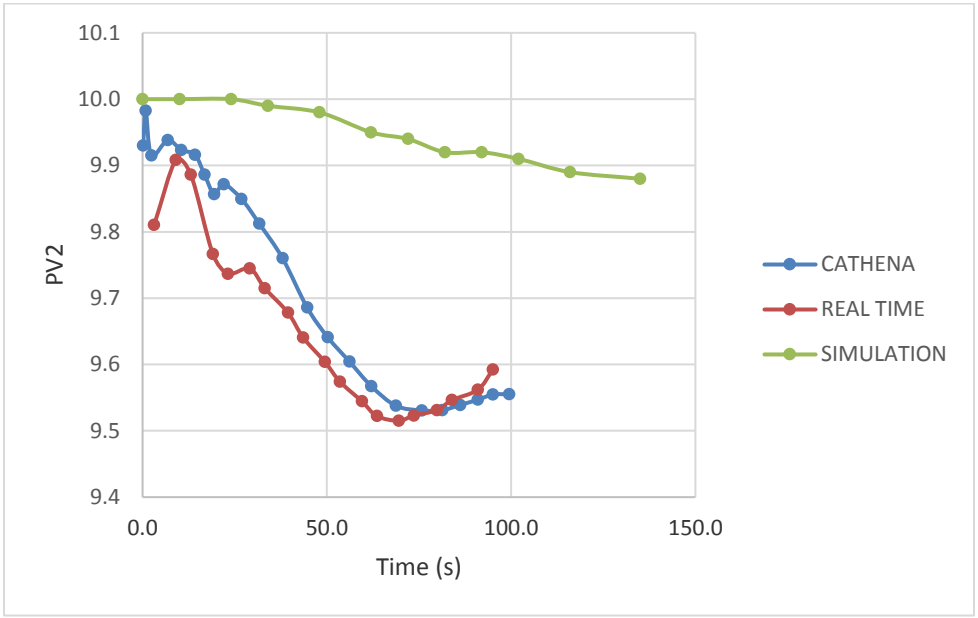

Figure 7.13 PV2 results by CATHENA, Simulation and Real time following a Turbine trip

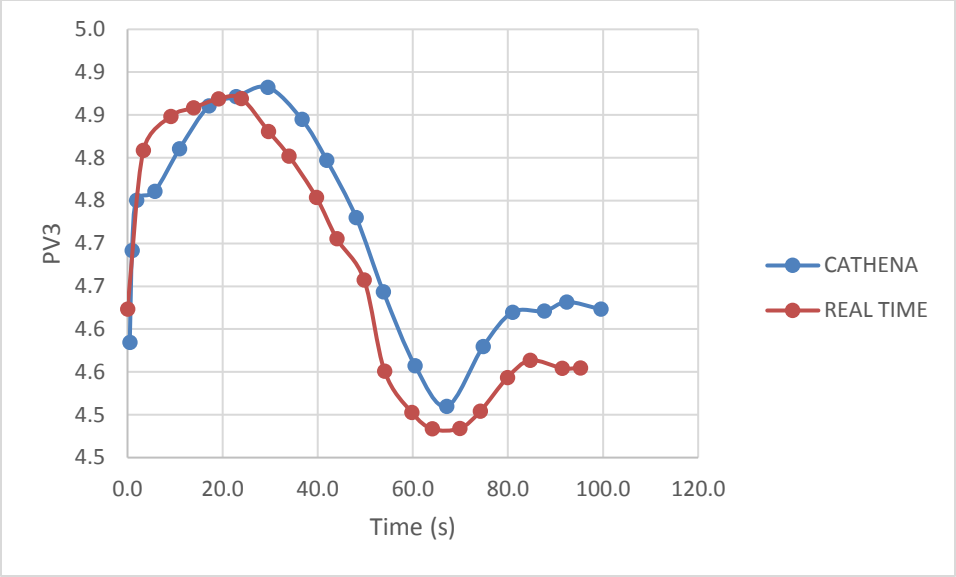

Figure 7.14 PV3 variation with time following a Turbine trip

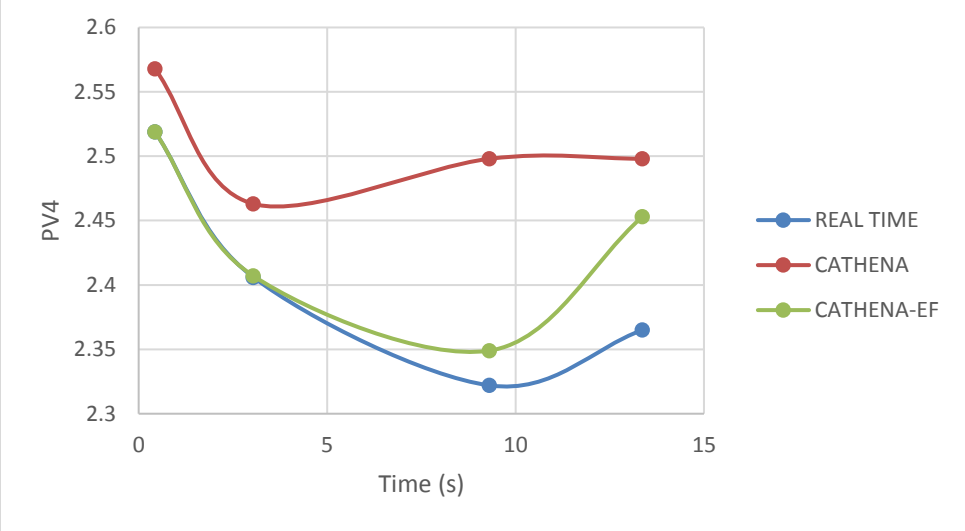

Figure 7.15 PV4 results with error function

Figures 7.12-7.14 are plots of results obtained from the following: running CATHENA simulations, experimental data and from the CANDU simulator. These results relate to case study 2 described in chapter 4. In figure 7.12, PV1 (Core thermal power) values are plotted against time following a turbine trip. The curve labeled CATHENA represents results from

CATHENA simulations [79], the curve labeled "SIMULATION" represents results obtained from the CANDU simulator while the curve labeled 'REAL TIME' represents experimental results [79]. The results presented in this section are related to the Uncertainty Quantification & Error reduction section in the methodology framework presented in chapter 3.

It is seen clearly from figures 7.12-7.14 that simulation results do not match real time data and as demonstrated in table 2.1, these differences can be within control or safety limits and may have implications on response actions in the event of reactor transients. In figure 7.15 however, a reduction is noticed in the error between simulation results by CATHENA and real time data after incorporating an error function. This error reduction is expected to go a long way in improving the accuracy of simulations in predicting fault propagation.

The error function used for reducing the error in figure 7.15 is given by equation 7.2.

$$EF = 0.0004x^3 - 0.0064x^2 + 0.0153x - 0.0544 \tag{7.2}$$

Where x is the time after the Turbine trip.

The mean absolute error (MAE) is given by equation 7.3,

$$MAE = \frac{\sum_{i=1}^{n} \left| y_i - \overline{p_i} \right|^2}{n} \tag{7.3}$$

Where y_i and $\overline{p_i}$ are the real time outputs and the average of the outputs of the models respectively.

The MAE between CATHENA and real time data represented in figure 7.15 is 0.019 while the MAE between the error model and real time is 0.012. The lower value of MAE by the incorporation of the error model indicates a more accurate model in relation to seeking a solution close to real time.

7.4 Risk Estimation for Steam Generator Tube Rupture (SGTR)

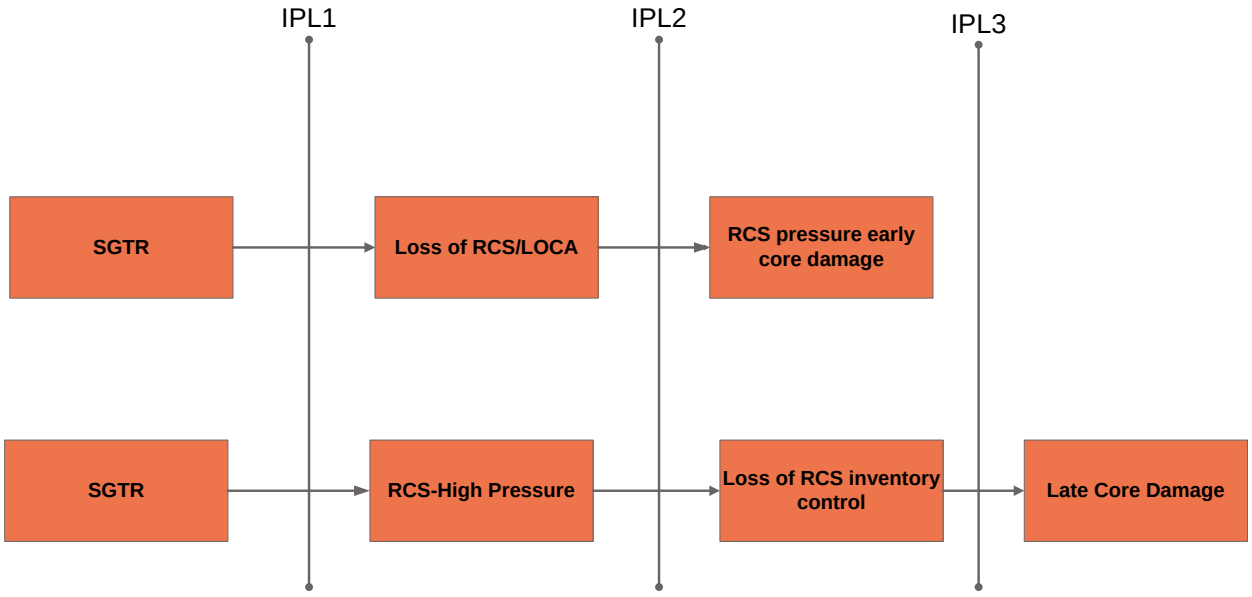

Figure 7.16 Fault propagation scenarios for Steam Generator Tube Rupture.

During the operation of a NPP, several initiating events may lead to the propagation of faults in various components. Steam Generator Tube Rupture (SGTR) is a phenomenon that is essential for consideration in performing safety assessment of SG integrity due to its degradation. Probability Risk Assessment (PRA) has been prescribed by the USNRC (NUREG-1570) for estimating the risks associated with operating a degraded SG. In this study, some results obtained from a PRA of SG integrity were used to perform safety verification of NPP based on some selected fault propagation scenarios.

Safety systems are designed as part of the plant to prevent the occurrence of initiating events. If, however these events do occur, there are still safety systems that act as Independent Protection Layers (IPLs) to check the propagation of faults. The vertical lines in figure 7.16 represent some of these IPLs which can be in the form of passive safety systems, inherent safety design or active safety systems. An initiating event may either lead to faults/failures or be curtailed by safety systems.

Figure 7.16 depicts some fault propagation scenarios that may result in large releases of fission products following the rupture of SG tubes. These releases may result from core damage if protection layers or systems fail. The first fault propagation scenario involves the occurrence of SGTR followed by loss of reactor cooling system (RCS) and core heat removal. This scenario requires once-through cooling, if it fails, a high RCS pressure early core damage occurs.

The second fault propagation scenario starts with SGTR occurring followed by a successful reactor trip and primary-secondary heat removal. The RCS however remains at high pressure and coolant inventory is assumed to be lost. RCS inventory control will be lost following the depletion of the Reactor Water Safety Tank (RWST). The High Pressure Safety Injection (HPSI) suction will be aligned to an empty containment sump. This scenario leads to a late core damage.

Safety verification involves a comparison between the total risk associated with a process and the target risk. The target risk is usually set by the regulatory body such as the USNRC, CNSC or the IAEA. Risk estimation methods described earlier were used to estimate the total risk associated with the fault propagation scenarios identified. This result was then

compared with the risk target set by the USNRC for safety verification. In estimating the risk for a fault propagation scenario, the following equation was used.

$$Risk(path - i) = R_i \times PFDi \times..\times R_n \times PFDn \quad (7.4)$$

Where the meaning of the terms are described in table 7.1.

Table 7.1 Risk estimation parameters

Symbol	Description	Magnitude
R1	Steam Generator Tube Rupture	2.7
R2	Early core damage	5.5E-08
R3	Late core damage	5.5E-08
R4	Loss of RCS/LOCA	2.4E-15
PFD1	Probability of failure on demand of IPL1	0.05
PFD2	Probability of failure on demand of IPL2	0.01
PFD3	Probability of failure on demand of IPL3	0.0045

The total risk estimation is given as,

$$Total\ Risk = \sum_{i=1}^{n} Risk(path - i) \quad (7.5)$$

From equation 7.4, the risk associated with fault propagation path 1 is estimated as,

$$Risk(path - 1) = R_1 \times PFD1 \times R_2 \times PFD2 \times R_3 \quad (7.6)$$

$$= 2.7 \times 0.05 \times 5.5E - 08 \times 0.01 \times 5.5E - 08$$

$$\approx 4.08E - 18$$

Risk associated with fault propagation path 2 is estimated as,

$$Risk(path-2) = R_1 \times PFD1 \times R_2 \times PFD2 \times R_3 \times PFD3 \times R_4 \quad (7.7)$$

$$= 2.7 \times 0.05 \times 5.5E-08 \times 0.01 \times 5.5E-08 \times 0.0045 \times 2.4E-15$$

$$\approx 4.41E-35$$

Therefore, the total risk is estimated from equation 7.5 as,

$$Total\ Risk = Risk(path-1) + Risk(path-2)$$

$$\approx 4.08E-18 + 4.41E-35$$

$$\approx 4.08E-18$$

The USNRC safety goal states that the cancer fatality risk associated with exposure from NPP accidents to the population near an operating NPP should not exceed one-tenth of one percent [25]. The target risk considered in this study therefore was 1.0E-03. Since the estimated risk is far lower than the target risk, the SGTR accident considering the fault propagation scenarios evaluated is safe.

The risk estimation results presented in this section were based on selected fault propagation scenarios related to SGTR accident. In order for a direct application of uncertainty quantification results in this context, the scenarios presented above need to be extended to include the analysis of more safety systems and their possible failure. As part of an extension of the current study in the future, a more comprehensive number of fault propagation scenarios would be evaluated. A direct application of uncertainty quantification results would then be possible.

7.5 Results of CATHENA Simulation of Edward's Blowdown Problem

CATHENA simulation results are presented in this section. The model considered here has been described earlier in chapter 3.

Mass flow rises from zero to about 160 kg/s within 0.02 seconds, then falls smoothly to almost zero by 0.4 seconds. The pressure near the ruptured disc drops off quickly as the water there becomes steam almost immediately, while the pressure at the closed end drops off more slowly. Pressure recovery starts at about 0.004 seconds. This is caused by a pressure wave being reflected off the closed end of the pipe and moving back towards the open end. Pressure then bleeds down to atmospheric by ~0.4 seconds. The void near the rupture disc goes from 0.0 to ~0.6 within about 0.04 seconds, then more slowly to 1.0 by ~0.4 seconds. Void near the closed end rises more slowly, reaching ~0.2 by about 0.08 seconds, then more quickly to ~0.8 by about 0.15 seconds, then approaching 1.0 asymptotically by the end of the simulation. The above can be seen in figures 7.17-7.20.

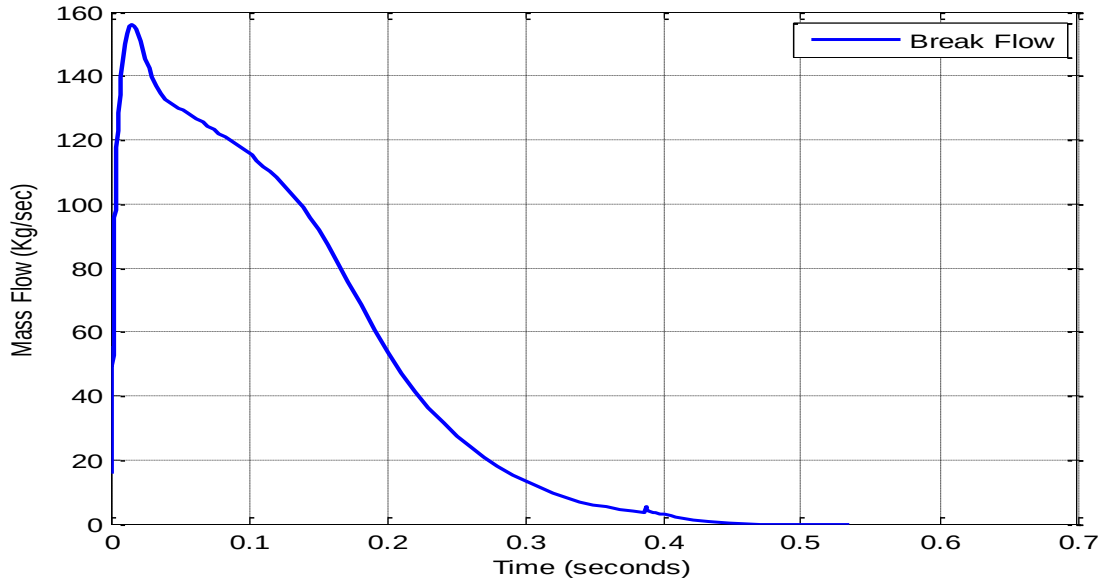

Figure 7.17 Mass Flow Rate during pipe blowdown transient.

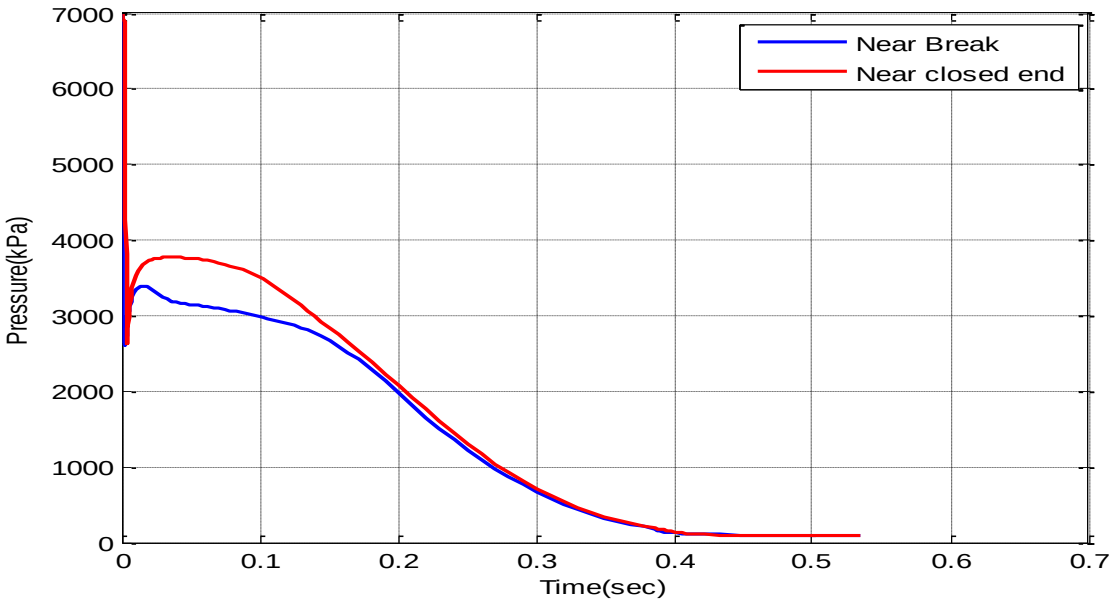

Figure 7.18 Pressure (Entire simulation) during pipe blowdown transient.

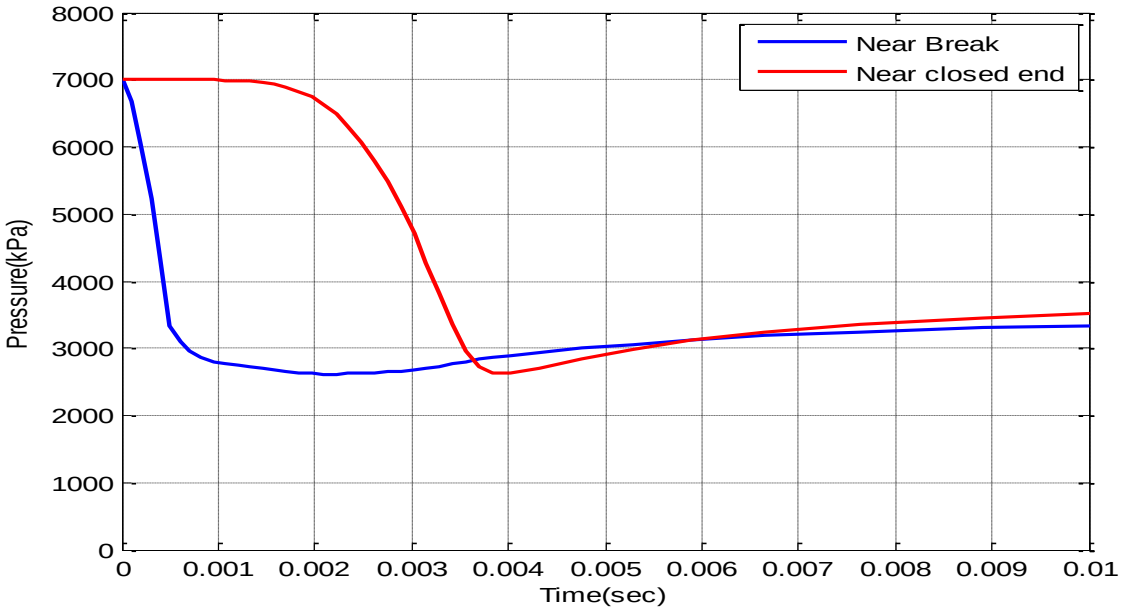

Figure 7.19 Pressure (Smaller time step) during pipe blowdown transient.

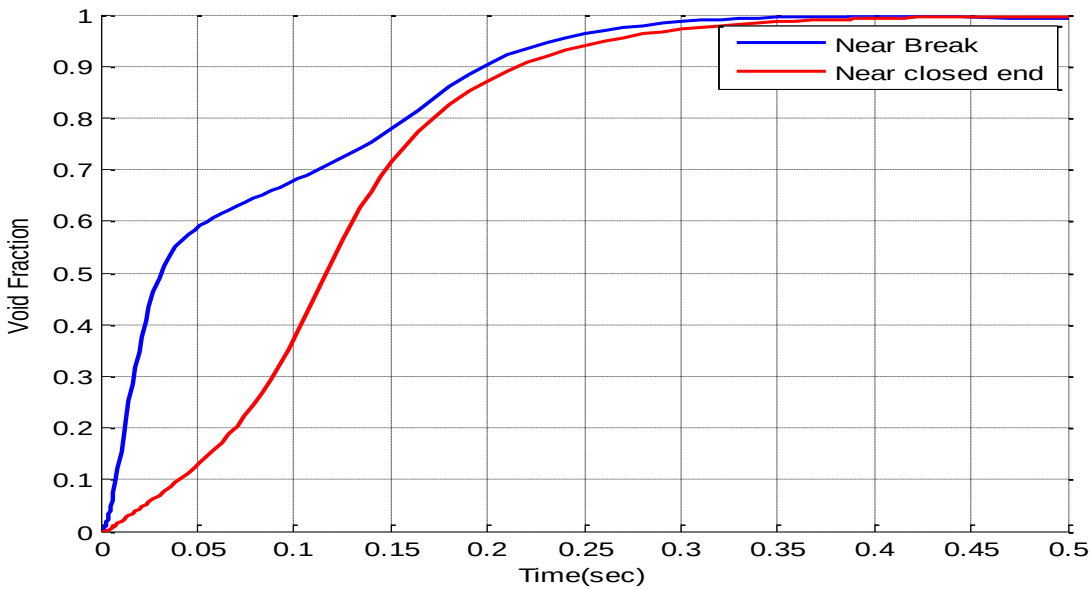

Figure 7.20 Void Fraction during pipe blowdown transient

7.6 FSN Results for Case Study 1

In order to illustrate the FSN methodology described in chapter 3, an example of a steam generator used in CANDU and other NPPs is selected for this purpose. Table 7.2 shows the FSN for this case. The example shows symptoms that can be observed during plant operation and for each symptom, a semantic network may be defined as well as a prediction of the likely causes for observing such a symptom. Both Fuzzy Expert System (FES) and Bayesian Belief Network (BBN) can be appropriately used as the semantic network for the symptoms.

Table 7.2. FSN case for steam generator system

Symptom ID	Symptom	Impact	Semantic Network (BBN/FES)	Causes
1	Low SG1 level	0.7	FES 1	C1, C3
2	Low Reactor Power	0.3	BBN 1	C1, C2
Cause ID	Cause	Impact		Diagnosis
1	Impaction of particles	0.25		D1
2	Incorrect Installation	0.25		D2
3	Sensor Degradation	0.5		D3
Diagnosis ID	(Sensor, Features)	Impact		Repair
1	D1: (S1,F1)	0.69		R1
2	D2: (S1,F2)	0.75		R2
3	D3: (S2,F3)	0.45		R3
Repair ID	Repair	Impact		
1	Clean Valve	0.33		
2	Proper Installation	0.33		
3	Sensor Replacement	0.33		

Sensor ID	Name	Location	Description
S1	LCV 101	Steam Generator Level Ctrl.	Liquid control valve opening (%)
S2	Flow Transmitter	Steam Generator 1 inlet	Flow Transmitter at feedwater inlet

Feature ID	Name	Description	Detection
F1	LCV 101 fails open	Liquid Control valve fails in the open position	LCV 101 remains at 100% open, Steam Generator 1 level increase, Turbine trip
F2	LCV 101 fails closed	Liquid Control valve fails in the closed position	LCV 101 remains at 0% open, Steam Generator 1 level decrease, Reactor trip
F3	SG1 FW FT Irrational	Steam Generator 1 feedwater flow transmitter irrational	Flow transmitter reads -1.0, Steam Generator 1 level increase, Reactor neutron power decrease slightly

Finally, the FSN is made up of a sensor component which describes some sensors that are used to measure and indicate the features of interest as well as a description of relevant features/faults and how they are detected.

7.6.1 Utilizing Fuzzy Expert System (FES) in FSN

Fuzzy logic can be utilized in representing human expert knowledge in a particular domain of application and in reasoning with that knowledge in order to arrive at useful inferences or actions. The conventional binary logic is crisp and allows for only two states (TRUE or FALSE). This logic is therefore not suitable for handling fuzzy descriptors, such as “fast”, “slow” and “weak”. Fuzzy logic permits the extension of binary, crisp logic to qualitative, subjective, and approximate situations, which characterize majority of real life and engineering problems. The application of fuzzy logic in control systems for example results in more optimal control of such systems. Fuzzy logic tolerates the use of imprecise data. Since imprecise knowledge characterizes most problems, the use of fuzzy logic to

incorporate such imprecise into a system has advantages over conventional techniques based on binary logic. The use of fuzzy logic in control systems for instance is also flexible compared to conventional control algorithms such as the proportinal-integral-derivative controller. Fuzzy reasoning is easy since the mathematical concepts that form the foundation of fuzzy logic are simple to understand. In fuzzy logic, the knowledge base is represented by if-then rules of fuzzy descriptors. An example of a fuzzy rule applied in FSN for the steam generator would be, "If the steam generator level is low and the neutron power is normal, then failure mode is "LCV fails closed", which contains the fuzzy descriptors *low* and *normal*. A fuzzy descriptor is usually represented by a membership function. This function assigns a membership grade between 0 and 1 for each possible value of the fuzzy descriptor it represents where a membership grade of 1 implies a 100 % certainty of an element in that set.

A fuzzy inference system has been demonstrated for the selected steam generator system by implementing the following processes in order to arrive at a set of fuzzy rules applicable in the FSN.

1. A set of linguistic rules (protocols) made up of fuzzy variables as inputs (process variables) and output (failure modes) were developed.

2. A set of membership functions for process output variables and input variables were obtained based on the knowledge of the system behavior.

3. The "fuzzy AND" operation (min) and the "fuzzy implication" operation (min) were applied on each rule in Step 1, and Step 2 was used to obtain the multivariable rule base

function Ri (a multidimensional array of membership values in the discrete case) for that rule.

The steps outlined above were used with the aid of the CANDU 9 simulator to obtain the following rule base, which was implemented using the "fuzzy logic" toolbox in MATLAB [87]:

1. *IF "NP" IS "N" AND "SGL" IS "H" AND "LCVO" IS "VH" THEN "Failure Mode" IS "LCV101 fails open"*
2. *IF "NP" IS "L" AND "SGL" IS "VH" THEN "Failure Mode" IS "LCV101 fails open"*
3. *IF "NP" IS "VL" AND "SGL" IS "L" AND "LCVO" IS "VH" THEN "Failure Mode" IS "TURBINE TRIP"*
4. *IF "NP" IS "N" AND "SGL" IS "L" AND "LCVO" IS "VL" THEN "Failure Mode" IS "LCV101 fails closed"*
5. *IF "NP" IS "N" AND "SGL" IS "VL" AND "LCVO" IS "VL" THEN "Failure Mode" IS "LCV101 fails closed"*
6. *IF "NP" IS "L" AND "SGL" IS "VVL" THEN "Failure Mode" IS "LCV101 fails closed"*
7. *IF "NP" IS "N" AND "SGL" IS "H" AND "LCVO" IS "H" THEN "Failure Mode" IS "FW FT irrational"*
8. *IF "NP" IS "N" AND "SGL" IS "H" AND "FF" IS "VL" THEN "Failure Mode" IS "FW FT irrational".*

Where, N=Normal, H=High, VH=Very High, L=Low, VL=Very Low, VVL=Very Very Low, NP=Neutron Power, SGL=Steam generator 1 level, LCVO=LCV101 opening (%), FF=Feed Flow and FW FT=Feedwater flow transmitter.

Figures 7.21-7.26 show plots of fuzzy surfaces and membership functions for the fuzzy inference system described above. The triangular membership function was selected due to its extensive use in literature.

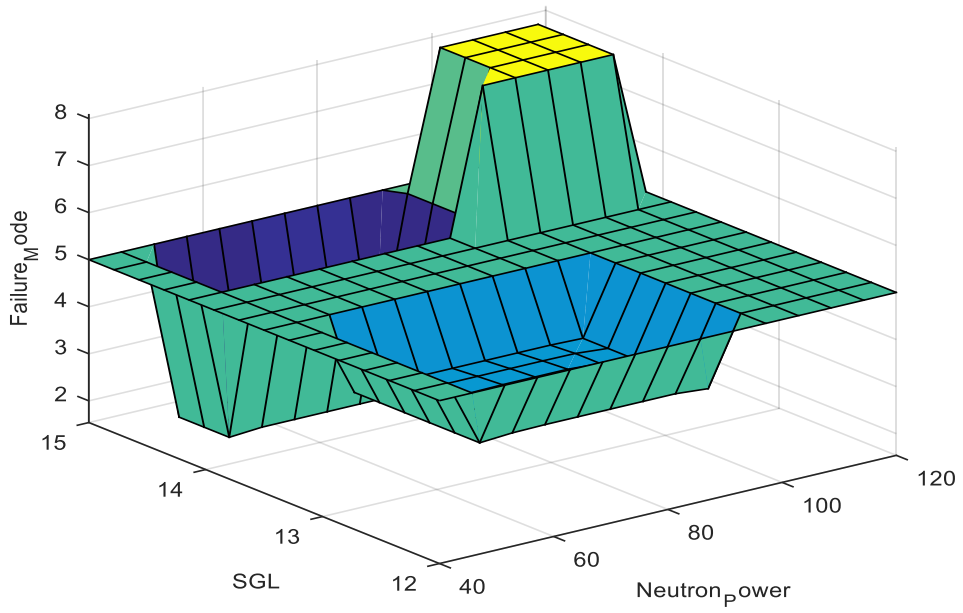

Figure 7.21 ‘NP’ against ‘SGL’ fuzzy surface plot

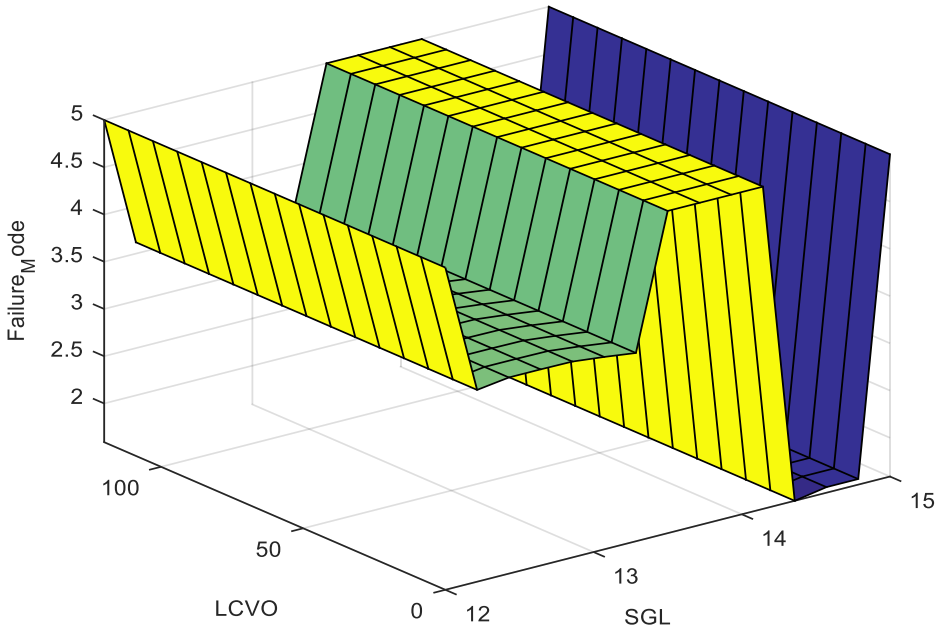

Figure 7.22 ‘SGL’ against ‘LCVO’ fuzzy surface plot

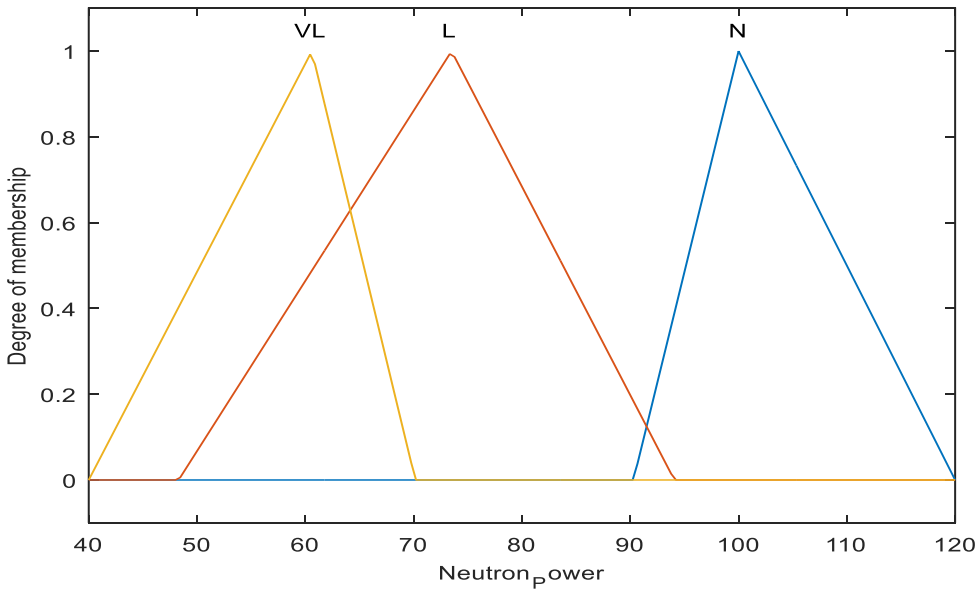

Figure 7.23 ‘NP’ membership functions

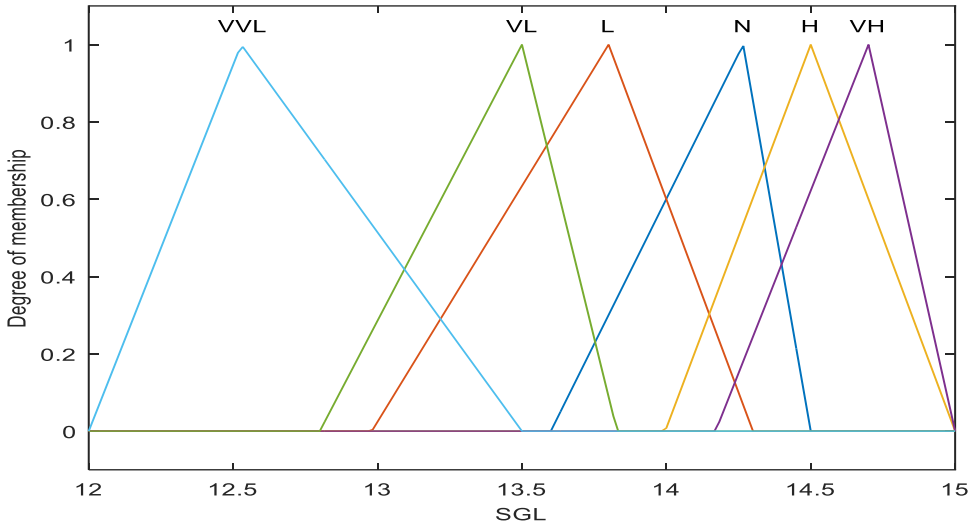

Figure 7.24 ‘SGL’ membership functions

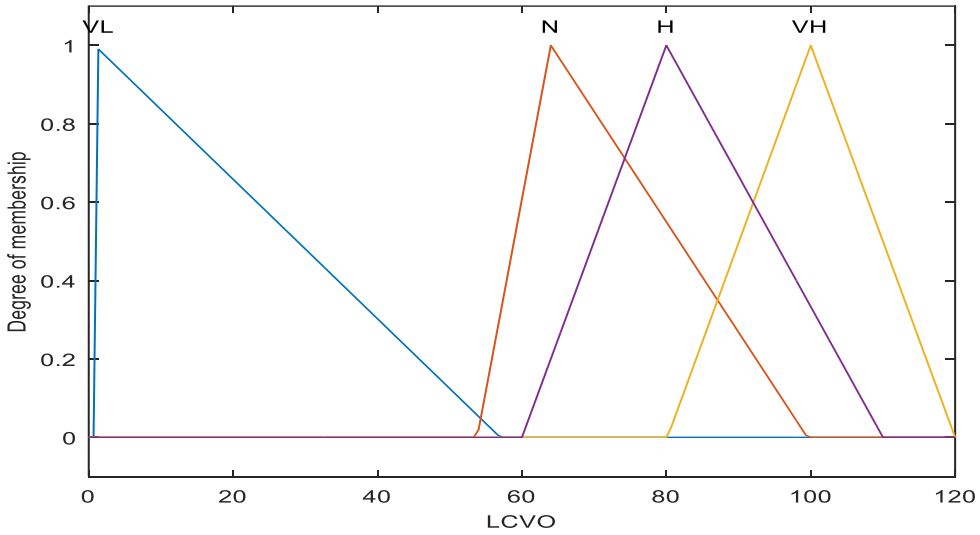

Figure 7.25 ‘LCVO’ membership functions

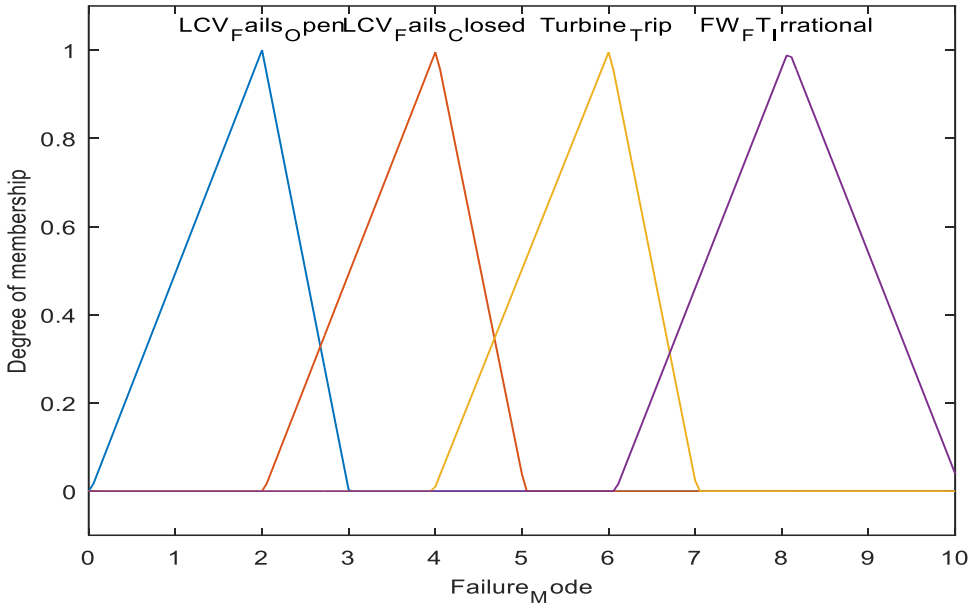

Figure 7.26 Failure Mode membership functions

7.6.2 Bayesian Belief Network (BBN) Application in FSN

BBN mainly involves the compact representation of joint probability distributions using conditional independence. It is made up of both qualitative and quantitative parts. The qualitative part is referred as directed acyclic graph (DAG) which comprises nodes (random variables) and edges (direct influence). The quantitative part comprises a set of conditional probability distributions. BBN is useful due to the possibility of representing knowledge in a modular form as well as internal algorithms for inference and learning.

In applying BBN for FSN, posterior probabilities (evidence based probabilities of events) are used to explain the causes of faults based on observed symptoms. Human expert knowledge of a system, historical data and simulation results are used to construct the

BBN. The inference mechanism in BBN is utilized in the FSN either to diagnose, predict or identify inter-causal faults. Symptoms of faults are entered as evidence and the inference mechanism is able to identify likely causes in the diagnosis. Based on the evidence of process variable values, faults can be predicted using the inference mechanism. A combination of causes can also be used to infer a symptom using the inference mechanism.

BBN is constructed for the steam generator case of a CANDU NPP. Fault propagation, symptoms and node probabilities are assigned based on scenario simulation using the CANDU 9 simulator [84] as well as expert knowledge of the plant operation.

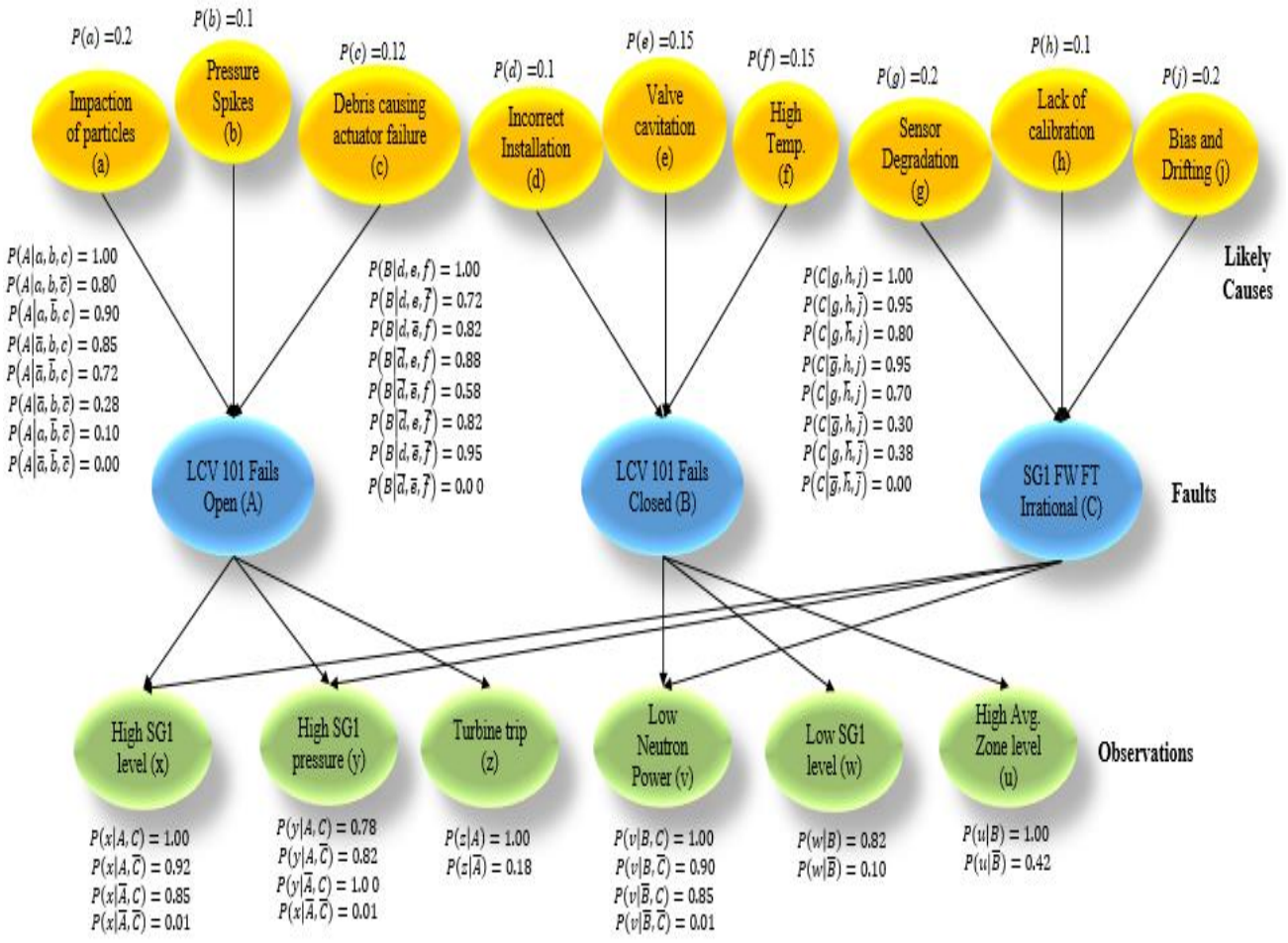

Figure 7.27 BBN for Steam Generator faults

In figure 7.27, the BBN structure for steam generator faults is shown. Likely causes of faults are indicated together with the various faults and the resulting observations. The prior probabilities as well as the posterior probabilities obtained after learning and inferencing the BBN are also shown in the figure. The BBN can be queried in various ways in order to obtain posterior probabilities as described below:

Diagnostic Query

If '*High SG1 level (x)*' is observed, what is the probability that the cause is '*Impaction of particles (a)*'?

Answer:

$$P(a|x) = 29\ \%\ \text{True}$$

71 % False

Therefore, there is a 29 % probability that '*High SG1 level (x)'* observed was caused by the *Impaction of particles (a)'*.

Predictive Query

What is the probability of observing a '*Turbine trip (z)*' given that '*Pressure spikes (b)*' had occurred?

Answer:

$$P(z|b) = 54\ \%\ \text{True}$$

46 % False

Therefore, there is a 54 % probability of observing a '*Turbine trip (z)'* following the occurrence of '*Pressure spikes (b)*'.

Inter-causal Query

What is the probability that a '*Turbine trip (z)*'observed was caused by a combination of '*Pressure spikes (b)'* and '*Bias and drifting (j)*'?

Answer:

$$P(z|b,j) = 52\ \%\ \text{True}$$

48 % False

Therefore, there is a 52 % probability that '*Turbine trip (z)'* observed was caused by a combination of *'Pressure spikes (b)' and 'Bias and drifting (j)'.*

7.7 Linking Uncertainty Quantification Results with FSN

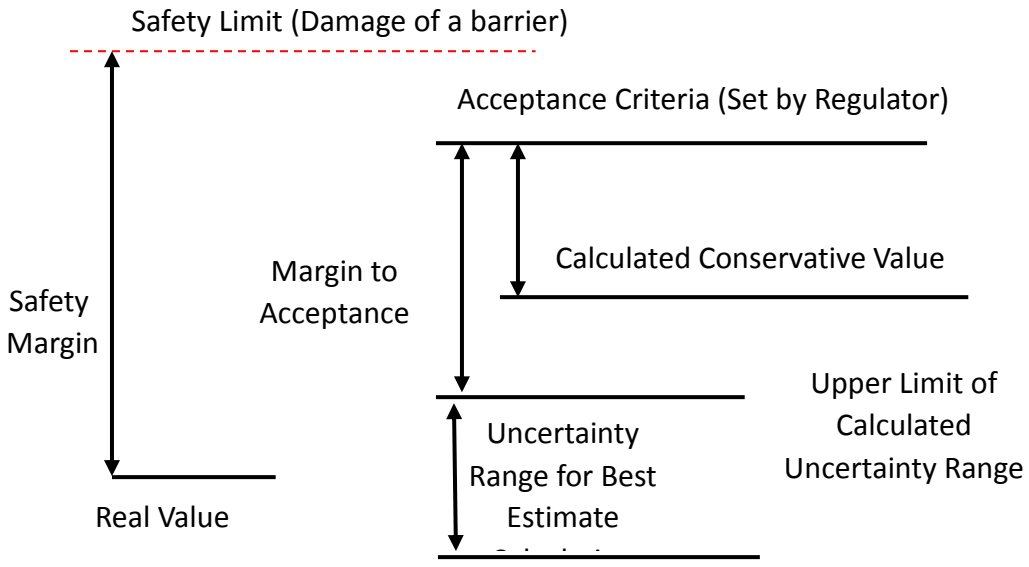

Figure 7.28 Safety Margins Concept [89]

In the conservative approach, the results of parameter estimates are limited by acceptance criteria set by the regulatory bodies. In the best estimate approach, uncertainty ranges are used to express parameter results calculated as shown in figure 7.28. Safety margins can therefore be reduced with the knowledge of uncertainties and sensitivities associated with code calculations as has been shown in this thesis.

The Fault Semantic Network (FSN) can be linked with uncertainty quantification results in the following manner: in FSN, rules are used to describe the transition between different plant states. These rules can be updated using knowledge obtained from the uncertainty quantification exercise. The updated rules reflect the fact that safety margins would be reduced without compromising the acceptance criteria as long as the upper limit of the uncertainty range is not exceeded. FSN rules related to the RD-14 facility can be updated with the uncertainty quantification results as follows:

(1) If *"Pressure"* is less than 7.4 MPa and less than 5.56 MPa, then *"Failure Mode"* is *"Unsafe".*

(2) If *"Pressure"* is greater than 7.4 MPa and less than 9.24 MPa, then *"Failure Mode"* is *"Safe".*

(3) If *"Pressure"* is greater than 7.4 MPa and greater than 9.24 MPa, then *"Failure Mode"* is *"Unsafe".*

(4) If *"Temperature"* is less than 270 ^{0}C and less than 233 ^{0}C, then *"Failure Mode"* is *"Unsafe"*.

(5) If *"Temperature"* is greater than 270 ^{0}C and less than 307 ^{0}C, then *"Failure Mode"* is *"Safe"*.

(6) If *"Temperature"* is greater than 270 ^{0}C and greater than 307 ^{0}C, then *"Failure Mode"* is *"Unsafe"*.

The above rules can be continuously updated in the FSN rule base and this can be used to perform safety verification for any operating plant under various conditions. Under any normal or abnormal operational scenario, the FSN can be utilized to provide insight into the plant safety status. This insight would be based on the defined rule base. In this manner, the use of uncertainty quantification results and FSN would provide a good means for safety verification and enhancement.

Fuzzy rules which form the integral FSN rule base will be updated using the above results. The process of updating these rules will include modifications of the rules to reflect these results. Tuning of the FSN will involve changing the fuzzy membership functions for process variables as inputs and failure modes as outputs. The updated membership functions will then be applied to the overall system and new evidence of plant conditions will be compared to the updated membership functions for appropriate feedback and actions.

CHAPTER 8: CONCLUSIONS AND RECOMMENDATIONS

8.1 Review

This chapter concludes this thesis and presents some recommendations. The main innovative contributions of the thesis are outlined and major aspects of the methods developed in the thesis are highlighted. Main results obtained and their significance are also presented. The chapter concludes with recommendations for further studies and useful applications of results presented in this thesis.

8.2 Conclusion

This thesis has presented uncertainty quantification and fault diagnosis methods. It has also reviewed existing literature relevant to the study. The methodology framework based mainly on the stochastic uncertainty quantification approach and safety verification based on FSN were presented and some case studies were described. The issue of NPP safety is essential and this study is expected to enhance current safety analysis and verification tools.

A stochastic uncertainty and sensitivity analysis method has been presented in this study. The methodology discussed has promising potential for safety analysis applications in the nuclear and other industries. Although computationally expensive in terms of time taken to complete code simulations, the use of high performance computing techniques is expected to minimize the effect of such draw backs.

The global uncertainty in output pressure was estimated by computing the standard deviation after varying two input parameters within specified ranges. The global uncertainty obtained for output pressure was approximately 0.61 % and that for mass flow

rate was 0.57 %. The significance of the global uncertainty in terms of the input uncertainty contributions was obtained after computing the correlation coefficient between inputs and the outputs for a specified number of time steps. For the number of time steps considered, the total correlation coefficient between initial pressure and the output pressure was approximately 1.0 while that between the initial temperature and output pressure was approximately 0.6. This implies that there is approximately 1.73KPa change in output pressure expected given a 10 % covariance in initial pressure and an initial temperature uniformly distributed between 200 and 300^0 C temperature. The initial pressure however contributes more to this uncertainty observed in the output pressure. For the mass flow, there is a 50.52 Kg/s change expected given a 10 % covariance in initial pressure and an initial temperature uniformly distributed between 200 and 300^0 C.

A methodology has been presented for fault propagation analysis in NPPs based on FSN. Both the fuzzy logic method and the Bayesian Believe Network which is based on conditional probability were used to demonstrate the FSN. The FSN uses expert knowledge, operational history and simulation results as input in developing a database for subsequent analysis. The fuzzy inference system consists of inputs (process variables) and outputs (failure modes) as well as membership functions. The BBN consists of estimated prior probabilities and posterior probabilities as well as an inference mechanism.

A case study of faults associated with the steam generator in a CANDU was used to demonstrate the methodology presented. The results show that the FSN is capable of providing valuable information useful for plant safety and for executing effective maintenance activities. The proposed methodology when extended to more systems of an NPP can be implemented and deployed in real time as a co-simulation tool. In this way,

both operating organizations of NPPs as well as industry regulators may find this tool useful for safety verification purposes as well as for accident and disaster prevention. In this regard, the proposed solution method can serve as a valuable tool that gives insight to operators and decision makers in order to implement timely intervention to prevent catastrophic scenarios.

Although the methods developed in this study were demonstrated using applications related to nuclear power plants, these methods can also be applicable in other industries and disciplines. In the automotive industry for example where unmanned vehicle technology is currently under research and development, the methods developed in this work can be useful in enhancing safety of automated driving when implemented.

8.3 Innovative Contributions of this Study

This study was undertaken to develop and implement methods for performing uncertainty quantification and to verify the safety of NPPs. The proposed methods were applied to quantify uncertainty and demonstrate safety verification in real world scenarios. The main contributions of this study are summarized as follows:

8.3.1 Stochastic Uncertainty Quantification Framework

1. A framework for performing uncertainty quantification for safety verification applications has been developed. The framework integrates conventional computational tools to facilitate uncertainty and sensitivity analysis with the advantage of providing more information to analysts and code developers on output parameter characteristics and distributions. In comparison with the conservative

approach, the proposed framework when implemented is expected to enhance understanding of safety margins when undertaking safety analysis. The stochastic uncertainty and sensitivity approach proposed will provide a valuable means of estimating distributions of safety important parameters that may be used by code developers, users and regulators to achieve better output during safety verification.

2. The Fault Semantic Network (FSN) based on the Bayesian Belief Network was used to demonstrate safety verification in NPPs. This approach if extended to cover other plant systems would enhance safety analysis of existing plants throughout their life cycle. With the development of a comprehensive database of faults, process variables (PVs) and interactions between PVs, the FSN would play a significant role in fault diagnosis, propagation analysis and safety verification if implemented in existing plants.
3. The link between FSN and uncertainty quantification results has been established. This will enable the updating of the FSN rule base for safety verification of operating plants under various conditions. The updated rule base can be used to effectively tune the FSN based on evidence. In this way, the status of any plant or process can be effectively estimated given the dynamic nature of conditions that may prevail at any given time.

8.3.2 Case Studies

The uncertainty quantification and safety verification methods proposed in this study were applied to a total of four case studies. Two transients (small break LOCA and pipe blowdown) were simulated with CATHENA and input parameter uncertainty propagation

was performed. Two faults (liquid control valve failure and turbine trip) were simulated using the CANDU 9 simulator and the results were used to demonstrate safety verification with FSN. These cases are regarded credible with significant impacts on plant safety and operation.

8.4 Recommendations and Future Work

Based on the results obtained in this study, the following recommendations and an outlook on the future direction of the research are presented in this section.

8.4.1 Recommendations

To Plant Owners and Operators: It is recommended that current trends and best practices in performing safety analysis such as using the probabilistic approach is embraced. The probabilistic approach may be used as a supplemental methodology to the existing deterministic methods being used. In this way, safety and plant economics would be enhanced due to better understanding of realistic safety margins and limits.

To Industry Regulators: It is highly commendable that regulatory bodies such as the CNSC and NRC are engaged with various stakeholders in conducting research in the use of stochastic methods for performing safety analysis. The use of best estimate codes supported by uncertainty and sensitivity analysis has been identified to play a major role in demonstrating the safety case of existing power plants as well as new builds. Particularly, extensive research is required in the use of stochastic uncertainty quantification methods such as in the coupling of neutronic and thermal hydraulic codes to simulate transient and accident scenarios.

To Code Developers: As identified in chapter 2, the sources of uncertainties associated with code simulations are many and the task of minimizing these uncertainties is a huge one. It is recommended that results from researchers such as those presented in this thesis be taken into account during code revisions and design. This would contribute to enhancing code accuracy in predicting complex processes such as transients that may occur in power plants.

8.4.2 Future Work

The following are proposed for the future direction of this research:

8.4.2.1 Use of SUSA and Other Codes

Input parameter uncertainty propagation was investigated in this study. Input parameters were varied and the effects on selected outputs were estimated. It is expected that other stochastic tools such as SUSA developed by GRS would be used to perform uncertainty and sensitivity analysis. SUSA facilitates the use of more input parameters than those used in this study.

8.4.3 Proposed Implementation in Operating Plants

The methods developed in this study are proposed to be implemented in existing operating plants such as Bruce Power, Pickering and Darlington. As an example, the following is a summary of such a proposal with Bruce Power comprising objectives, research activities, deliverables and expected benefits:

8.4.3.1 Objectives

(1) Identify uncertainties, rank their importance and estimate their influence on safety parameter computations.

(2) Avoid risk by reaching an acceptable quality level.

(3) Demonstrate compliance with regulatory thresholds.

8.4.3.2 Research Tasks

(1) Perform uncertainty quantification for selected scenarios using stochastic methods (Phase 1).

(2) Identify best estimate codes, select and simulate fault scenarios (Phase 1).

(3) Perform sensitivity analysis for selected scenario with available methods such as SUSA and COSSAN-X (Phase-1).

(4) Validate uncertainty quantification and sensitivity analysis results obtained (Phase-1).

8.4.3.3 Deliverables

(1) Program Code: provide Bruce Power the code of the proposed system for safety verification and compliance support, which could run on their computer systems, as integrated with existing safety analysis systems.

(2) Training: conduct a training session for Bruce Power personnel on the use of the proposed system.

(3) Publication: publish two manuscripts to reflect the proposed innovation (1 conference paper and 1 journal paper) (Phase-1).

(4) Final Report: submit the final report, which includes simulation and test results using selected case studies and recommendations (Phase-1).

8.4.3.4 Expected Benefits

(1) Estimate the probability distributions of important safety parameters instead of single values of unknown accuracy.

(2) Enhance the validation of thermal hydraulic codes for safety analysis applications.

(3) Satisfy regulatory requirements on demonstrating safety margins and acceptance criteria for best estimate computer codes.

(4) The sensitivity analysis would provide useful information for code improvement, design modifications and uncertainty reduction.

REFERENCES

[1] Hossam A. Gabbar, Emmanuel K. Boafo. 2016. FSN-based co-simulation for fault propagation analysis in nuclear power plants. *Process Safety Progress*, vol 35, no. 1, pp 53-60.

[2] Bhushan, M., Rengaswany, R. Design of sensor location based on various fault diagnostic observability and reliability criteria. *Computers and chemical engineering*, Vol 24(2000).735-741.

[3] Demuth, H., Beale, M., Hagan, M. MATLAB Neural Network Toolbox 5, Users guide (2007).

[4] Gabbar, H.A. Integrated framework for safety control design of nuclear power plants. *Nuclear Engineering and Design* 240(2010) 3550-3558.

[5] Gabbar HA. Qualitative fault propagation analysis. *Journal of Loss Prevention in the Process Industries* 2007; 20(3):260–70.

[6] Gabbar, H. A. Design of computer-aided plant enterprise safety management in plant enterprise engineering environment. Ph.D. thesis, Okayama University, Graduate School of Natural Science & Technology, 2001.

[7] Gabbar, H.A. Improved qualitative fault propagation analysis. *Journal of Loss Prevention in the Process Industries* 20 (2007), 260–270.

[8] Gabbar, H. A., Sayed, H. E., Osunleke, A. S., Masanobu, H. Design of fault simulator. *Reliability Engineering and System Safety* 94 (2009) 1289–1298.

[9] Gabbar, H.A. Fault semantic networks for accident forecasting of LNG plants. Knowledge-based and Intelligent Information and Engineering Systems, Lecture Notes in Computer Science 6277 (2010), 427–437.

[10] Gross, K.C., Singer, R.M., Wegerich, S.W., Herzog, J.P. Application of a model-based fault detection system to nuclear plant signals. In: Proceedings of the *9th International Conference on Intelligent Systems Applications to Power Systems*, 6e10 July 1997, Seoul, Korea.

[11] Haasl, D. F. Advanced concepts in fault tree analysis. System safety symposium. Seattle: Boeing Company, (1965) pp. 8–9.

[12] Hadad, K., Mortazavi, M., Safavi, A., Mastali, M. Enhanced neural network based fault detection of a VVER nuclear power plant with the aid of principal component analysis. *IEEE Trans Nuclear Science* 55 (2008), 6e3611.

[13] Hart, R.S. CANDU Technical Summary. Atomic Energy of Canada Limited (AECL). Revised Edition, 1997.

[14] Iri, M., Aoki, K., O"Shima, E., Matsuyama, H. "An Algorithm for Diagnosis of System Failures in the Chemical Process" *Computer & Chemical Engineering*, Vol.3 (1979). pp.489.

[15] Lee, S.J., Seong, P.H. Development of automated operating procedure system using fuzzy colored petri nets for nuclear power plants. *Annals of Nuclear Energy* 31(2004) (8), 849–869.

[16] A. Saltelli, K. Chan, E. Scott, Sensitivity Analysis, Wiley Series in Probability and Statistics, vol. 535, John Wiley and Sons, Chichester, 2000.

[17] Moray, N.P., Huey, B.M. Human factors research and human safety. In: *Proceedings of Panel on human factors research needs in nuclear regulatory research*, Committee on Human Factors, Commission on Behavioral and Social Sciences. National Research Council, Washington, DC, (1988) pp. 13–19.

[18] Nasimi, E., Gabbar, H A. FSN-based fault modeling in CANDU stations. *Annals of Nuclear Energy* 65 (2014) 325–337.

[19] O'Hara, K. Cost of Operations Affects Plantfulness of Problem-Solving Behaviour. In: Proceedings of CHI'94, *Conference on Human Factors in Computing Systems*, Boston, MA, USA, (1994) pp. 105–106.

[20] Qaiser, S.H., Bhatti, A.I., Iqbal, M., Qadir, J. System Identification and Robust Controller Design for Pool Type Research Reactor. *13th IEEE IFAC International Conference on Methods and Models in Automation and Robotics*, 2 - 3 August 2007, Poland.

[21] Raghuraj, R., Bhushan, M., Rengaswany, R. Locating Sensors in Complex Chemical Plants based on fault diagnostic observability criteria, *AICHE journal*, Vol 45(1999) pp310-322.

[22] Rastogi, A., Gabbar, H.A. Fuzzy-Logic-Based Safety Verification Framework for Nuclear Power Plants. *Society for Risk Analysis*. DOI: 10.1111/j.1539-6924.2012.01899.x, 2012.

[23] Sandham, W., Leggett, M. (Eds.). Geophysical Applications of Artificial Neural Networks and Fuzzy Logic. *Kluwer Academic Publishers*, 2003.

[24] E. Patelli, H.J. Pradlwarter, G.I. Schu¨eller, Global sensitivity of structural variability by random sampling, Comput. Phys. Commun.181 (2010) 2072–2081. doi:10.1016/j.cpc.2010.08.007.

[25] Upadhyaya, B.R., Li Fan, Perillo, Perillo, S.R.P., Hines, J.W. Load-following, Co-generation, and Sensor Placement S for Small modular reactors. *Nuclear Safety and Simulation*, Vol 2(4), (2011), pp307-317.

[26] Upadhyaya, B.R., Perillo S.R.P. Advanced Instrumentations and control for small and medium reactors with demonstration, Vol5: Multi-modular integral pressurized water reactor control and operational configuration for a flow control loop. USNRC, DE-FG07-07I014895/U NE/ (2011).

[27] H.Wang, Zhihuan Song, Hui Wang. Statistical process monitoring using in proved PCA with optimized sensor locations. *Journal of process control*. Vol 12(6)735-744, 2002.

[28] Xin, J., Ray, A., Edwards, R.M. Integrated Robust and resilient control of nuclear power plants for Operational safety and high performance. *IEEE Transactions on Nuclear Science* 55 (2), 807-817, 2010.

[29] Zhao, K., Upadhyaya, B.R. Model based approach for fault detection and isolation of helical coil steam generator systems using principal component analysis. *IEEE Transactions on Nuclear Science* 53 (4), 2343-2352, 2006.

[30] Frank, P. M. Fault diagnosis in dynamic system using analytical and knowledge based redundancy - a survey and some new results, *Automatica* 26(3): 459–474, 1990.

[31] A. Saltelli, Making best use of model valuations to compute sensitivity indices, Comput. Phys. Commun. 145 (2002) 280–297.

[32] Isermann, R. On the applicability of model-based fault detection for technical processes, *Control Engineering Practice* 2(3): 439–450, 1994.

[33] Patton, R. J. and Chen, J. A review of parity space approaches to fault diagnosis, Preprints of *IFAC/IMACS Symposium SAFEPROCESS'91*, Baden-Baden, pp. 239–255 (Vol.1). Invited Survey Paper, 1991.

[34] Poulizeos, A. D. and Stravlakakis, G. S. (eds). Real Time Fault Monitoring of Industrial Processes, *Int. Series on Micro-Based and Int. Sys. Eng*., Vol.12, Series Editor Tzafestas, S., Kluwer Academic Press, 1994.

[35] Chen, J. Robust Residual Generation for Model-based Fault Diagnosis of Dynamic Systems, PhD thesis, Dept. of Electronics, University of York, York, UK, 1995.

[36] Patton, R. J. and Chen, J. A review of parity space approaches to fault diagnosis for aerospace systems, J. of Guidance, *Control and Dynamics* 17(2): 278–285, 1994.

[37] Willsky, A. S. A survey of design methods for failure detection in dynamic systems, *Automatica* 12(6): 601–611, 1976.

[38] R. J. Patton, J. Chen, S.B.Nielsen. Model-based methods for fault diagnosis; some guide-lines. *Transactions of the Institute of Measurement and control*, 17(2): 73-83, 1995.

[39] Frank, P. M. Fault diagnosis in dynamic system via state estimation - a survey, in Tzafestas, Singh and Schmidt (eds), *System Fault Diagnostics, Reliability & Related Knowledge-based Approaches*, D. Reidel Press, Dordrecht, Vol 1, pp. 35–98, 1987.

[40] Patton, R. J., Frank, P. M. and Clark, R. N. (eds). Fault Diagnosis in Dynamic Systems, Theory and Application, *Control Engineering Series*, Prentice Hall, London, 1989.

[41] Yu, D. L., Shields, D. N. and Mahtani, J. L. A nonlinear fault detection method for a hydraulic system, *Proc. of the IEE Int. Conf.: Control' 94*, Peregrinus Press, Conf. Pub. No. 389, Warwick, UK, pp. 1318–1322, 1994.

[42] Gertler, J. and Kunwer, M. K. Optimal residual decoupling for robust fault diagnosis, Proc. of Int. Conf. on Fault Diagnosis: *TOOLDIAG'93, Toulouse*, pp. 436–452, 1993

[43] Chow, E. Y. and Willsky, A. S. 1984. Analytical redundancy and the design of robust detection systems, IEEE Trans. Automat. Contr. AC-29(7): 603–614.

[44] Lou, X., Willsky, A. S. and Verghese, G. C. 1986. Optimally robust redundancy relations for failure detection in uncertain systems, Automatica 22(3): 333–344.

[45] Gertler, J., Fang, X. W. and Luo, Q. 1990. Detection and diagnosis of plant failures; the orthogonal parity equation approach, in C. Leondes (ed.), Control & Dynamics Systems, Academic Press, pp. 157–216. Vol.37.

[46] Isermann, R. 1984. Process fault detection based on modelling and estimation methods: A survey, Automatica 20(4): 387–404.

[47] Isermann, R. 1987. Experiences with process fault detection via parameter estimation, in Tzafestas, Singh and Schmidt (eds), System Fault Diagnostics, Reliability & Related Knowledge-based Approaches, D. Reidel Press, Dordrecht, pp. 3–33.

[48] Isermann, R. 1993. Fault diagnosis of machine via parameter estimation and knowledge processing - tutorial paper, Automatica 29(4): 815–835.

[49] Patton, R. J., Chen, J. and Siew, T. M. 1994. Fault diagnosis in nonlinear dynamic systems via neural networks, Proc. of the IEE Int. Conf.: Control' 94, Peregrinus Press, Warwick, UK, pp. 1346–1351. Conf. Pub. No. 389.

[50] Patton, R. J. and Chen, J. 1992b. Robustness in model-based fault diagnosis, in D. Atherton and P. Borne (eds), Concise Encyclopedia of Simulation and Modelling, Pergamon Press, pp. 379–392.

[51] Frank, P. M. and Ding, X. 1994. Frequency domain approach to optimally robust residual generation and evaluation for model-based fault diagnosis, Automatica 30(4): 789–804.

[52] W. Cauer, Theorie der linearen Wechselstromschaltungen, vol. 1, Akad. Verlags-Gesellschaft Becker und Erler, Leipzig, 1941.

[53] Patton, R. J. 1991. Fault detection and diagnosis in aerospace systems using analytical redundancy, IEE Computing & Control Eng. J. 2(3): 127–136.

[54] Tzafestas, S. G. and Watanabe, K. 1990. Modern approaches to system/sensor fault detection and diagnosis, Journal A 31(4): 42–57.

[55] Speyer, J. L. and White, J. E. 1984. Shiryayev sequential probability ratio test for redundancy management, J. of Guidance, Control and Dynamics 7: 588–595.

[56] Clark, R. N. 1989. State estimation schemes for instrument fault detection, in R. J. Patton, P. M. Frank and R. N. Clark (eds), Fault Diagnosis in Dynamic Systems: Theory and Application, Prentice Hall, chapter 2, pp. 21–45.

[57] Frank, P. M. and Ding, X. 1994. Frequency domain approach to optimally robust residual generation and evaluation for model-based fault diagnosis, Automatica 30(4): 789–804.

[58] Emami-Naeini, A. E., Akhter, M. M. and M., R. S. 1988. Effect of model uncertainty on failure detection: the threshold selector, IEEE Trans. Automat. Contr. AC-33(2): 1106–1115.

[59] Frank, P. M. and Kiupel, N. 1993. Fuzzy supervision and application to lean production, Int. J. System Sci. 24(10): 1935–1944.

[60] Shen, Q. and Leitch, R. 1993. Fuzzy qualitative simulation, IEEE Trans. on Sys., Man & Cybernetics SMC-23(4): 1038–1061.

[61] Sorsa, T., Koivo, H. N. and Koivisto, H. 1991. Neural networks in process fault diagnosis, IEEE Trans. Systems, Man & Cybernetics 21(4): 815–825.

[62] Watanabe, K., Matsuura, I., Abe, M., Kubota, M. and Himmelblau, D. M. 1989. Incipient fault diagnosis of chemical processes via artificial neural networks, AIChE J. 35(11): 1803–1812.

[63] IAEA, 2009. Safety Assessment for Facilities and Activities. General Safety Requirements Part 4. Number GSR part 4, STI/PUB/1375.

[64] Edoardo Patelli, H. Murat Panayirci, Matteo Broggi, Barbara Goller, Pierre Beaurepaire, Helmut J. Pradlwarter, Gerhart I.Schu¨ eller. 2012. General purpose software for efficient uncertainty management of large finite element models. Finite Elements in Analysis and Design 51 (2012) 31–48.

[65] Horst Glaeser. 2008. GRS Method for Uncertainty and Sensitivity Evaluation of Code Results and Applications. Science and Technology of Nuclear Installations Volume 2008, Article ID 798901, 7 pages doi:10.1155/2008/798901.

[66] J. Myung, Tutorial on maximum likelihood estimation, J. Math. Psychol. 47 (1) (2003) 90–100.

[67] C.A.Schenk, G.I.Schu¨eller, Uncertainty Assessment of Large Finite Element Systems, Lecture Notes in Applied and Computational Mechanics, vol. 24,Springer-Verlag,Berlin/Heidelberg/NewYork,2005ISBN:978-3-540- 25343-3.

[68] E. Vanmarcke, Random Fields: Analysis and Synthesis, MIT Press, Cambridge, MA, 1998; Web Edition by Rare Book Services, Princeton University, Princeton NJ, Cambridge, MA, 1998.

[69] *Hanna BN,* et al. One-step semi-implicit method for solving the transient two-fluid equations that is noncourant limited. 11th National Heat Transfer Conference, Denver, 1985.

[70] *Richards DJ,* et al. ATHENA: a two-fluid code for CANDU LOCA analysis. Presented at the Third International Topical Meeting on Reactior Thermalhydraulics, Newport, Rhode Island, 1985.

[71] J.P. Mallory and P.J. Ingham. CATHENA Simulation of Thermosiphoning in a Pressurized-Water Test Facility. Nuclear Journal of Canada /1:2/ pp. 240-249.

[72] Lecture Notes on General Introduction to CATHENA by System Code Development Thermalhydraulics Branch, Canadian Nuclear Laboratories. September, 2015.

[73] Bereznai, G., 2001b. Nuclear power plant systems and operation, simulator user manual. Faculty of Energy Systems and Nuclear Science, University of Ontario Institute of Technology (UOIT), Oshawa, Ontario.

[74] Canadian Nuclear Safety Commission (CNSC). 2014. Regulatory Document REGDOC-2.4.1. Deterministic Safety Analysis. PWGSC catalogue number CC172-108/1-2014E-PDF ISBN 978-1-100-23790-9.

[75] E.-L. Pelletier and E. Varin. 2011. A Direct Coupling between RFSP and CATHENA Using PVM. Atomic Energy of Canada Limited, Montreal, Québec, Canada.

[76] B. Rouben, "RFSP-IST, The Industry Standard Tool Computer Program for CANDU reactor Core Design and Analysis", Proceedings of the 13th Pacific Basin Nuclear Conference, Shenzhen, China, October 21-25 (2002).

[77] B.N. Hanna, "CATHENA: A Thermalhydraulic Code for CANDU Analysis", Nucl. Eng. Design 180: 113-131, 1998.

[78] J.V. Donnelly and E.M. Nichita, "Verification of Two-Group *CERBERUS for a Loss-of-Coolant Analysis in a Simplified Reactor Model", in *Proceedings of the 39th Annual Canadian Nuclear Association Conference* and the 20th Annual *Conference of the Canadian Nuclear Society*, Montréal, Québec, 1999 May 30-June 2.

[79] J.H. Choi, H.R. Hwang, and J.T. Seo, CATHENA code validation with Wolsong 4 plant commissioning test data, *Proceedings of the Korean Nuclear Society Autumn Meeting*, Seoul, Korea, 2001.

[80] Dan Gabriel Cacuci, Mihaela Ionescu-Bujor. 2010. Sensitivity and Uncertainty Analysis, Data Assimilation, and Predictive Best-Estimate Model Calibration. *Handbook of Nuclear Engineering*, DOI: 10.1007/978-0-387-98149-9_17, Springer Science+Business Media LLC.

[81] Hyoung Tae Kim. 2012. An open calculation of RD-14M small-break LOCA experiments using CATHENA code. *Annals of Nuclear Energy* 46 (2012) 63–75.

[82] McGee, G.R. et al, 'RD-14 Test B8603-Small Inlet-Header Break with Emergency Coolant Injection", AECL, Report RD-14-86-03, April, 1986.

[83] M. Shoukri and A. Abdul-Razzak. 1990. FUEL CHANNEL REFILLING DATA ANALYSIS, A research report prepared for the Atomic Energy Control Board Ottawa, Canada, April, 1990.

[84] CANDU-9 Simulator. http://www.cti-simulation.com/ctisimulation/CANDU.htm

[85] Hora SC, Iman RL (1989) Expert opinion in risk analysis: the NUREG-1150 methodology. *Nuclear Science Engineering* 102:323.

[86] Bonano EJ, Apostolakis GE (1991) Theoretical foundations and practical issues for using expert judgments in uncertainty analysis of high level radioactive waste disposal. *Radioactive Waste Management Nuclear Fuel Cycle* 16:137

[87] MATLAB Release 2015b, The MathWorks, Inc., Natick, Massachusetts, United States.

[88] E. Alhassan, H. Sjostrand, P. Helgesson, A.J. Koning, M. Osterlund, S. Pomp, D. Rochman. 2014. Uncertainty and correlation analysis of lead nuclear data on reactor parameters for the European Lead Cooled Training Reactor. *Annals of Nuclear Energy* 75 (2015) 26–37.

[89] IAEA. 2008. Best estimate safety analysis for nuclear power plants: uncertainty evaluation. — Vienna: International Atomic Energy Agency, Safety reports series, ISSN 1020–6450; no. 52.

[90] Clotaire Geffray, Rafael Macián-JuanTechnische. 2015. Multi-scale uncertainty and sensitivity analysis of the TALL-3Dexperiment. *Nuclear Engineering and Design* 290 (2015) 154–163.

[91] W.R. Marcum, A.J. BriganticOregon. 2015. Applying uncertainty and sensitivity on thermal hydraulic subchannel analysis for the multi-application small light water reactor. *Nuclear Engineering and Design* 293 (2015) 272–291.

[92] Cacuci, D.G., Ionescu-Bujor, M.I., 2010. Sensitivity and Uncertainty Analysis, Data Assimilation, and Predictive Best-Estimate Model Calibration. Handbook of Nuclear Engineering, DOI: 10.1007/978-0-387-98149-9_17, Springer Science+Business Media LLC.

[93] David J. Smith and Kenneth G.L. Simpson, 2004. Functional Safety – A straightforward Guide to applying IEC 61508 and Related Standards, Second edition, *Elsevier Butterworth-Heinemann*, ISBN 0 750662697, Oxford, Great Britain.

APPENDIX I: List of Publications Related to this Thesis

1. **Emmanuel Boafo**, Hossam A.Gabbar. 2016. Stochastic Uncertainty Quantification for Safety Verification Applications in Nuclear Power Plants. *Nuclear Engineering and Technology* – Under Review.
2. Hossam A.Gabbar, **Emmanuel K.Boafo**. FSN-based co-simulation for fault propagation analysis in nuclear power plants. *Process Safety Progress*, vol. 35, No. 1, March, 2016. American Society of Chemical Engineering.
3. **Emmanuel Boafo**, Elnara Nasimi, Luping Zhang, Hossam A.Gabbar. FSN-based Co-Simulation for Real Time Safety Verification of Nuclear Power Plants. *Mechanical Engineering Journal* - Accepted.
4. **Emmanuel Boafo**, Elnara Nasimi, Luping Zhang, Hossam A.Gabbar. Co-Simulation for Real Time Safety Verification of Nuclear Power Plants. The *23rd International Conference on Nuclear Engineering*, May 17th-21st, 2015, Chiba, Japan.

APPENDIX II: List of Publications Not Related to this Thesis

1. Thomas Sleeman, Dominique Paterson, Derek Steele, C.A. Barry Stoute, David Newell, Cole Simkin, Hossam A. Gabbar, **Emmanuel Boafo**. 2016. Evaluation and Optimization of Thermoelectric Generator Network for Waste Heat Utilization in Nuclear Power Plants and Non-Nuclear Energy Applications. *Annals of Nuclear Energy* – Under Review.
2. Hossam A.Gabbar, Luping Zhang, **Emmanuel Boafo**, Daniel Bondarenko, C.A. Barry Stoute. Simulations of High-Current Plasma Beam by Continuum and Statistical Mechanical Models. *World Journal of Nuclear Science and Technology*, 2016, 6, 103-114.
3. **E.K. Boafo**, E. Alhassan, E.H.K. Akaho, Utilizing the burnup capability in MCNPX to perform depletion analysis of an MNSR fuel- Annals of Nuclear Energy, Vol 73C, November, 2014, Page 478-483.
4. Luping Zhang, Sayf Elgriw, **Emmanuel Boafo**, Daniel Bondarenko, Hossam A.Gabbar. The Simulation of High-Current Intersecting Plasma Beams by MHD and Monte Carlo Methods. *British Journal of Applied Science & Technology* 11(3): 1-12, 2015, Article no.BJAST.20264 ISSN: 2231-0843.
5. J.L. Muswema, G.B Ekoko, J.K.-K. Lobo, V.M. Lukanda, **E.K. Boafo.** 2016**.** *TRICO II* core inventory calculation and its radiological consequence analyses. *Nuclear Engineering and Radiation Science*, Vol. 2 / 024501-1, Transactions of ASME.
6. J.L. Muswema, G.B. Ekoko, V.M. Lukanda, J.K.K Lobo, E.O. Darko, **E.K. Boafo**. Source Term Derivation and Radiological Safety Analysis for the TRICO II

Research Reactor in Kinshasa. *Nuclear Engineering and Design*, vol 281, page 51-57, 2015.

7. J.L Muswema, J.K. Gbadago, E.O. Darko, **E.K. Boafo**. Atmospheric Dispersion Modeling and Radiological Safety Analysis for a Hypothetical Accident of Ghana Research Reactor-1 (GHARR-1). *Annals of Nuclear Energy*, Vol. 68, June 2014, Page 239–246.
8. F. Ameyaw, M. Nyarku, J. Boffie, J. K. Gbadago, **E. Boafo**, E. T. Glover. Characterization of Radioisotope and Shield Content of Stored Disused Sealed Radioactive Sources in Ghana. *Journal of Hazardous, Toxic, and Radioactive Waste*, American Society of Civil Engineers, 2016. DOI: 10.1061/ (ASCE) HZ.2153-5515.0000319.
9. **E.K. Boafo,** E.H.K. Akaho, B.J.B. Nyarko, S.A. Birikorang, G.K. Quashigah, Fuel burnup calculation for HEU and LEU cores of Ghana MNSR. *Annals of Nuclear Energy*, vol. 44c, page 65-70 in June, 2012.

APPENDIX III: MATLAB SCRIPT FOR GENERATING RANDOM CATHENA INPUT FILES

```
if isunix
    Sexecutable='cat3_5drev2.exe.sh';
else
    % TODO:
    Sexecutable='cat3_5drev2.exe.bat';
end

%% BE SURE OpenCOSSAN has been initialised

% Reset the random number generator in order to obtain always the same
results.
% DO NOT CHANGE THE VALUES OF THE SEED
OpenCossan.resetRandomNumberGenerator(51125)

%% Tutorial Connector: CATHENA
%

% In this examples 3 quantities are connected with OpenCOSSAN
% (ReservoirPressure, InitialPressure and InitialTemperature)
%
ReservoirPressure=Parameter('value',1.013E5);
InitialPressure=RandomVariable('Sdistribution','normal','mean',7,'cov',
0.1);
InitialTemperature=RandomVariable('Sdistribution','uniform','lowerBound
',200,'upperBound',300)

RVSET=RandomVariableSet('CSmembers',{'InitialPressure'
'InitialTemperature'});
Xinput=Input('CSmembers',{'RVSET'
'ReservoirPressure'},'CXmembers',{RVSET ReservoirPressure});
%
% The outputs are collected from a file (edwards_press.dat)

%% Create the Injector
% An injector is screated by scanning the file PipeBlowdown.inp.cossan
containing 3 indentifiers
Sfolder=fileparts(mfilename('fullpath'));% returns the current folder
SfilePath=fullfile(Sfolder,'Connector','CATHENA');

Xinj = Injector('Sscanfilepath',SfilePath,...
                'Sscanfilename','PipeBlowdown.inp.cossan',...
                'Sfile','PipeBlowdown.inp');

% Show the content of the identifier
display(Xinj)
%% Output files
% The output is collected from the file edwards_press.dat
% Since the data are written in a table format is convinient to use the
% method TableExtractor
%
```

```
Xte1=TableExtractor('Sdescription','Extractor for the tutorial
CATHENA', ...
    'Luseload',false,...
    'LextractColumns',true, ...
    'Srelativepath','./', ... % relative path to the Sworkingdirectory
where result file is located
    'Sfile','edwards_press.dat',...
    'Nheaderlines',27,...
    'Sdelimiter',' ',...
    'CcolumnPosition',{6},...
    'Soutputname','out');

% It is also possible to read a single value or post processing the
data
% using a MIO function after the execution of the SOLVER.

%% Construct the connector
Xc = Connector('Stype','cathena',... solver identification
    'Ssolverbinary',fullfile(SfilePath,Sexecutable),... Solver binary
    'Sexeflags','',... execution flags
    'Smaininputfile','PipeBlowdown.inp',... main input file
    'Smaininputpath',SfilePath,... absolute path to the original main
input file
    'Sexecmd','%Ssolverbinary %Smaininputfile %Sexeflags',...
construction of the execution command
    'SpostExecutionCommand',[' cp ' eval('SfilePath') filesep
'edwards_press.dat .'],... % SEE NOTE BELOW
    'LkeepSimulationFiles',false,...
    'CXmembers',{Xinj Xte1}); % objects included in the Connector

% The SpostExecutionCommand is used to simulate the execution of the
% solver. The output file is copied into the working directory and the
% extracted by the TableExtractor.

%% Define the model

Xeval = Evaluator('CXmembers',{Xc}); % Members of the evaluator (one or
more solvers)

% Create the Model
Xm = Model('Xinput',Xinput,'Xevaluator', Xeval);

% Test the model performing a deterministic analysis
Xout=Xm.deterministicAnalysis;

OutDataseries=Xout.getValues('Sname','out');

OutDataseries.plot

% Set Simulation properties
Xmc = MonteCarlo('Nsamples',300);

%% Perform Monte Carlo
Xout1 = Xmc.apply(Xm);
```

APPENDIX IV: MATLAB SCRIPT FOR CREATING AND UPDATING BBN

```
function [bnet, names, marg, loglik] = SGBBN()
%   Function to create bayesian Belief Network for Flexible Rotor
Faults


names = {'Impaction of particles(a)', 'Pressure Spikes(b)', 'Debris
causing actuator failure(c)', 'Incorrect Installation(d)', 'Valve
Cavitation(e)', 'High Temperature(f)', ...
         'Sensor Degradation(g)', 'Lack of calibration(h)','Bias and
Drifting (j)', ...
         'LCV101 Fails Open(A)','LCV101 Fails Closed(B)', 'SG1 FW FT
Irrational(C)', ...
         'High SG1 level(x)', 'High SG1 Pressure(y)', 'Turbine
Trip(z)', 'Low SG1 level(w)', 'Low Neutron Power(v)','High Avg Zone
level(u)'};
ss = length(names);

intrac = {...
  'Impaction of particlea(a)', 'LCV101 Fails Open(A)';
  'Pressure Spikes(b)', 'LCV101 Fails Open(A)';
  'Debris causing actuator failure(c)', 'LCV101 Fails Open(A)';
  'Incorrect Installation(d)', 'LCV101 Fails Closed(B)';
  'Valve Cavitation(e)', 'LCV101 Fails Closed(B)';
  'High Temperature(f)', 'LCV101 Fails Closed(B)(C)';
  'Sensor Degradation(g)', 'SG1 FW FT Irrational(C)';
  'Lack of calibration(h)', 'SG1 FW FT Irrational(C)';
  'Bias and Drifting(j)', 'SG1 FW FT Irrational(C)';
  'LCV101 Fails Open(A)', 'High SG1 level(x)'; 'LCV101 Fails Open(A)',
'High SG1 Pressure(y)';'LCV101 Fails Open(A)','Turbine Trip(z)';
  'LCV101 Fails Closed(B)', 'Low SG1 level(w)'; 'LCV101 Fails
Closed(B)', 'Low Neutron Power(v)'; 'LCV101 Fails Closed(B)', 'High Avg
Zone level(u)';
  'SG1 FW FT Irrational(C)', 'High SG1 level(x)'; 'SG1 FW FT
Irrational(C)', 'High SG1 Pressure(y)';'SG1 FW FT Irrational(C)', 'Low
Neutron Power(v)'};

[intra, names] = ESCL_Adj_Matrix(intrac, names, 0);
gObj = biograph(intra,names);
gObj = view(gObj);
discrete_nodes = 1:ss; % No. of discrete nodes
node_sizes = 2*ones(1,ss); % States of nodes, binary in this simple
case (FALSE = 1, TRUE = 2)
bnet = ESCL_Mk_Bnet(intra, node_sizes, 'names', names, 'discrete',
discrete_nodes);

%G = bnet.dag;
%ESCL_Draw_Bnet(G);

bnet.CPD{bnet.names('Impaction of particlea(a)')} =
ESCL_Tabular_CPD(bnet, bnet.names('Impaction of particlea(a)'), 'CPT',
[0.8 0.2]);
```

```
bnet.CPD{bnet.names('Pressure Spikes(b)')} = ESCL_Tabular_CPD(bnet,
bnet.names('Pressure Spikes(b)'), 'CPT', [0.9 0.1]);
bnet.CPD{bnet.names('Debris causing actuator failure(c)')} =
ESCL_Tabular_CPD(bnet, bnet.names('Debris causing actuator
failure(c)'), 'CPT', [0.88 0.12]);
bnet.CPD{bnet.names('Incorrect Installation(d)')} =
ESCL_Tabular_CPD(bnet, bnet.names('Incorrect Installation(d)'), 'CPT',
[0.9 0.1]);
bnet.CPD{bnet.names('Valve Cavitation(e)')} = ESCL_Tabular_CPD(bnet,
bnet.names('Valve Cavitation(e)'), 'CPT', [0.85 0.15]);
bnet.CPD{bnet.names('High Temperature(f)')} = ESCL_Tabular_CPD(bnet,
bnet.names('High Temperature(f)'), 'CPT', [0.85 0.15]);
bnet.CPD{bnet.names('Sensor Degradation(g)')} = ESCL_Tabular_CPD(bnet,
bnet.names('Sensor Degradation(g)'), 'CPT', [0.8 0.2]);
bnet.CPD{bnet.names('Lack of calibration(h)')} = ESCL_Tabular_CPD(bnet,
bnet.names('Lack of calibration(h)'), 'CPT', [0.9 0.1]);
bnet.CPD{bnet.names('Bias and Drifting(j)')} = ESCL_Tabular_CPD(bnet,
bnet.names('Bias and Drifting(j)'), 'CPT', [0.8 0.2]);

bnet.CPD{bnet.names('LCV101 Fails Open(A)')} = ESCL_Tabular_CPD(bnet,
bnet.names('LCV101 Fails Open(A)'), 'CPT', [1.0 1.0 0.9 1.0 0.8 0.9 0.8
0.1 0.0 0.0 0.1 0.0 0.2 0.1 0.2 0.9]);
bnet.CPD{bnet.names('LCV101 Fails Closed(B)')} = ESCL_Tabular_CPD(bnet,
bnet.names('LCV101 Fails Closed(B)'), 'CPT', [0.9 0.8 0.7 0.05 0.1 0.2
0.3 0.1,0.0 0.0 0.1 0.0 0.2 0.1 0.2 0.9]);
bnet.CPD{bnet.names('SG1 FW FT Irrational(C)')} =
ESCL_Tabular_CPD(bnet, bnet.names('SG1 FW FT Irrational(C)'), 'CPT',
[0.8 0.6 0.75 0.7 0.4 0.3 0.55 0.05 0.2 0.4 0.25 0.3 0.6 0.7 0.45
0.95]);

bnet.CPD{bnet.names('High SG1 level(x)')} = ESCL_Tabular_CPD(bnet,
bnet.names('High SG1 level(x)'), 'CPT', [0.9 0.6 0.7 0.1 0.1 0.4 0.3
0.9]);
bnet.CPD{bnet.names('High SG1 Pressure(y)')} = ESCL_Tabular_CPD(bnet,
bnet.names('High SG1 Pressure(y)'), 'CPT', [0.8 0.7 0.5 0.1 0.2 0.3 0.5
0.9]);
bnet.CPD{bnet.names('Turbine Trip(z)')} = ESCL_Tabular_CPD(bnet,
bnet.names('Turbine Trip(z)'), 'CPT', [1.0 0.0 0.9 0.1]);
bnet.CPD{bnet.names('Low SG1 level(w)')} = ESCL_Tabular_CPD(bnet,
bnet.names('Low SG1 level(w)'), 'CPT', [0.8 0.2 0.1 0.9]);
bnet.CPD{bnet.names('Low Neutron Power(v)')} = ESCL_Tabular_CPD(bnet,
bnet.names('Low Neutron Power(v)'), 'CPT', [0.7 0.6 0.5 0.25 0.3 0.4
0.5 0.75]);

engine = ESCL_Jtree_Inf_Engine(bnet);
evidence = cell(1,ss);
evidence{bnet.names('High SG1 level(x)')} = 1;
evidence{bnet.names('High SG1 Pressure(y)')} = 2;
evidence{bnet.names('Turbine Trip(z)')} = 2;
evidence{bnet.names('Low SG1 level(w)')} = 2;
evidence{bnet.names('Low Neutron Power(v)')} = 2;
[engine, loglik] = ESCL_Enter_Evidence(engine, evidence);

marg = ESCL_Marginal_Nodes(engine, bnet.names('LCV101 Fails Open(A)'));
marg.T
```